Origins of Structure and Energetics of van der Waals Clusters from ab Initio Calculations

Grzegorz Chałasiński*,†

Department of Chemistry, University of Warsaw, Pasteura 1, 02-093 Warszawa, Poland, Department of Chemistry and Biochemistry, Southern Illinois University, Carbondale, Illinois 62901, and Department of Chemistry, Oakland University, Rochester, Michigan 48309

Małgorzata M. Szczęśniak*

Department of Chemistry, Oakland University, Rochester, Michigan 48309

Received November 4, 1993 (Revised Manuscript Received July 31, 1994)

Contents

I. Introduction

The concept of intermolecular forces has been central to the molecular theory of matter since the work of van der Waals. A great deal of effort has been expended in an attempt to establish a relationship between the properties of bulk matter and intermolecular forces. Historically, the studies in this area have proceeded in two directions. On one hand, the quantum and statistical mechanical apparatus has been developed which could translate the input from quantum mechanical treatment of intermolecular interactions into the properties of bulk materials. On the other hand, the inverse problem of molecular theory has also been addressed in an attempt to obtain the information on intermolecular forces from direct measurements of the macroscopic properties.[1–3]

A molecular description of condense phase properties relies on the full characterization of pairwise interactions, as well as on the knowledge of many-body forces. van der Waals dimers of closed-shell species, atoms, and/or molecules have traditionally served as an important source of information on pair interactions to theoreticians and experimentalists

† Permanent address: Department of Chemistry, University of Warsaw, Pasteura 1, 02-093 Warszawa, Poland.

0009-2665/94/0794-1723$14.00/0

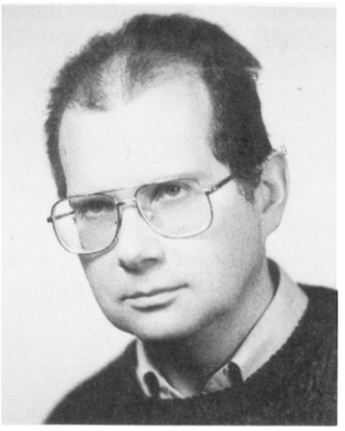

Grzegorz Chałasiński was born in Warsaw, Poland. He earned his M.S. degree in chemistry from the University of Warsaw in 1971. He received his Ph.D. degree in theoretical chemistry in 1977 from the University of Warsaw for work in ab initio perturbation theory of intermolecular interactions. He was a visiting professor at the University of Utrecht (1979–1980) and a Postdoctoral Fellow at the University of Utah (1985–1987). Since 1988 he has collaborated with M. M. Szczęśniak and S. Scheiner of Southern Illinois University at Carbondale. He is now a professor of chemistry at the University of Warsaw.

Małgorzata M. Szczęśniak was born in Wrocław, Poland. She received a M.S. degree in chemistry from the University of Wrocław in 1973. In 1978 she received her Ph.D. degree in theoretical chemistry from the University of Wrocław. She was a Postdoctoral Fellow with Professor S. Scheiner at Southern Illinois University at Carbondale. Also at SIU she held a Visiting Assistant Professor position (1983–1989) and Associate Research Professor position (1989–1991). In 1991 she joined the faculty of Oakland University in Rochester, MI.

alike. Trimeric species allow insights into three-body forces. Larger clusters are often regarded as intermediates between gas and condensed phases of matter. The primary goal of these studies has been to understand the nature of intermolecular potential over the entire configurational space, the so-called potential energy surface (PES). In binary complexes of polyatomic molecules the intermolecular surface is in general a function of six intermolecular degrees of freedom. One of its most important characteristics is its anisotropy.

From the experimental perspective, the insights into the anisotropic forces which determine the shape of potential energy surfaces rely on experiments which can directly sample the extended regions of PES, and on mathematical schemes which invert the experimental measurements to yield the anisotropic multidimensional surfaces. Recent advances in far-IR laser spectroscopy allowed for direct measurements of the low-frequency vibrations of van der Waals bonds.[2–13] Such spectra are believed to probe the extended regions of PES both below and above the barriers to internal motion, and for this reason this technique has been dubbed vibration–rotation–tunneling (VRT) spectroscopy.[8,9] Simultaneously, a great deal of progress has been achieved in computational approaches which directly determine the multidimensional PESs and the associated intermolecular dynamics from VRT spectra. This strategy is now pursued in several laboratories.[5–11]

The first principle calculations have been used to evaluate potential energy surfaces since the dawn of modern computational chemistry. These investigations have generated an immense amount of PES data on systems ranging from the He dimer to DNA base pairs and also larger clusters. The results have been summarized in a number of monographs and review articles.[14–23] The first thematic issue of *Chemical Reviews* on the topic of intermolecular interactions, which appeared some six years ago, provided a fairly complete account of ab initio results on van der Waals interactions.[24–26] Over the past years a better understanding of these interactions at the fundamental level has been achieved. Due to rapid progress in computational algorithms and computer hardware, the ab initio techniques are now capable of providing potential energy surfaces for these systems with an accuracy which can fully compete with that of experimental investigations.

From the most fundamental perspective, the shapes of PESs result from an interplay of the four basic components of interaction energy, electrostatic, exchange, induction, and dispersion. Each of these components has a different physical origin, properties, and behavior with respect to intermolecular degrees of freedom. An individual examination of these components helps determine the effects the anisotropies of the individual components have on the entire surface. The dominant contributions at any given range of geometries can be easily identified. More importantly, a relationship can be established between the interaction energy and the intrinsic properties of the constituent fragments, thus providing a more complete understanding of the interaction phenomenon. Therefore, any meaningful ab initio attempt to understand the underlying origins of anisotropic forces employs some type of energy partitioning into these fundamental effects. This point of view, which is deeply rooted in classical theory of intermolecular forces, will be highlighted in the present review. Our primary focus is on the underlying factors which govern the interaction energies across a wide spectrum of interacting systems. We will discuss the ab initio results for a variety of dimers and trimers ranging from weak van der Waals complexes to hydrogen-bonded species.

The review consists of two major parts. The first part describes the state-of-the-art ab initio theory of van der Waals interactions at the post-Hartree–Fock level of theory. Our emphasis is on the methods which provide a rigorous quantitative quantum mechanical description of the intermolecular forces, and allow for the identification of physically meaningful

terms which originate from the classic theory of intermolecular forces. The quantum mechanical basis is provided by the Møller–Plesset perturbation theory[27–29] also known as the many-body perturbation theory.[30–33] Within the symmetry-adapted perturbation formalism,[34–38] this theory allows for the most natural description of interaction energy in the form of a sum of electrostatic, induction, dispersion, and exchange interactions. It also offers a logical framework for step-by-step inclusion of electron correlation effects on these forces within both the perturbation and the supermolecular approaches.[39–44] The four fundamental components are first described within the independent particle model level (i.e. HF), and next, by progressive inclusion of *intramonomer* and *intermonomer* electron correlation effects, a more complete description of these forces is achieved. Following the formal description of the theory, we discuss some practical aspects which are important in the actual computations of potential energy surfaces, such as the basis set selection, the basis set superposition error, and the convergence of the perturbation expansion. With an increasing number of investigators from various disciplines reaching for Møller–Plesset perturbation formalism via quantum chemistry codes, such as Gaussian,[45,46] these somewhat technical problems are of great importance to a large community of researchers.

The second part describes the results for specific complexes. In the broad context of the structure and energetics of van der Waals clusters, our main objective is to relate the interaction energies to the intrinsic properties of the monomers involved, and in particular, we intend to elucidate the factors which determine the anisotropy of individual components of the interaction. The complexes of molecules bound to rare gases offer many clues to the understanding of the more complex molecule–molecule interactions. A rare gas atom in these complexes may be viewed as a structureless probe of the molecule's properties. For this reason a great deal of attention is devoted to these complexes, particularly involving Ar. On the basis of these results, we attempt to elucidate factors which determine the shapes of potential energy surfaces in the short, intermediate, and long range of intersystem distances and to verify such classic concepts as molecular shape, lone electron pair, etc. and their role in the more directional interactions such as hydrogen bonding.

Finally, a number of trimeric species are also discussed. The selected trimers are designed to provide a gradual transition from nonpolar to polar clusters. The physical origin and properties of three fundamental nonadditive components (exchange, induction, and dispersion) in these trimers are discussed to gain insights into the nature and importance of three-body forces across a wide spectrum of interacting systems.

II. Essentials of ab Initio Theory of Weak Intermolecular Interactions

Since the seminal papers of London,[47–49] it has been known that there are four fundamental building blocks of the van der Waals interaction energies: electrostatic, induction, dispersion, and exchange.[50–54] The origin of the first three may be traced to the monomer properties: permanent multipole moments and polarizabilities (static and dynamic). The electrostatic energy results from permanent electric multipole interactions; the induction energy arises from the interactions of permanent multipole moments of one monomer with the multipole moments induced in another monomer; the dispersion energy originates in a mutual polarization of the electronic charge distributions of interacting monomers (interactions of instantaneous multipoles which are related to dynamic multipole polarizabilities). The exchange interaction energy is a repulsive effect, a result of the Pauli principle which forbids the electrons of one monomer to penetrate the occupied space of the partner. It may be conceptually related to the electron charge densities of interacting monomers which avoid each other.

Sometimes an additional type of interaction energy is postulated called the "charge-transfer" energy.[55,56] So far the term has eluded rigorous definition and is strongly dependent on both theoretical formalism and basis set effects.[57,58] In rigorous treatments it is encompassed primarily by the induction component, but is also related to the exchange effects. It should only be invoked as a conceptual visualization rather than a well-defined physical effect.

Another aspect to be aware of is that four fundamental components are not strictly additive and an exact treatment must also reveal coupling terms, e.g. induction–dispersion or exchange–dispersion.

A contemporary ab initio theory of electronic structure offers approaches of varying degrees of sophistication to both intermolecular and intramolecular interactions. The primary condition for an ab initio treatment to be useful in intermolecular problems is that it must not neglect any of the four fundamental interaction terms. The ab initio theory is most conveniently considered at two levels: the Hartree–Fock (HF) level (independent particle model), and post-Hartree–Fock level (electron-correlated level). Today, the HF level is reduced to a fairly routine SCF approach and may be accurately carried out even for large systems of biological interest.[59] The post-Hartree–Fock level calculations still present a largely nontrivial task which requires a thorough understanding of both the electron correlation theory and basis set effects. It is also convenient to discuss the ab initio theory of intermolecular forces at these two levels.

At the lowest level we assume HF approximation for monomers. Then all four fundamentals are evaluated with the HF monomer wave functions. They are related to the HF permanent moments, HF static and dynamic polarizabilities, and HF electron charge densities. Such a treatment precludes the appearance of the intramonomer correlation effects, but does allow for the intermonomer correlation ones which arise between the HF monomers—the HF dispersion energy.

At the post-HF level, electron correlation is allowed for in monomers. Then all four fundamentals should be evaluated with correlated monomer wave functions. This means that they now may be related to the monomer properties calculated at the correlated

level. At this level of theory the intramonomer correlation effects, as well as inter-intramonomer couplings, may be recovered to the extent which depends on a given correlated treatment applied.

The most complete and consistent realization of the post-Hartree–Fock ab initio approach is provided by the intermolecular Møller–Plesset perturbation theory (referred also to as symmetry-adapted perturbation theory).[34–38] On the one hand, it directly reproduces all four fundamental terms at consecutive orders beginning with the HF level through the limiting case provided by the complete treatment of correlation via the coupled cluster theory.[30,31] On the other hand, I-MP perturbation theory is closely related to the supermolecular approach to intermolecular forces based on the MP perturbation theory and CC approaches.[39–44]

A. Brief Overview of Intermolecular MP Perturbation Theory

The I-MP perturbation theory takes advantage of the fact that both the theory of intermolecular forces and the theory of electron correlation may be naturally developed within the perturbation theory framework. The I-MP perturbation theory is a double perturbation formalism with two perturbations representing the intermolecular interaction and the intramonomer correlation, respectively. The problem is that the classic RS perturbation theory does not account for intermolecular electron exchange effects (in other words does not enforce the Pauli principle in the overlap region). Because the electrons are kept within their original subsystems, application of the RS perturbation theory to intermolecular interactions was termed "polarization approximation" by Hirschfelder.[60] To circumvent this difficulty one must employ a symmetry-adapted formalism which forces proper antisymmetrization of the wave function in the course of the perturbation expansion.[61–64] The problem of symmetry forcing has no unique solution from the purely mathematical point of view. However, the demand that the symmetry-adapted perturbation theory preserves the physically meaningful contents of the classic approach, and remains technically applicable to many-electron systems, considerably narrows the number of possible formalisms. In fact the only viable approach is the one which adopts the so called *weak symmetry forcing*.[61] The weak symmetry forcing consists of performing a formally standard RS expansion for the wave function which is *a posteriori* antisymmetrized to obtain the energy corrections. Such an idea has been analyzed by many researchers[60,62,65,66] and was found efficient in model calculations of H_2^+ [66,67] and H_2.[68] Below, we follow the approach of Jeziorski, Szalewicz, and collaborators who developed the SAPT formalism which is applicable to many-electron systems and referred to as I-MP.[35–38] The related perturbation expansion may be presented in the form

$$E_{\mathrm{int}} = \sum_{i=1,j=0}^{\infty} \epsilon^{(ij)} \qquad (1)$$

where the corrections $\epsilon^{(ij)}$ are of the ith order with respect to the interaction, and of the jth order with respect to intramonomer correlation. In addition, $\epsilon^{(ij)}$ may be considered as composed of two physically different components, the polarization component and the exchange component:

$$\epsilon^{(ij)} = \epsilon^{(ij)}_{\mathrm{pol}} + \epsilon^{(ij)}_{\mathrm{exch}} \qquad (2)$$

The first component is the perturbation correction which arises in the "polarization approximation" that is in classic RS perturbation theory. The exchange effects are included in the second term, $\epsilon^{(ij)}_{\mathrm{exch}}$. A classification chart of various terms is given in Table 1. One can find there which components of $\epsilon^{(ij)}$ contribute to the particular fundamental energy contributions at the HF and correlated levels of theory. We begin with the polarization terms. At the HF level we obtain:

(1) $\epsilon^{(10)}_{\mathrm{es}}$—the electrostatic energy between HF monomers.[52,69,70] It describes the electrostatic interactions of the permanent multipole moments of the monomers computed in the HF approximation. It also includes the charge overlap terms which arise due to the overlap of the monomer electronic charge densities. They have a damping effect on the multipole terms.

(2) $\epsilon^{(20)}_{\mathrm{ind}}$—second-order induction energy (also referred to as uncoupled-Hartree–Fock (UCHF) induction).[71] It describes interactions between permanent and induced multipole moments resulting from the electric polarization of one monomer by the permanent moments of another monomer. The process is described within the HF approximation. Since the monomer electronic charge distributions are modified, damping charge overlap terms are also present.

(3) $\epsilon^{(20)}_{\mathrm{disp}}$—the second-order dispersion energy.[71,72] It results from quantum mechanical charge fluctuations (interactions of correlation-induced instantaneous electric moments). Similar to electrostatics and induction, it also includes charge overlap effects. Since this correlation is of the zeroth order in the intramonomer correlation operator, it is often referred to as the dispersion energy between Hartree–Fock monomers or uncoupled-Hartree–Fock (UCHF) dispersion.

(4) Higher order induction and dispersion interactions of HF monomers ($\epsilon^{(30)}_{\mathrm{disp}}$ and $\epsilon^{(30)}_{\mathrm{ind}}$, etc.).

At the correlated level one finds the correlation corrections to the above terms:

Table 1. Classification of I-MP Perturbation Theory Corrections

fundamental component	HF level	intracorrelated level	additive?
electrostatics	$\epsilon^{(10)}_{\mathrm{es}}$	$\epsilon^{(1j)}_{\mathrm{es}}(\epsilon^{(1j)}_{\mathrm{es,r}})$	yes
exchange	$\epsilon^{(10)}_{\mathrm{exch}}(\epsilon^{\mathrm{HL}}_{\mathrm{exch}})$	$\epsilon^{(1j)}_{\mathrm{exch}}$	no
induction	$\epsilon^{(20)}_{\mathrm{ind}}(\epsilon^{(20)}_{\mathrm{ind,r}})$	$\epsilon^{(2j)}_{\mathrm{ind,r}}(\epsilon^{(2j)}_{\mathrm{ind,r}})$	no
	$\epsilon^{(30)}_{\mathrm{ind}}(\epsilon^{(30)}_{\mathrm{ind,r}})$	$\epsilon^{(3j)}_{\mathrm{ind}}(\epsilon^{(3j)}_{\mathrm{ind,r}})$	no
and related exchange–induction terms			
dispersion	$\epsilon^{(20)}_{\mathrm{disp}}$	$\epsilon^{(2j)}_{\mathrm{disp}}$	yes
	$\epsilon^{(30)}_{\mathrm{disp}}$	$\epsilon^{(3j)}_{\mathrm{disp}}$	no
and related exchange–dispersion terms			

(1) $\epsilon_{es}^{(1j)}$—denote the intramonomer correlation corrections to the electrostatic term.[40,73] One may view this correction as the effect of correlating the permanent multipole moments. This results in modification of their Coulombic interactions. The charge overlap effects are also modified.

(2) $\epsilon_{ind}^{(2j)}$—denote the intramonomer correlation corrections to the induction term.[44] One may interpret them as a result of changes in the polarization process due to the correlation effects on the multipole moments and polarizabilities. The charge overlap effects are also modified.

(3) $\epsilon_{disp}^{(2j)}$—represent the terms which couple the intermonomer correlation effects and the intramonomer correlation effects.[36]

Next to some terms in Table 1, modified symbols are shown in brackets. They denote modified induction and electrostatic correlation corrections. An additional letter "r" stands for "response" and corrections marked with "r" sum the orbital relaxation terms through the infinite order.[74,75] The relaxation terms arise because the monomer HF orbitals have to readjust after the field of the partner monomer is switched on. The orbital relaxation terms are formally of a nonzero order with respect to the intramonomer correlation, yet they account for the effect which is still within the independent particle approximation. They present a better alternative since they are directly related to the supermolecular MP perturbation theory[40,41,43,44,75] (cf. section II.B) and correspond to the expressions for monomer properties that satisfy the Hellmann–Feynman theorem.[76]

The dispersion energy may also be calculated at an intermediate approximation as $\epsilon_{disp,RA}^{(2)}$.[77,78] This energy is sometimes referred to as the ring approximation dispersion energy[78] or the time-dependent HF (TDHF) dispersion energy.[79–84] The relation to the TDHF dynamic polarizabilities of monomers provides an argument for classifying $\epsilon_{disp,RA}^{(2)}$ as a better variant of Hartree–Fock dispersion interaction energy. Consequently, the difference between $\epsilon_{disp,RA}^{(2)}$ and $\epsilon_{disp}^{(20)}$ has been attributed to "apparent intramonomer correlation effects".[83,85,86] This interpretation has been criticized on the grounds that, unless the Casimir–Polder approach is used,[87] the real intramonomer correlation equations must be solved.[77,78]

According to eq 2, every polarization correction is accompanied by an exchange term. These terms are crucial to the convergence of the series of eq 1. This is because the polarization approximation provides a divergent expansion except for one- and two-electron monomers.[70,88] The exchange terms provide the necessary damping effects to force convergence of the series.[66,68]

The first-order exchange term, $\epsilon_{exch}^{(10)}$,[69,70] is interpreted as the result of the exchange of electrons (quantum mechanical tunneling) between unperturbed monomers described at the HF level. It is a very important term as it provides the necessary repulsion to properly balance attractive terms in the van der Waals minimum. In practical applications it is convenient to consider this term along with some minor terms of no physical interpretation, the so called "zeroth-order exchange" terms.[70,89] Then the name ϵ_{exch}^{HL} indicated in parentheses (Table 1) is used. By adding ϵ_{exch}^{HL} to $\epsilon_{es}^{(10)}$, the familiar Heitler–London interaction energy is obtained. The ϵ_{exch}^{HL} term is often referred to as the "exchange–repulsion" or "Heitler–London exchange". The ϵ_{exch}^{HL} term may be corrected for intramonomer correlation by allowing for higher order corrections with respect to the second index to produce $\epsilon_{exch}^{(1j)}$ exchange correlation corrections[90–92] (cf. Table 1).

There are two other exchange terms of interest which are only mentioned in Table 1. These are the exchange–induction and exchange–dispersion contributions. They represent the exchange effects that accompany the induction and dispersion terms, respectively.

In higher orders the perturbation expansion eq 1 branches out into a multitude of terms representing various couplings of several effects; for instance, an induction–dispersion–exchange term appears in the third order. Certainly, we need some insights into these complex, although in general, secondary terms. However, in practice a partitioning of the interaction energy would be useless if the number of these terms were too large. Therefore, application of the I-MP theory must involve a judicious choice of the most important terms to achieve a desired accuracy of the resulting interaction energy. The first results for a few van der Waals complexes are very promising and suggest that the theory may provide accurate interaction energies.

B. Insight into Supermolecular MP Perturbation Theory

In S-MP theory the interaction energy is defined as the difference between the energy of the total complex ("supermolecule") and constituent monomers. For instance, for a cluster ABC composed of three monomers: A, B, and C, the interaction energy is defined as

$$\Delta E = E^{ABC} - \sum_{X=A,B,C} E^{X} \qquad (3)$$

where E^{ABC} is the trimer energy and E^{X} denote monomer energies of X = A, B, and C. In S-MP the interaction energy is not expressed in the form of individual components as in the perturbation theory of intermolecular forces. The individual terms, such as electrostatic, induction, dispersion, and exchange are only implicitly and collectively reproduced in ΔE. To understand the behavior of such a mixture of physically different effects without decomposition into well-defined contributions is impossible. Fortunately, the intrinsic relationship between S-MP and I-MP perturbation formalisms enables us to identify various intermolecular contributions within the S-MP interaction energies. To simultaneously include both pair interactions and nonadditive effects in larger clusters let us consider the case of a trimer. At the ith order of S-MP perturbation theory, the total energy of the trimer ABC can be decomposed as[42]

$$E^{(i)}_{ABC} = \sum_{X=A,B,C} E^{(i)}_X + \sum_{X=A,B,C} \Delta E^{(i)}_X + \sum_{X>Y=A,B,C} \Delta E^{(i)}_{XY} + \Delta E^{(i)}_{ABC} \quad (4)$$

where (i) denotes a particular order of MP perturbation theory, but it could also represent any other size-consistent treatment of the correlation effects, such as coupled cluster (CC) theory. The second, third, and fourth terms describe, respectively, the one-, two-, and three-body contributions. The one-body term describes the effects of the geometry relaxation of subsystem X in the trimer. A two-body term $\sum\Delta E^{(i)}_{XY}$ describes the interaction between pairs of monomers, and the $\Delta E^{(i)}_{ABC}$ term represents the three-body contribution arising between the relaxed-geometry monomers arranged in the same way as they occur in the complex. Unless explicitly stated, we will consider no effects due to the relaxation of monomer geometries.

The expressions for the first four $\Delta E^{(n)}$ are given in Table 2.

The SCF interaction energy, ΔE^{SCF} is composed of already familiar HF electrostatic and exchange terms:[39]

$$\Delta E^{SCF} = \epsilon^{(10)}_{es} + \epsilon^{HL}_{exch} + \Delta E^{SCF}_{def} \quad (5)$$

A new term here is ΔE^{SCF}_{def}. It originates from the mutual induction effect. In contrast to perturbation $\epsilon^{(n0)}_{ind,r}$ terms, which describe classic induction, ΔE^{SCF}_{def} may be viewed as the quantum induction which includes exchange effects. Indeed, quantum mechanics does not allow monomer electronic densities to deform freely. Instead, the induction process must be subject to the Pauli exclusion principle. To better appreciate the content of ΔE^{SCF}_{def} and its physical interpretation, let us consider the situation where the exchange effects are absent. (It may be exemplified by the interaction of a molecule and a proton.[75]) Then ΔE^{SCF}_{def} may be represented as the infinite sum[75]

$$\Delta E^{SCF}_{def} = \sum_{n=2}^{\infty} \epsilon^{(n0)}_{ind,r} \quad (6)$$

However, if the exchange effects are present, the series becomes rapidly divergent.[75] More seriously, the polarization approximation leads generally to a qualitatively wrong description of the induction process. As pointed out by Gutowski and Piela[57] (cf. also[25,58,93]) the reason is the lack of enforcement of the antisymmetry principle which creates a possibility of nonphysical electron charge transfer. That is, whenever the redistribution of electrons among monomers provides an energy lowering, the induction process will carry out such a redistribution *regardless of the Pauli principle violation*. Gutowski and Piela advanced a convincing example of $He-Li^+$ interaction where the induction process carried through to infinity appears to remove electrons from the He atom to create the Li^- anion with four electrons at the valence 1s shell.

Table 2. The Relationship between S-MP and I-MP Perturbation Theories

order	supermolecular MP: $E_{int} = \sum\Delta E^{(i)}$	intermolecular MP: $E_{int} = \sum\epsilon^{(ij)}$
(0+1)	$\Delta E^{SCF} = \Delta E^{HL} + \Delta E^{SCF}_{def}$	$\Delta E^{HL} = \epsilon^{(10)}_{es} + \epsilon^{(10)}_{exch}$ $\Delta E^{SCF}_{def} = \epsilon^{(20)}_{ind,r} + \epsilon^{(30)}_{ind,r} + \ldots +$ exch−def
(2)	$\Delta E^{(2)}$	$= \epsilon^{(20)}_{disp} + \epsilon^{(12)}_{es,r} + \Delta E^{(2)}_{exch} + \Delta E^{(2)}_{def}$
(3)	$\Delta E^{(3)}$	$= \epsilon^{(30)}_{disp} + \epsilon^{(21)}_{disp} + \epsilon^{(13)}_{es,r} + \Delta E^{(3)}_{exch} + \Delta E^{(3)}_{def}$
(4)	$\Delta E^{(4)}$	$= \epsilon^{(40)}_{disp} + \epsilon^{(31)}_{disp} + \epsilon^{(22)}_{disp} + \epsilon^{(14)}_{es,r} + \Delta E^{(4)}_{exch} + \Delta E^{(4)}_{def}$

The only remedy is to enforce the antisymmetry condition at every step of the induction process. Formally, using the language of I-MP perturbation theory, we may write an improved version of eq 6

$$\Delta E^{SCF}_{def} = \sum_{n=2}^{\infty} \epsilon^{(n0)}_{ind,r} + \text{exch}-\text{def} \quad (7)$$

where "exch−def" stands for the exchange−deformation effects. So far neither a satisfactory definition nor evaluation of these effects has been achieved despite some interesting attempts,[57,94-96] and even practical applications of I-MP perturbation theory employ the SCF−deformation energy rather than any of the SAPT approximations.

Yet, the exchangeless second-order induction energy offers a useful approximation to ΔE^{SCF}_{def} provided it is always controlled against the latter. There is already some experience collected which can be summarized as follows:

(1) In general, $\epsilon^{(20)}_{ind,r}$ is close to ΔE^{SCF}_{def} in the region of the minimum (and further) of the PES at the HF level. (Applying this rule one should keep in mind that in the dispersion-bound complexes, if the minimum at the SCF curve occurs at all, it does not coincide with the true one.) If the $\epsilon^{(20)}_{ind,r}$ is evaluated with the basis set of the whole complex, it overestimates ΔE^{SCF}_{def}.

(2) In some cases $\epsilon^{(20)}_{ind,r}$ may be a particularly poor approximation to ΔE^{SCF}_{def}, even qualitatively. If the basis set allows for delocalization of electrons (i.e. one employs bond functions and/or the basis set of the dimer to describe the monomer) the unphysical charge transfer may take place. For instance, in the interaction of a chlorine anion with Ar, a substantial unphysical polarization of the negative ion is observed, which is attributed to the partial delocalization of a negative charge to Ar.

(3) If the multipole approximation of $\epsilon^{(20)}_{ind,r}$ is used, or if $\epsilon^{(20)}_{ind,r}$ is evaluated with enforcement of the localization of electrons at the monomers (e.g. by describing the monomer in its own basis set), the problem of an nonphysical charge transfer is circumvented, at least at the numerical level. However, the physical delocalization effects are also blocked, and consequently, the $\epsilon^{(20)}_{ind,r}$ term calculated in this manner usually underestimates ΔE^{SCF}_{def}.

(4) The uncoupled Hartree−Fock induction, $\epsilon^{(20)}_{ind}$, has similar properties to $\epsilon^{(20)}_{ind,r}$ and offers another

useful approximant of ΔE_{def}^{SCF}. It provides values of the induction effect which are smaller in magnitude.

In the second order, $\Delta E^{(2)}$, we see already familiar terms, such as the UCHF dispersion and the electrostatic–correlation:[39-41]

$$\Delta E^{(2)} = \epsilon_{disp}^{(20)} + \epsilon_{es,r}^{(12)} + \Delta E_{exch}^{(2)} + \Delta E_{def}^{(2)} \quad (8)$$

There are also the exchange and deformation terms, collected somewhat symbolically (their rigorous explicit forms are not known) within two terms: $\Delta E_{exch}^{(2)}$ and $\Delta E_{def}^{(2)}$. The first one gathers the exchange–correlation and exchange–dispersion effects. The second includes intramonomer correlation effects to the SCF deformation term ΔE_{def}^{SCF}. $\Delta E_{def}^{(2)}$ may be viewed as composed of the induction correlation terms ($\epsilon_{ind,r}^{(2j)}$ and $\epsilon_{ind,r}^{(3j)}$ in Table 1) along with exchange counterparts summed up to infinity.

The general expression for the nth order correction may be postulated (cf. also ref 42):

$$\Delta E^{(n)} = \epsilon_{es,r}^{(1,n)} + \sum_{i=0}^{n-2} \epsilon_{disp}^{(n-i,i)} + \Delta E_{def}^{(n)} + \Delta E_{exch}^{(n)} \qquad n = 2, 3, \ldots \quad (9)$$

where $\epsilon_{es,r}^{(1,n)}$ is the electrostatic correlation correction (which collects $\epsilon_{es,r}^{(1,0,n)}$ and $\epsilon_{es,r}^{(1,n,0)}$ related to the nth order intramolecular correlation at A and B, respectively[73]), and $\epsilon_{disp}^{(n-i,j)}$ are the dispersion correlation corrections, described in the previous section. $\Delta E_{def}^{(n)}$ represents the intra- and intermonomer correlation component to the deformation effect, and $\Delta E_{exch}^{(n)}$ represents the intramonomer correlation effects to the exchange–repulsion and exchange–dispersion effects.

C. Relation to Other Supermolecular Approaches

A partitioning of the interaction energy is very important, both from a theoretical point of view (we are able to understand the physics behind the numbers) and a practical point of view (we control much better the completeness and accuracy of a particular calculation). It is no surprise, then, that all serious supermolecular attempts to evaluate intermolecular forces strive to introduce some means of partitioning the interaction energy. Several methods introduce the decomposition of interaction energies in the framework of a localized-orbital approach in a more or less explicit form.[97-105] In this context we should mention two approaches which seem to be the most advanced and have been used for some time. These are the localized MP2 method[101,102] and the interacting correlated fragments (ICF) method.[97-99] Both are based on the idea of inter- and intramonomer correlation separation which is achieved through localization of molecular orbitals. In the localized MP2 approach ΔE^{SCF} is partitioned as shown in eq 5, and $\Delta E^{(2)}$ as follows:[101]

$$\Delta E_{AB}^{MP2\text{-}corr} = \Delta MP2^{A} + \Delta MP2^{B} + E_{AB}^{disp} \quad (10)$$

where $\Delta MP2^{A}$ and $\Delta MP2^{B}$ are the intramonomer correlation contributions and the E_{AB}^{disp} is the intermonomer energy contribution. The first two, besides the monomer correlation energy, contain the electrostatic and exchange correlation contributions. The deformation correlation effects are also expected to belong to these two terms. The third term corresponds to our $\epsilon_{disp}^{(20)}$ together with the exchange–dispersion term. The advantage of this approach, with respect to I-MP, is its complete and consistent dissection of the MP2 energy. There is some disadvantage in a less rigorous relationship with the theory of intermolecular interactions as the fundamental terms appear blended with their exchange counterparts.

D. Relation to Other Perturbation Approaches

An important variant of the ab initio perturbation theory of intermolecular interactions was developed by van der Avoird and Wormer.[106-110] Their formalism may be viewed as the *multipole-expanded* I-MP theory. Basically, the electrostatic and exchange terms are evaluated as in the I-MP theory. Furthermore, in calculations of the respective correlation corrections these authors adopt a similar philosophy as I-MP. The difference is that the induction and dispersion components are in the form of a truncated multipole expansion *a posteriori* damped by some model damping functions to avoid divergence of the multipole series. The advantages of this approach are (i) an explicit relationship with the multipole expansion of the interaction energy, (ii) an analytical form of the induction and dispersion terms and their intermolecular orientation dependence, (iii) individual van der Waals induction and dispersion coefficients are neither distance nor orientation dependent and may be obtained in a single ab initio calculation and with high accuracy. A certain drawback is an *ex post* model treatment of charge overlap and exchange effects. It should be stressed, though, that the theory is *open-ended*, and one can always replace less accurate components by some better approximations. The relationship to the I-MP theory may be very useful in this context. On the other hand, the I-MP theory may use the multipole-expanded results to better elucidate the physical origin of individual terms, and subsequently to use the multipole expansion to design analytical expressions.

E. Brief Characteristics of Methods

After outlining different ab initio methods, it is useful to underscore some of their major virtues and problems.

The attractive features of S-MP are as follows:

(1) It is size consistent at every level of the theory. That is, formally, the same amount of electron correlation is included in both the monomers and in the dimer.

(2) It is free of arbitrary choices and approximations.

(3) It covers the long, medium, and short ranges in a uniform way.

(4) If MP perturbation theory appears poorly convergent or divergent, extension to the fully complete and general CC technique is well defined and natural.

(5) It is easy to apply due to the wide availability of the state-of-the-art quantum chemistry codes.

However, the fact that the interaction energy is calculated indirectly causes some inconveniencies. Because of basis set effects, it is generally impossible to calculate monomer and dimer energies in eq 3 with a smaller error than the interaction energy. Therefore, one should ensure a consistent evaluation of the eq 3, which means a basis set consistent calculation of monomer and dimer energies. The basis set consistency requirements leads to the counterpoise technique to avoid the so-called basis set superposition error (cf. section III.A.1). Another problem is that S-MP alone offers little insight into the nature of the interaction. This drawback may be largely alleviated by parallel I-MP calculations, or by a localized MP2 approach.[100-102]

The I-MP perturbation theory is the most natural and elegant way of expressing the interaction energy which directly provides us with individual components. It should be stressed that without I-MP there would be little understanding of S-MP results. I-MP is also size consistent, and since the interaction energy is calculated directly, it is basis set consistent and does not require any counterpose corrections. The inconvenient side of the I-MP expansion is that it involves extra convergence problems of the expansion with respect to the interaction operator, combined with enforcing the Pauli principle. Because the convergence properties may vary from system to system, and there is some arbitrariness in the choice of higher order corrections, a comparison with the S-MP and/or S-CC results is often necessary and always useful. In fact, the state-of-the-art I-MP calculations employ the SCF interaction energy from S-MP rather than its SAPT approximation. We believe that one should view I-MP and S-MP as largely complementary, and the question as to which one is better has little foundation.

The problems with both approaches, supermolecular and intermolecular, begin when dealing with open-shell systems, transition states, and excited states which require multireference starting points. In these cases a single-reference MP perturbation theory is not a good choice, although it still may be efficient in some instances.

At this point, the CI-type methods, such as MR-SDCI[100] and ICF,[97,98] become very important. Whereas they do not seem to be competitive with MP perturbation theory and CCSD(T) as long as one deals with well-behaving closed-shell systems, they are necessary for open-shell ones. A major obstacle involved in these methods is the size-inconsistency problem which requires special corrections which are never exact. Moreover, the size inconsistency couples with basis set inconsistency and removal of the basis set superposition error becomes more involved. In contrast to S-MP perturbation theory, these methods are less transparent to a user. They require a great deal of expertise in configuration interaction techniques and in judicious choices of one-particle basis sets and configuration basis sets. A great success of this approach was a very accurate benchmark calculation of He_2.[98,100] High-quality results for alkaline earth metal dimers[111] should also be mentioned. Calculations for a system with many electron valence shells (the Ar dimer) have been less accurate so far.[112]

Table 3. Summary of Nonadditive Effects Arising in S-MP

order of S-MP	nonadditive I-MP term	n-body nonadditivity	asymptotic behavior	
			a	b
ΔE^{SCF}	$\epsilon_{exch}^{HL}\,\epsilon_{exch}^{(10)}$	3, 4, ..., n-body	e^{-aR}	
	ΔE_{def}^{SCF}	3, 4, ..., n-body	R^{-n}	e^{-aR}
$\Delta E^{(2)}$	$\Delta E_{def}^{(2)}$	3, 4, ..., n-body	R^{-n}	e^{-aR}
	$\Delta E_{exch}^{(2)}$	3, 4, ..., n-body	e^{-aR}	
$\Delta E^{(3)}$	$\epsilon_{disp}^{(30)}$	3-body	R^{-9}	
	$\Delta E_{def}^{(3)}$	3, 4, ..., n-body	R^{-n}	e^{-aR}
	$\Delta E_{exch}^{(3)}$	3, 4, ..., n-body	e^{-aR}	
$\Delta E^{(4)}$	$\epsilon_{disp}^{(40)}$	4-body	R^{-12}	
	$\epsilon_{disp}^{(31)}$	3-body	R^{-9}	
	$\Delta E_{def}^{(4)}$	3, 4, ..., n-body	R^{-n}	e^{-aR}
	$\Delta E_{exch}^{(4)}$	3, 4, ..., n-body	e^{-aR}	

[a] One of the subsystems has a permanent moment. [b] No permanent moments.

F. Ab Initio Theory of Nonadditive Effects

According to the perturbation theory of intermolecular forces, any nonadditive interaction is composed of three fundamental nonadditives: exchange, polarization, and dispersion. The relationship between S-MP and I-MP theories outlined above can easily be extended to nonadditive interactions if we keep in mind which I-MP corrections are additive (cf. Table 1). The perturbational contents of the S-MP nonadditive interaction energies are shown in Table 3. It is seen that all the fundamental nonadditivities are included if the S-MP calculations are carried out through the third order. Furthermore, such MP3 calculations will reproduce these nonadditivities at least at the HF level of theory (in case of dispersion nonadditivity it is UCHF level of theory). In trimers of rare gases, where the overall nonadditivity is largely determined by the dispersion effect, a more advanced treatment of dispersion which takes into account the inter−intra correlation coupling may be necessary (see below).

The exchange nonadditivity is perhaps the most difficult to interpret physically, as it results from the nonclassical exchange effect which may be related to overlap. It is known that in the interactions of three spherically symmetric species, such as rare gas atoms, the exchange nonadditivity is attractive in the configuration of the equilateral triangle and repulsive in the collinear-trimer configuration. This fact can be explained in terms of a different overlap in both cases. In an interacting pair of atoms, the electron clouds of individual atoms will modify to avoid overlap, and thus the electrons will be pushed out from the interatomic region. A third atom will experience less overlap when it approaches perpendicular to the bond formed by the other two (as in the configuration of a triangle), and more overlap if it approaches either of the terminal atoms as in the linear configuration. The first approach is energetically favorable (attractive) since it involves a reduced

overlap, and the second approach is energetically unfavorable, as it involves enhanced overlap.

When one rare gas atom in the trimer is replaced by a molecule, the behavior of the exchange nonadditivity is additionally complicated by the fact that the exchange effect is a function of the orientation of a molecule. In our calculations we have observed both positive and negative values of this nonadditivity and in some instances (e.g. Ar_2HCl, Ar_2HF, see below) the anisotropy of this component was found to be so strong that it controlled the orientation behavior of the entire three-body effect. To understand this type of orientational behavior one needs to analyze it in terms of some physical model. Cooper and Hutson,[117] following some earlier works of Jansen,[119,120] have suggested that this process can be split into two events. First, the avoidance of overlap of the two Ar atoms creates a quadrupole moment on the Ar_2 part of the cluster, the so called exchange quadrupole. Next, the exchange quadrupole can interact electrostatically with the dipole located at a polar molecule, for example. Indeed, the interaction of two Ar atoms produces a negative quadrupole moment, indicating that the electron density is pushed out from the region of the van der Waals bond. The interaction of the exchange quadrupole with the positive end of a dipole should be repulsive, and the interaction of the exchange quadrupole with the negative end of a dipole should be attractive. Such an interpretation is in the spirit of the Hellmann–Feynmann view of a chemical bond, from which it follows that the quantum effects (exchange effects in this case) govern the modifications of the charge distributions, but the bonding itself results from the classic electrostatic interaction of charge clouds. This model approach to exchange nonadditivity seems very promising, at least in some types of clusters.

The rigorous ab intio values of the three-body exchange term within our treatment involve the evaluation of the Heitler–London energy for the trimer and for all the pairs of monomers. The Heitler–London exchange nonadditivity is obtained as the energy difference. Since the electrostatic part of the HL energy is additive, the effect obtained in this manner contains only the exchange nonadditivity.

The polarization nonadditivity is much easier to interpret.[120] In the trimer, the field generated by one of the monomers modifies the charge distributions of the other two which in turn modify their mutual electrostatic interaction. Consequently, the polarization nonadditivity can be either attractive or repulsive, unlike the pair polarization which always leads to more stabilization. In the case of the three spherically symmetric atoms, the polarization nonadditivity has a purely nonclassical charge-overlap character. In the interactions involving a molecule with two Ar atoms, the field generated by multipole moments of a molecule induces moments on both Ar atoms. The induced moments can either attract or repell one another depending on their mutual orientations. An analytical modeling of such an effect can be accomplished via the multipole approximation, which should, at least in principle, provide a rough description of its anisotropy. In trimers composed of polar monomers the interpretation is even simpler: If a pair of monomers is allowed to polarize one another the field which the third monomer experiences is different from the combined fields of the two monomers in the pair.

An ab initio treatment of polarization nonadditivity is based on the fact that the orbitals of individual monomers undergo deformations due to the field of the other monomers. Only such deformations of orbitals are allowed, however, which do not violate the Pauli principle pertaining to the intermonomer electron exchanges; otherwise, the electrons of one monomer would try to occupy the already occupied orbitals of the others. In the supermolecular SCF calculations such modifications are carried out to self-consistency and the Pauli principle is automatically enforced. For this reason, this effect is called the SCF–deformation (ΔE_{def}^{SCF}) nonadditivity. Some nonexchange approximations to ΔE_{def}^{SCF}, which originate from the intermolecular perturbation theory, have been customarily used:[122,123]

$$\sum_{n=2} \epsilon_{ind}^{(n0)} \quad \text{and} \quad \sum_{n=2} \epsilon_{ind,r}^{(n0)}$$

In the first series the perturbed orbitals do not adjust to the remaining orbitals of the same monomer, while the second series includes orbital relaxation within monomers. Only the second series converges asymptotically to ΔE_{def}^{SCF}; it is thus a proper nonexchange approximation to ΔE_{def}^{SCF}.

The nonadditivity of dispersion energy has a straightforward interpretation in terms of the electrostatic interactions of instantaneous multipoles which result from the intersystem electron correlation. For this reason the leading term has been dubbed the triple dipole effect.[124] If three monomers are collinear, the arrangement of instantaneous dipoles is favorable and the term is attractive. If, however, the monomers are in the triangular configuration, the instantaneous dipoles induced by monomer A on B and C are in repulsive orientation. In the first approximation the three-body dispersion term can be evaluated using the three-body $\epsilon_{disp}^{(30)}$ correction which does not involve the multipole approximation. In such a treatment the multipole terms higher than the triple-dipole are also implicitly included along with the charge-overlap effects. This approximation corresponds to the UCHF level of theory which describes the interaction of the Hartree–Fock (i.e. uncorrelated) monomers. More accurate approaches to the dispersion nonadditivity which correspond to either partially or fully correlated monomers require highly correlated treatments[125] (see below).

III. Numerical Aspects

A. Bottleneck: Basis Set Problem

If it had not been for the basis set problem, a vast number of accurate ab initio potentials for the interactions of closed shell systems would have already been calculated. This is because the molecu-

lar electronic structure theory necessary for these calculations is already available, as outlined in previous sections. If applied at the high level, that is through fourth-order including triple excitations (either within I-MP or S-MP frameworks), it is efficient enough to provide the interaction energy accurate within a few percent. A few cases for which the MP4 treatment seems to be insufficient are discussed later in section III.B.

There are two main aspects of the basis set problem. The first is universal for any approach: to obtain reasonable results one must employ an extended basis set which satisfies the demands of molecular properties and interaction energy, not just those of the total molecular energy. These demands largely depend on the physical nature of the interaction considered. In H-bonded complexes, or in clusters involving polar or ionic species, the major concern is the electrostatic energy which requires a proper description of the lowest multipole moments and of charge overlap effects. In interactions of ions with nonpolar molecules or atoms, one of the dominant effects is the induction energy (related to lower multipole polarizabilities) which encompasses the charge-transfer effects. Finally, in the dimers of rare gases the dispersion energy serves as the major attractive contribution. This term is the most difficult to reproduce since it is a pure correlation effect. Certainly, all interactions involve the exchange energy, which provides the repulsion necessary to create the attraction−repulsion equilibrium in the van der Waals region and is sensitive to the outer regions of the wave function, sometimes referred to as the "tail". Therefore, a judicious choice of a basis set should be based on a faithful description of the multipole moments, static and dynamic multipole polarizabilities, and the electron density at long distances.

Second, any supermolecular calculation of the interaction energies involves the so-called basis set extension effect—BSE effect. That is, a calculation of the energy of the entire complex reproduces the energy of a constituent monomer within the basis set of the *entire complex* rather than within the *monomer's* basis sets. The difference between the monomer energy obtained with its own basis set (monomer-centered basis set, MCBS) and the basis set of the entire cluster (e.g. dimer- or trimer-centered basis sets, DCBS or TCBS) is usually large—on the order of the interaction energy itself. This leads to an apparent inconsistency involving the subtraction of energies obtained with different basis sets in eq 3. The basis set extension effect on the monomer energies is termed the basis set superposition error (BSSE).[24,25,126-130]

1. Basis Set Superposition Error

To remedy the above-mentioned inconsistency all the energies in eq 3, i.e. those of monomers and that of the dimer, should be derived within the same basis set. The prescription formulated by Boys and Bernardi,[131] called "counterpoise procedure"; states that if the interaction energy is obtained as the difference of the dimer and the monomer energies, all the energies should be evaluated within the same basis of the whole dimer. This prescription is quite obvious since it requires that the dimer and the monomers be treated in the basis set consistent way. After all, if we weigh a bucket of potatoes the weight of the bucket should be fully subtracted to get the weight of the potatoes. The problem is that the calculated interaction energies are often too small in magnitude, and the counterpoise correction makes them even smaller. So, instead of choosing a superior basis set, we are tempted to blame the counterpoise procedure that it somehow overcorrects the interaction energy (as if, continuing the "potato analogy", we tried to manipulate the weight of the bucket instead of adding more potatoes to earn a better price).

There are essentially two well-established arguments in favor of the counterpoise technique. First the uncorrected results often reveal nonsensical features which disappear when the CP correction is applied. The CP corrected results are generally more stable with respect to basis set effects.[43,129,132-136] However, neither the basis set stability nor the proximity to an accurate result should serve as satisfactory proofs. Much more persuasive is the second argument which stems from the relationship between I-MP interaction energies and the S-MP results. Only the CP-corrected S-MP values were shown to agree quantitatively with the I-MP results which are free from BSSE. The examples of such an agreement have been provided in refs 25, 39, 43, 127, 128, and 130. (See also van Duijneveldt et al. in this volume, ref 137.) Some of the most convincing results have been presented in ref 43. It is unfortunate that the perturbational arguments in favor of the CP technique are tacitly disregarded by many of the participants in the "BSSE debate".

Some researchers are still not satisfied with the CP method.[138-141] They dispute the fact that the interaction energy contained in the supermolecular energy is related to the DCBS description of monomer wave functions and their deformations (caused by induction, dispersion, and exchange effects). For example, the electrostatic energy corresponds to monomer wave functions described in DCBS, and is thus related to multipole moments obtained with DCBS. Since DCBS consists of the basis sets located at both monomers, the DCBS symmetry is different from that of the monomer symmetry. With good basis sets such a nonphysical basis set extension is insignificant and sometimes beneficial. In poor basis sets, however, this effect may lead to serious distortions (see the next section). For this reason the basis set extension effect on the electrostatic energy was termed the secondary basis set superposition error.[142]

Certainly, a basis set extension affects other properties of the interacting systems, not just the electrostatic energy, and it can be defined as a difference between the DCBS and MCBS values of this property.[25] It has been argued that it is desirable to eliminate basis set extension effects on the selected properties. One suggested approach of this type completely eliminates these effects on all the properties, including the interaction energy.[143] As it turns out, such a method yields inferior interaction energies in comparison to the standard CP method. For example, a proper description of the induction effect requires the inclusion of the charge delocalization

effects (charge-transfer effects). These effects are facilitated by the presence of the basis set on the other monomer.

Alternative treatments attempt to prevent the monomers from using the partner's basis set only when they are unperturbed, but permit them to do so once the deformation of the wave function is switched on.[138-140] So far these attempts have been only partly successful. The question remains whether such a selective treatment of basis set extension effects is well defined. It should be stressed that the DCBS approach is almost always beneficial, with the one exception of the electrostatic energy calculated with poor basis sets. The benefits outweigh the shortcomings, so even the I-MP calculations which are free from BSSE are routinely carried out with DCBS[36-38,92] and not with MCBS.

Another unconventional definition of BSSE has recently been proposed by Davidson and Chakravorty.[144] It views BSSE as a difference between the monomer energy obtained with the complete basis set and the monomer energy calculated with the basis set deprived of the partner's basis set. This definition lumps together two qualitatively different things, such as *errors in monomer energies*, and *deficiencies within the description of energy components*. From a practical point of view this approach does nothing to address the real issue which is: What is the proper interaction energy within a limited basis set?

A more thorough discussion of the basis set effects can be found in a recent review by Gutowski and Chałasiński[127] and in previous reviews.[24,25,145] At this point it is worthwhile to summarize the experience in this area:

(1) The interaction energies should always be calculated via the CP procedure. Even if the uncorrected energies seem better, they are meaningless.

(2) The magnitudes of CP correction must not be used to judge the quality of the interaction energy since they are in no way related to the error in the interaction energy.

(3) If the calculated interaction energy is not satisfactory, one must improve the basis set. The quality of the interaction energy components, rather than the magnitude of BSSE correction, should guide such improvements.

(4) If the monomer geometries are distorted in the course of dimer formation (e.g. bond lengths change, or angular deformations of monomers occur), one should first calculate the interaction energy with respect to deformed monomers, properly accounting for the CP correction. Next, the distortion energies of monomers should be calculated (either with MCBS or DCBS) and added to obtain the interaction energy between undistorted monomers.

There are, however, some instances where it is convenient to use a basis set which does not produce a large BSSE. The gradient optimization techniques are routinely coded without the CP corrections, so if these techniques are used, it is desirable that the BSSE correction to the energy gradient be small. Sometimes it is not clear how to apply the CP procedure, because the separation of the complex into monomers is not unique.[146,147] This is the case of transition states, reaction intermediates, and strongly bonded species, which may dissociate in a number of ways. Finally, in the case of size-inconsistent methods (e.g. MR-SDCI) the counterpoise technique is not straightforward and debatable.[98-100].

2. Choice of Basis Set

The majority of basis sets available in the literature are not readily applicable to the intermolecular interaction problems. This is because their optimization is focused on the lowering of the total atomic, ionic, and/or molecular energies, whereas the interaction energy is related to monomer properties (multipole moments and polarizabilities). In addition, the interaction energy is sensitive to the "tail" region of the wave function, a region of secondary importance to the total energy. A proper basis set must satisfy the demands of all four fundamental interaction energy components, such as electrostatics, induction, dispersion, and exchange. These demands may overlap to some extent, but in general they are not identical. A thorough discussion of the basis set dependence of the total interaction energy in the context of the basis set effects on its components was given in ref 41. Below, we will extend this discussion by including some of the most frequently used basis sets and by applying the same model, the equilibrium HF dimer. To this end, the interaction energy and its components have been evaluated for several commonly used basis sets of increasing size from 3-21G to 6-311G(2df,2pd).[45] The popularity of these basis sets stems from the fact that they are internally stored in the Gaussian-type programs. They are often referred to as standard basis sets. There is, however, nothing standard about them. The interaction energy components were derived within the DCBS and MCBS frameworks. It should be reiterated that the DCBS values of these components are implicitly reproduced in the S-MP interaction energies. The MCBS values are of interest in determining the magnitude of basis set extension effects on individual energy contributions. The basis set extension effect is defined as the difference between the DCBS and the MCBS values. To gauge the accuracy of the different terms we use accurate results obtained with large well-tempered polarized basis set (see ref 41 for details) augmented with bond functions (see below). The results are presented in the form of plots in Figures 1-5.

a. Electrostatic Energy. The electrostatic energy at the SCF level (Figure 1) and at the correlated level (Figure 2) is a very unstable term. At the SCF level, prior to approaching the best basis sets result, both the MCBS and the DCBS values oscillate around it. The MCBS results are better only for the 6-31G** basis set and the smaller ones. For larger basis sets, both the MCBS and the DCBS results are of comparable quality. It is worthwhile to note that the inclusion of diffuse functions (indicated by "+") considerably decreases the MCBS-DCBS difference. One important conclusion is that the basis set dependence of the total CP-corrected SCF interaction energy closely follows the basis set dependence of the electrostatic energy calculated with DCBS. The uncorrected SCF results, on the other hand, do not reflect behaviors of either the MCBS or the DCBS

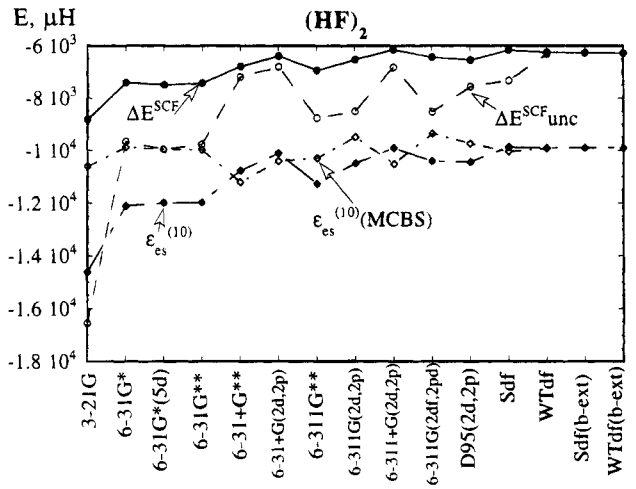

Figure 1. Basis set dependence of the total SCF interaction energy (CP-corrected, ΔE^{SCF}; CP-uncorrected, ΔE^{SCF}unc) and electrostatic component derived with DCBS ($\epsilon_{es}^{(10)}$) and MCBS ($\epsilon_{es}^{(10)}$(MCBS)) for $(HF)_2$ in equilibrium geometry of ref 186.

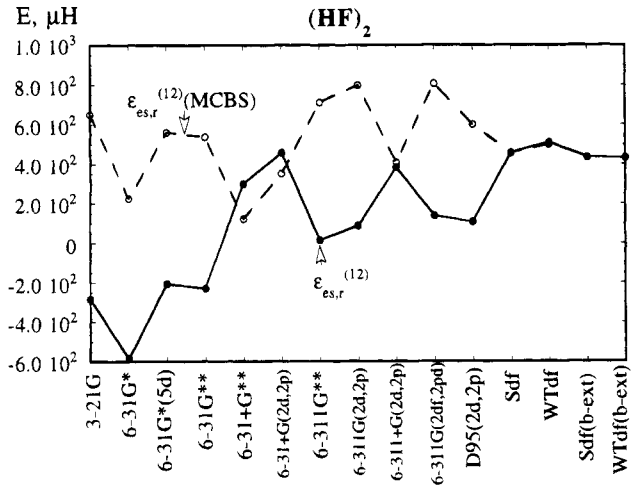

Figure 2. Basis set dependence of electrostatic correlation component derived with DCBS ($\epsilon_{es,r}^{(12)}$) and MCBS ($\epsilon_{es,r}^{(12)}$(MCBS)) for $(HF)_2$ in equilibrium geometry of ref 186.

electrostatic energies. At the correlated level the electrostatic interaction is represented by $\epsilon_{es,r}^{(12)}$, which is also very sensitive to the basis set (see Figure 2). The MCBS and the DCBS results are widely scattered except for those with diffuse functions. The latter reveal the small MCBS–DCBS differences and more quickly approach the largest basis set result.

b. Induction Energy. The SCF induction contribution can be described either as $\epsilon_{ind,r}^{(20)}$ or ΔE_{def}^{SCF}. So far the experience has been that this term, if evaluated with DCBS, saturates quickly (see Figure 3), and has little effect on the basis set dependence of the SCF interaction energy. The use of MCBS makes the induction effect grossly underestimated and basis set dependent. Moreover, it provides a worse approximation of ΔE_{def}^{SCF} than DCBS. In the case of induction the DCBS–MCBS difference is sometimes used to estimate the size of charge-transfer effects. The problem is that this difference is strongly basis set dependent and cannot be rigorously defined. The perturbation induction terms suffer from yet another

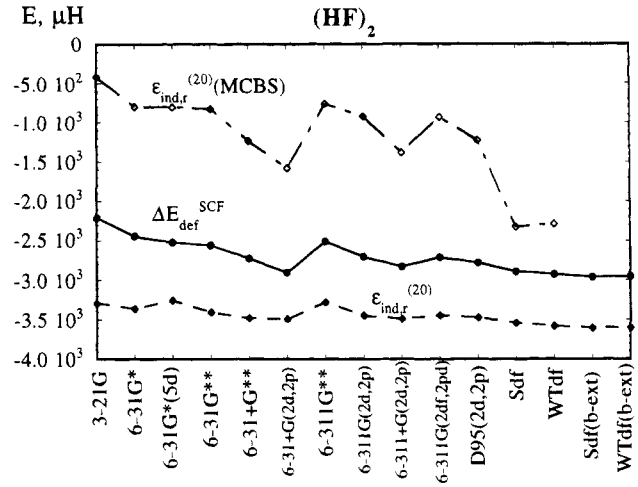

Figure 3. Basis set dependence of the SCF-deformation energy (ΔE_{def}^{SCF}) and induction components derived with DCBS ($\epsilon_{ind,r}^{(20)}$) and MCBS ($\epsilon_{ind,r}^{(20)}$(MCBS)) for $(HF)_2$ in equilibrium geometry of ref 186.

shortcoming discussed in section II.B. In view of the fact that the Pauli principle is not imposed, the induction energy may reveal an *unphysical charge transfer*; i.e. the electrons may flow to the partner's occupied space, violating the antisymmetry condition.[57] This effect is insignificant in MCBS since a finite monomer-centered basis set tends to effectively localize the electrons within the monomers. DCBS, on the other hand, facilitates the shifting of charge. In such cases the $\epsilon_{ind,r}^{(20)}$ terms calculated in DCBS may serve as a poor approximation to ΔE_{def}^{SCF}. To summarize, MCBS leads to the induction energies which are too small and too basis set dependent, while DCBS may cause a charge transfer which is physically forbidden. It should be reiterated that ΔE_{def}^{SCF}, which is reproduced in DCBS, and is subjected to Pauli principle, is free from the abovementioned drawbacks (cf. also section II.B).

The induction correlation terms (not shown in Figure 3b) are substantially smaller than $\epsilon_{ind,r}^{(20)}$ and reveal a similar behavior. The MCBS values are unstable with respect to basis set variations, and consistently smaller than the DCBS values.

c. Dispersion Energy. The dispersion energy (see Figure 4) has very high basis set demands which are difficult to satisfy. It requires polarization functions from low up to high angular quantum numbers. From a practical standpoint, the convergence slows down when the angular symmetry increases. In the same time, the technical difficulties associated with handling large number of basis functions rapidly rise.[148,149] Its behavior with respect to basis set differs from that of the electrostatic energy in that the dispersion energy is almost always too small in magnitude. Fortunately, the lack of higher polarization functions may be partly compensated by the basis set extension effect. That is, dispersion energies are vastly superior in DCBS than in MCBS.

d. Exchange Energy. The exchange contribution ϵ_{exch}^{HL} is relatively easy to reproduce with a reasonable set describing the occupied monomer orbitals (cf. Figure 5). The problems associated with a too rapid decay of Gaussian orbitals is circumvented by using

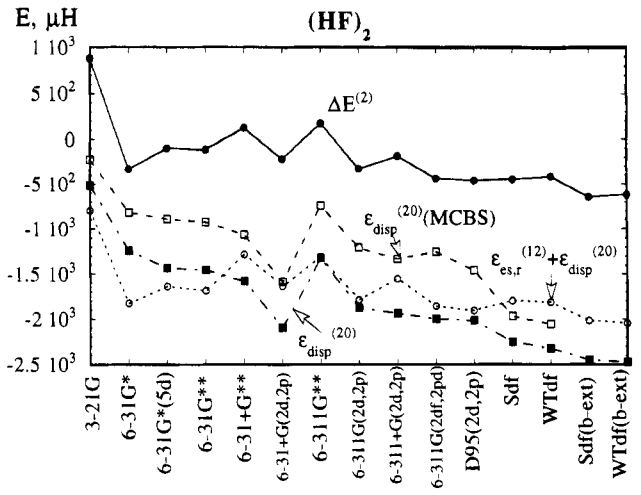

Figure 4. Basis set dependence of the second-order S-MP term ($\Delta E^{(2)}$) and the dispersion component derived with DCBS ($\epsilon_{disp}^{(20)}$) and MCBS ($\epsilon_{disp}^{(20)}$(MCBS)) for $(HF)_2$ in equilibrium geometry of ref 186.

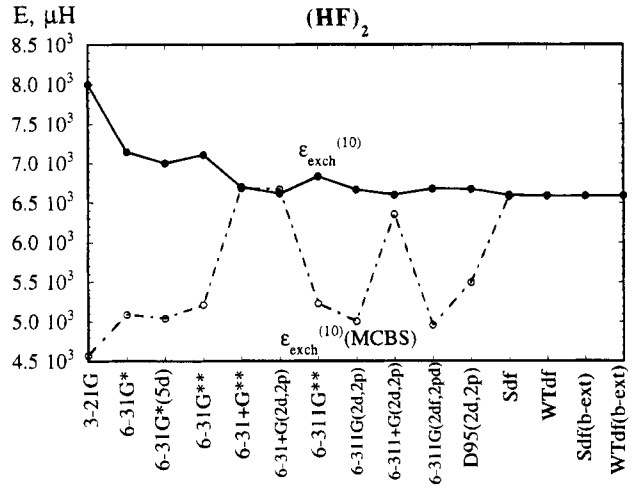

Figure 5. Basis set dependence of the HL exchange component derived with DCBS ($\epsilon_{exch}^{(10)}$) and with MCBS ($\epsilon_{exch}^{(10)}$(MCBS)) for $(HF)_2$ in equilibrium geometry of ref 186.

Table 4. Recommended Exponents of Polarization Functions Optimized for Dispersion Energy in the Following Molecules Interacting with He

	CH_4	NH_3	H_2O	H_2S	HF	HCl
f	C: 0.11[a]	N: 0.17	O: 0.18	S: 0.1	F: 0.275	Cl: 0.15
d (H)	0.12		0.18	0.15	0.075	0.15

[a] The *f*(C) exponent optimized for CO is equal to 0.258.

DCBS. It is also seen that the use of MCBS yields inadequate exchange energies. Higher order exchange terms, such as exchange correlation and exchange–dispersion, are also better described in DCBS, cf. ref 150 and 151, respectively. The higher order exchange effects may be collectively approximated by the difference (cf. eq 8):[40,41]

$$\Delta E_{exch}^{(2)} + \Delta E_{def}^{(2)} = \Delta E^{(2)} - (\epsilon_{es,r}^{(12)} + \epsilon_{disp}^{(20)}) \quad (11)$$

In contrast to $\epsilon_{es,r}^{(12)}$ and $\epsilon_{disp}^{(20)}$, this difference is very stable with respect to basis set variations.

To summarize, all terms, except for the electrostatics with poor basis sets (up to 6-311G**), are better reproduced by DCBS. This is automatically granted in the supermolecular approach and is a usual choice in I-MP calculations. "Standard" basis sets should be considered as inappropriate, and if they accidentally provide good results, this is due to a fortuitous cancellation of errors.

Two general regularities pointed out in ref 41 are also worth emphasizing. First, the total SCF interaction energies basis set effects closely follow the basis set effects on the electrostatic term (cf. Figure 1). Second, the total $\Delta E^{(2)}$ correlation basis set effects are practically determined by the basis set effects on both the dispersion and electrostatic correlation components (cf. Figure 4).

e. Efficient Medium-Sized Basis Set. The above discussion rationalizes a general recommendation for an efficient medium basis set. The basis set should be of at least DZ or TZ quality, contain diffuse valence orbitals, and also include diffuse polarization functions which are capable of reproducing the multipole moments and polarizabilities, as well as a significant portion of the dispersion energy. For atoms with occupied sp sets, this means that two d-type orbitals and one f-type orbital are needed. The two p and one d symmetry orbitals should be used for hydrogen. Several selections have been proposed in this context.[24,152–156] Our experience is that the Sadlej's medium-sized polarized basis set[155] offer the best choice. The first set of polarization functions in these basis sets is obtained as two contractions of four primitives. We recommend that they be augmented with one set of f symmetry orbitals on heavy atoms and one set of d symmetry orbitals on hydrogens. (In Table 4 we show the recommended values of the f exponents for some first- and second-row atoms for use with Sadlej's basis sets.) This prescription economizes on polarization functions that are necessary to describe the intramonomer correlation effects, and usually have much higher exponents than those needed for dispersion energy. There is good reason for such a strategy. In the dispersion-dominated complexes these spdf-type basis sets yield interaction energies which are some 15–25% too small. The reason for this underestimation is *not* the intramonomer correlation, but the extremely slow convergence of angular expansion of the dispersion energy.

In Tables 5–7 we provide some illustration of the above trends for the three model systems: Ar_2, ArHCl, and $(HF)_2$. These systems differ in the nature of their interactions. Ar_2 is purely dispersion bound. Ar–HCl is primarily dispersion bound with a considerable induction component. $(HF)_2$, a typical H-bonded complex, is predominantly electrostatic. One can see that the above strategy, without f functions centered at heavy atoms, provides only qualitative results for Ar_2 and ArHCl (the interaction energies at the MP4 level represent, respectively, only 50% and 60% of the accurate interaction energies). The inclusion of f symmetry functions provides a substantial improvement (ca. 80%), and we may consider these results as quantitative approximations. Similar changes, although smaller, are observed for $(HF)_2$ in its dispersion part. The total interaction energy in the latter case is dominated by the electrostatic effect at the SCF level and thus is

Table 5. Partitioning of the MP4 Interaction Energy (in μH) of Ar_2 (R = 7.5 a_0) (All Electron Calculations Unless Stated Otherwise)[a]

	spd	spdf	spdf(b-ext)	
		MP2 Results		
ΔE^{SCF}	196.9	196.7	194.0	
$\Delta E^{(2)}$	−450.0	−559.6	−624.0[b] −631.3	
$\Delta E(2)$	−255.1	−362.9	−429.9[b] −437.3	
		SCF Decomposition		
ϵ_{exch}^{HL}	−83.1	−83.0	−83.7	
$\epsilon_{es}^{(10)}$	291.1	291.4	290.2	
ΔE_{def}^{SCF}	−11.1	−11.8	−12.5	
$\epsilon_{ind,r}^{(20)}$	−94.9	−95.0	−96.6	
		$\Delta E^{(2)}$ Decomposition		
$\epsilon_{es,r}^{(12)}$	−22.1	−23.3	−36.5	
$\epsilon_{disp}^{(20)}$	−499.9	−614.3	−670.3	
$\Delta E_{exch}^{(2)}$	72.0	78.0	75.5	
		Higher-Order Terms		
$\Delta E^{(3)}$	87.6	85.7	85.9[b]	
$\Delta E_{SDQ}^{(4)}$	1.4	1.5	1.7[b]	
$\Delta E^{(4)}$	−42.4	−63.7	−76.4[b]	
$\Delta E(4)$	−207.8	−338.6	−420.4[b]	CCSD(T): −421.1[b]
$\Delta E(4)$ (R = 7.15 a_0)			−452.9[b] −468.3	
experiment[c]			−413.7	
		Other Results		
$\Delta E(4)$/t-aug-cc-pVQZ′ (R = 7.1 a_0)			−431.2[b,e]	
CCSD(T)/t-aug-ee-pVQZ (R = 7.1 a_0)			−418.1[b,e]	
experiment[d]			−453.5	

[a] The spd and spdf basis sets were taken from ref 180. The spdf(b-ext) is the spdf basis set augmented with a set of bond functions [3s3p2d1f] from ref 169a, located in the middle of the van der Waals bond. [b] Frozen-core result. [c] From the potential of Tang and Toennies,[182] quoted after ref 180, R = 7.5 a_0. [d] From ref 181 at R = 7.1 a_0. [e] From ref 164.

easier to reproduce with better accuracy.

f. Efficient Extended Basis Set. To get a smaller error in dispersion-bound complexes, of the order of 5%, we must first circumvent the slow convergence of the dispersion energy with respect to increasing symmetries of the polarization functions. However, at this level of accuracy one should also consider other factors such as: (i) basis set saturation of intramolecular correlation effects; (ii) higher order correlation effects, above the MP4 level of theory; (iii) role of inner shells, in particular, the core−valence correlation; and (iv) role of relativistic effects.

In this section we are primarily concerned with the basis set problem which is the most important. The basis sets appropriate for highly accurate benchmark calculations are the well-tempered sets of Huzinaga et al.,[157−159] the consistently correlated basis sets of Dunning et al.,[160] and the atomic natural orbitals of Almlöf and Taylor.[161,162] The energy-optimized sets of Partridge should also be mentioned.[163] However, even the largest basis sets from the above list must be supplemented by additional sets of diffuse polarization functions of high angular quantum numbers specially designed to saturate the dispersion term. In the benchmark He_2 calculations,[99,101,129] a balanced sequence of basis sets composed of intracorrelation and intercorrelation parts was used.[129] The same philosophy was pursued in calculations of the rare gas dimers by Woon[164,165] who employed the consistently correlated basis sets to saturate the intramonomer correlation and an additional systematic sequence to saturate dispersion. A similar attempt for the water dimer by Feller could not reach large enough basis sets to achieve results of a comparable quality.[166]

Such large basis set calculations can be performed for only a few small model systems. Fortunately, it is possible to achieve the ±5% level of accuracy by a small but very specific enlargement of the basis set which aims at overcoming the prohibitively slow convergence of the dispersion term. The enlargement includes the so-called bond functions.[100−102,149,167−170] The bond functions are usually located at the center of the van der Waals bond, although their positions may be varied to improve performance. We find that the effect of the bond functions is not strongly dependent on their location. The extreme efficiency of these functions is demonstrated in two examples, Ar_2 and ArHCl (Tables 5 and 6). The spdf-type basis sets, augmented with an extended set of bond functions from ref 169, yield the binding energies which are very close to the accurate values (101% and 105% of the accurate values for Ar_2 and ArHCl, respectively). The major cause of this improvement is rapid saturation of the dispersion term. However, rather important negative increments are also seen for the electrostatic correlation term (it is of a purely charge-overlap character). The changes of the other terms are less significant. Similar trends in the dispersion energy are observed for $(HF)_2$ (Table 7).

The bond functions seem to provide the dispersion term with a missing component which is otherwise difficult to reproduce. They improve a description of the dispersion effect half way between the interacting systems. This region is particularly difficult to describe using atom-centered basis sets, since the

Table 6. Partitioning of MP4 Interaction Energy (in μH) for Linear Configuration of Ar–HCl at R = 7.8888 a_0 (all Electron Calculations Unless Stated Otherwise)[a]

	spd[a]	spdf'[b]	spdf'(b-ext)	WTdf(b-ext)[c]
		MP2 Results		
ΔE^{SCF}	272.2	237.7	250.1	252.0
$\Delta E^{(2)}$	−826.6	−972.9	−1108.3	−1086.5
$\Delta E(2)$	−556.7	−735.1	−858.3	−834.5
		SCF Decomposition		
$\epsilon_{es}^{(10)}$	−163.2	−176.3	−165.9	−169.7
ϵ_{exch}^{HL}	733.5	730.3	735.7	739.3
ΔE_{def}^{SCF}	−298.1	−316.3	−319.8	−317.6
$\epsilon_{ind,r}^{(20)}$	−394.1	−409.9	−412.4	−407.9
		$\Delta E^{(2)}$ Decomposition		
$\epsilon_{es,r}^{(12)}$	−7.4	−18.0	−86.1	−67.0
$\epsilon_{disp}^{(20)}$	−926.6	−1060.1	−1120.8	−1126.4
$\epsilon_{ind,r}^{(22)}$	−41.3	–	−45.5	−38.1
$\Delta E_{exch}^{(2)}$	107.4	105.2	98.6	106.5
		Higher-Order Terms		
$\Delta E^{(3)}$	159.0	163.3	175.2	171.2
$\Delta E_{SDQ}^{(4)}$	14.1	14.3	14.6	23.9
$\Delta E^{(4)}$	−88.5	−120.0	−138.3	−132.1
$\Delta E(4)$	−484.0	−691.9	−821.4	−795.4
semiempirical[d]				−801.8 ± 14.0

[a] The spd and spdf' basis sets were taken from ref 183. The spdf'(b-ext) is the spdf' basis set augmented with a set of bond functions [3s3p2d] from ref 169a, located in the middle of the Ar–H distance. The WTdf(b-ext) basis is the well-tempered basis from ref 122 augmented with the same set of bond functions. [b] From Chałasiński et al., ref 183. [c] Frozen-core. [d] From Hutson, ref 184.

basis set expansion suffers from prohibitively slow convergence typical for expanding a function at one center in terms of basis set located at some remote center.

The application of bond functions presents some new problems. Because they represent an ansatz, which is specific for dispersion, their effect on the other interaction energy terms should be controlled. As discussed above, only the electrostatic energy is prone to distortion. Therefore, bond functions should be optimized under the constraint that they do not distort the SCF electrostatic energy.[101,102,162] Our experience is that one should additionally monitor the electrostatic correlation term, $\epsilon_{es,r}^{(12)}$, which is extremely basis set dependent. Fortunately, the dispersion energy is, to a large extent, insensitive to choice and location of bond functions which makes the above conditions easier to satisfy.

The single-point calculations with bond functions almost always yield considerably improved interaction energies which often match, or surpass, the empirical accuracy.[100–102,149,167–170] However, calculations for different points at the PES require a basis set consistent treatment to correctly predict the anisotropy of the interaction. There are geometries for which the "middle of van der Waals bond" seems to be easy to decide (for instance the T-shaped Ar–Cl_2 complex or the linear Ar–Cl_2 complex), but there are also geometries where it is not clear (a T-shaped-planar Ar–H_2O complex). These problems should be addressed to make bond functions even more useful.

Table 7. Partitioning of the MP4 Interaction Energy (in μH) of $(HF)_2$ (Optimized Geometry of ref 186; All Electron Calculations Unless Stated Otherwise)[a]

	S[b]	Sdf[b]	Sdf(b-ext)[c]	WTdf(b-ext)[c]
		MP2 Results		
ΔE^{SCF}	−6041	−6154	−6272	−6272
$\Delta E^{(2)}$	−276	−441	−641	−616
$\Delta E(2)$	−6317	−6595	−6913	−6888
		SCF Decomposition		
$\epsilon_{es}^{(10)}$	−9800	−9863	−9900	−9907
ϵ_{exch}^{HL}	6581	6598	6589	6591
ΔE_{def}^{SCF}	−2823	−2889	−2961	−2956
$\epsilon_{ind,r}^{(20)}$	−3484	−3539	−3602	−3602
		$\Delta E^{(2)}$ Decomposition		
$\epsilon_{es,r}^{(12)}$	442	457	436	430
$\epsilon_{disp}^{(20)}$	−2054	−2251	−2449	−2472
$\epsilon_{ind,r}^{(22)}$		−827	−808	−800
$\Delta E_{exch}^{(2)}$	1336	1353	1372	1426
		Higher-Order Terms		
$\Delta E^{(3)}$	−69	−98	−129[b]	−165
$\Delta E_{SDQ}^{(4)}$	244	233	222[b]	247
$\Delta E^{(4)}$	146	105	70[b]	111
$\Delta E(4)$	−6240	−6587	−6972[b]	−6942[c]
CCSD(T)			−7085[c]	
experiment[d]				−7116

[a] S denotes the medium-size polarized basis set.[155] Sdf is augmented with one d symmetry orbital at H and one f symmetry orbital at F.[41] Sdf(b-ext) includes a set of bond functions [3s3p2d1f] from ref 169a located in the middle of the van der Waals bond H–F. WTdf(b-ext) is the well-tempered basis set of ref 41, polarization functions and bond functions are the same as in Sdf(b-ext). [b] Frozen core approximation. [c] The effect due to relaxation of geometry of monomers is of the order of 5 μH. [d] The experimental result obtained by Quack and Suhm (ref 187) from the data of Miller (ref 188). [e] From Burcl et al., ref 185.

B. Convergence of Supermolecular MP Perturbation Theory

The question of the convergence of S-MP perturbation theory is of utmost importance to the practical calculations of interaction energies. The efficient perturbation expansion must be convergent. It should also recover the major portion of the interaction energy through the second order, and provide accurate results through the fourth order. The behavior of correlation corrections, $\Delta E^{(2)}$, $\Delta E^{(3)}$, and the components of $\Delta E^{(4)}$ ($\Delta E_{SDQ}^{(4)}$, etc.), should always be carefully examined. If the signs and magnitudes of these corrections raise doubts about the convergence of the whole series (for instance $\Delta E^{(2)}$ is not dominant, $\Delta E^{(4)}$ is much larger than $\Delta E^{(3)}$), it is recommended to check the $\Delta E_{SDQ}^{(4)}$ and $\Delta E_{SDTQ}^{(4)}$ results against the CCSD and CCSD(T) calculations. The better they agree, the better the convergence of MP perturbation theory is expected. If they disagree, MP perturbation theory may still provide a reliable estimate of the interaction energy, but one is advised to make an extra effort to understand why it is so.

van der Waals complexes, Ar_2 (Table 5), ArHCl (Table 6), and $(HF)_2$ (Table 7), exemplify a desired behavior of the MP perturbation theory series. Basically, the MP4 level of theory provides an accurate estimate of D_e which is slightly refined at the CCSD-

Table 8. Convergence of the S-MP Interaction Energies in Dimers of Hydrides (Energies Are in μH)

S-MP term	$(H_2O)_2$ *a*	$(H_2O)_2$ *b*	$(HF)_2$ *c*	$(NH_3)_2$ *d*	$(CH_4)_2$ *e*	CH_4NH_3 *f*	CH_4H_2O *g*
ΔE^{SCF}	−5746	−5769	−6272	−2641	236	−149	151
$\Delta E^{(2)}$	−1261	−1179	−641	−1801	−832	−749	−1251
$\Delta E^{(3)}$	56	−16	−129	158	15	−6	46
$\Delta E^{(4)}_{SDQ}$	207	207	222	158	39	52	59
$\Delta E^{(4)}$	−30	16	70	−129	−63	−62	−127

[a] From Szczęśniak et al. (ref 189), equilibrium dimer, Sf basis set. [b] From Rybak et al. (ref 36). [c] From Burcl et al. (ref 185), Sdf(b-ext) basis set. [d] From Szczęśniak et al. (ref 190), equilibrium trimer geometry; Sf basis set. [e] From Szczęśniak et al. (ref 191), equilibrium dimer (A-conf, R = 7.5 a_0), Sf basis set. [f] From Szczęśniak et al. (ref 192), equilibrium dimer (C−H−N configuration, R(C−N) = 7.6 a_0), S basis set. [g] From Szczęśniak et al. (ref 168), equilibrium dimer (F−H configuration R(C−O) = 6.8 a_0), Sf basis set.

(T) level. The MP perturbation theory convergence may, however, depend on the basis set. For example, in Ar_2 (see Table 5) the difference between MP4(SDTQ) and CCSD(T) is practically zero with the spdf(b-ext) basis set, but amounts to 13 μH with the extensive basis set of Woon[164] (due to the change in T contributions).

The convergence properties of MP theory largely depend on a considered system, and the general regularities should be discussed in the context of the interaction type. Owing to the relationship between the I-MP and S-MP theories, we can often use the knowledge of the physical contents of the individual $\Delta E^{(n)}$ corrections to predict the convergence properties of the series. For electrostatically bound complexes, such as $(HF)_2$ (Table 7), the ΔE^{SCF} term prevails as the van der Waals minimum is determined by the balance between the attractive electrostatic and repulsive exchange interactions, accompanied by smaller induction. The dispersion term is of secondary importance, and the electrostatic correlation is small. Consequently $\Delta E^{(2)}$ is relatively small. $\Delta E^{(3)}$ and $\Delta E^{(4)}$ are 1 order of magnitude smaller than $\Delta E^{(2)}$ and cancel each other to a large extent. In Table 8 we show other examples where the behavior of correlation corrections is similar: $(H_2O)_2$, $(NH_3)_2$, and CH_4H_2O.

For dispersion-bound complexes, Ar_2 and ArHCl, represented in Tables 5 and 6, the typical features are (i) the bulk of exchange repulsion is present in ΔE^{SCF}, (ii) the dominant $\epsilon^{(20)}_{disp}$ attraction is accumulated in $\Delta E^{(2)}$, (iii) $\Delta E^{(3)}$ and $\Delta E^{(4)}$, which are determined by intramonomer correlation corrections to dispersion, are much smaller than $\Delta E^{(2)}$ and cancel each other to some extent. Yet, they are absolutely necessary to achieve a good agreement with the experimental well depth.

It is tempting to search for some patterns of convergence of higher terms that would be valid for a large number of complexes. For instance, it is sometimes assumed that the $\Delta E^{(3)}$ and $\Delta E^{(4)}$ corrections cancel each other.[24] Indeed, such a cancellation occurs in the above discussed cases, as well as in complexes shown in Tables 5, 6, and 8. However, two comments are in order. First, this is not *always* true. For example, in the complexes involving one- or two-electron species (H, He, H_2), both corrections are usually negative[171,172] (known exceptions are He−benzene[173] and He−Cl_2[174]). Another example, where both $\Delta E^{(3)}$ and $\Delta E^{(4)}$ are negative is the Ne dimer[164] and CH_4−NH_3 (Table 8). Second, even if $\Delta E^{(3)}$ and $\Delta E^{(4)}$ have opposite signs, they rarely cancel exactly, and the residue may be significant [see $(CH_4)_2$, CH_4-NH_3 and CH_4H_2O in Table 8]. Finally, the balance of $\Delta E^{(3)}$ and $\Delta E^{(4)}$ may be different for various locations on the PES. The conclusion is that any a priori assumptions about the signs of $\Delta E^{(3)}$ and $\Delta E^{(4)}$ have little foundation.

Table 9. Convergence of the S-MP Interaction Energies (in μH) in He−F^- at the Equilibrium Distance (R = 6.5 a_0)

S-MP term	ref 175	this work
ΔE^{SCF}	−237	−238.8
$\Delta E^{(2)}$	−4	−14.5
$\Delta E^{(3)}$	−104	−110.6
$\Delta E^{(4)}$	117	117.3
ΔE(4)	−228	−242.2
$\Delta E^{CCSD(T)}$		−320.0
I-MP	−255[a]	
model potential		−311[b]

[a] From ref 92. [b] From Ahlrichs et al. (ref 193), R = 6.47 a_0.

Another regularity which is observed is that $\Delta E^{(4)}_{SDQ}$ appears to be always repulsive and the contribution from triples, $\Delta E^{(4)}_T$ appears to be always negative. We have not seen any exceptions so far.

One interesting observation about the dispersion term $\epsilon^{(20)}_{disp}$ is that it overestimates the exact dispersion energy for the complexes with the III period elements, and underestimates the exact dispersion energy for the complexes of the I and II period elements. The next dispersion correction, $\epsilon^{(21)}_{disp}$, which appears in $\Delta E^{(3)}$ (cf. eq 9) is positive in the former case and negative (or negligibly positive) in the latter, which changes the overall dispersion energy in the desired direction.[77] Since $\epsilon^{(21)}_{disp}$ dominates the $\Delta E^{(3)}$ term in dispersion-bound complexes, its sign and value may be used to predict the effects of the truncation of the MP perturbation theory series on the second order. One effect of such a truncation is that for complexes involving III period elements, the MP2 calculations employing dispersion-saturated basis sets may yield values below the accurate the ones (cf. Ar_2 and ArHCl with best basis sets in Tables 5 and 6).

The convergence of MP perturbation theory should not be taken for granted. Some examples worth mentioning where the convergence problems occur are He−F^- and Be_2.

In the He−F^-, dimer Sadlej and Diercksen[175] demonstrated that the convergence of the MP perturbation theory series through the fourth order is suspicious; the $\Delta E^{(n)}$ corrections oscillate, and the $\Delta E^{(4)}$ term dominates (see Table 9). The well depth is reasonable (70% of D_e from the extended Tang−Toennies model potential), but this is because it is dominated by the SCF contribution. The correlation terms through the fourth order cancel almost exactly. Using the fourth-order I-MP Moszyński et al.[92] reproduced this result showing that the unusual behavior is due to the large intramonomer correlation effects in the diffuse F^- electron charge cloud. In

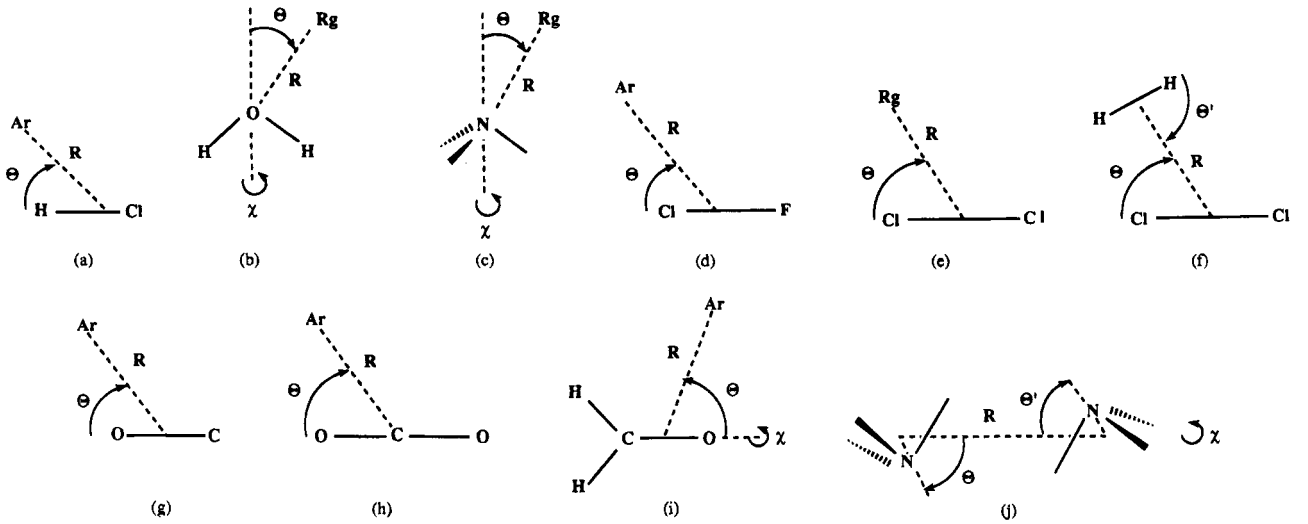

Figure 6. Definitions of geometrical parameters of the complexes discussed in section IV. b, c, i, and h the arrangements shown correspond to $\chi = 0°$.

particular, the electrostatic correlation and exchange correlation terms were found to be unusually large. However, only the CCSD(T) calculation managed to closely approach the experimental result (within a few percent). One can also see in Table 9 that the MP4 value of correlation contribution amounts to only 3% of the total CCSD(T) correlation contribution!

Another unusual case, but different from HeF^-, is that of the beryllium dimer. According to Černušak et al.,[176] the MP4 estimate of D_e agrees very well with the full CI result (3030 μH[172] vs 2960 μH[177]). However, the fact that the CCSD(T) result is poor (2020 μH) and the CCSD(T) curve does not have a proper shape, casts doubt on the assertion of ref 176. A great deal of sensitivity to the basis set has also been reported. The problems with Be_2 have been attributed to avoided crossing between two hypothetical diabatic curves: one dissociating into $2s^2(^1S)$ atoms and the other dissociating into $2s2p(^3P)$ atoms.[179] Consequently, single reference MP perturbation theory, as well as CC, are no longer adequate, and one has to conclude that the accurate MP4 result is due to a fortuitous cancellation of terms. Only the full CI has been successful in providing accurate results for Be_2.[177]

The above discussion is intended to provide general ideas as to what can be expected in the S-MP calculations of the interaction energies and the possible problems.

IV. Ab Initio Studies of van der Waals Dimers

The van der Waals complexes involving a rare gas (Rg) atom bound to a molecule are extremely useful models in the studies of intermolecular forces. Due to the fact that Rg is spherically symmetric, potential energy surfaces of these complexes involve only three intermolecular degrees of freedom. This feature greatly simplifies many aspects of the calculations. More importantly, it allows for the analysis of the forces in the simplest terms possible. For example, Rg may be viewed as a structureless probe of the intrinsic properties of molecules to which it is bound. At short and intermediate intersystem distances, such a probing may reveal the shape of the electron density of a molecule. At long distances Rg may be used to detect molecule's propensity for the dispersion and induction interactions. These two features are crucial to the overall anisotropy of PES.

It should be mentioned that in the Rg–molecule interaction, the multipole electrostatic energy is absent. This eliminates one important source of basis set effects. More fundamentally, the dispersion and induction energies behave variationally with respect to the basis set enlargement. The exchange energy, on the other hand, is fairly basis set independent. On this basis, we can expect that the calculated interaction energies will represent upper bounds to the true energies. This is a very important consideration in attempts to determine the accuracy of calculated interaction potentials.

In certain instances the relative simplicity of these complexes (low number of degrees of freedom) permits the rigorous inversion of spectroscopic information to generate semiempirical potential energy surfaces. The availability of semiempirical surfaces is of utmost importance to ab initio approach, as they help calibrate the computational approaches.

One of the most often chosen Rg atoms in these complexes is Ar. Due primarily to its relatively strong Lewis base character, Ar can form a wide variety of complexes ranging from typical van der Waals "nonbonding" interactions to incipient donor–acceptor complexes. In the forthcoming sections several complexes of the Ar–molecule type will be discussed and compared with complexes involving other Rg atoms or closed-shell species, such as Be. The coordinate systems of the complexes considered are shown in Figure 6. The summary of the recommended equilibrium parameters for the discussed complexes is included in the Appendix Table A1.

A. Ar–HCl: A Prototype van der Waals Complex

The ArHCl system is one of the basic prototypes of anisotropic intermolecular forces. In Figure 7a,b the anisotropies of SCF and correlated interaction energies, respectively, are illustrated.[183]

The anisotropy of ΔE^{SCF} is principally determined by the exchange component, ϵ_{exch}^{HL}. The electrostatic

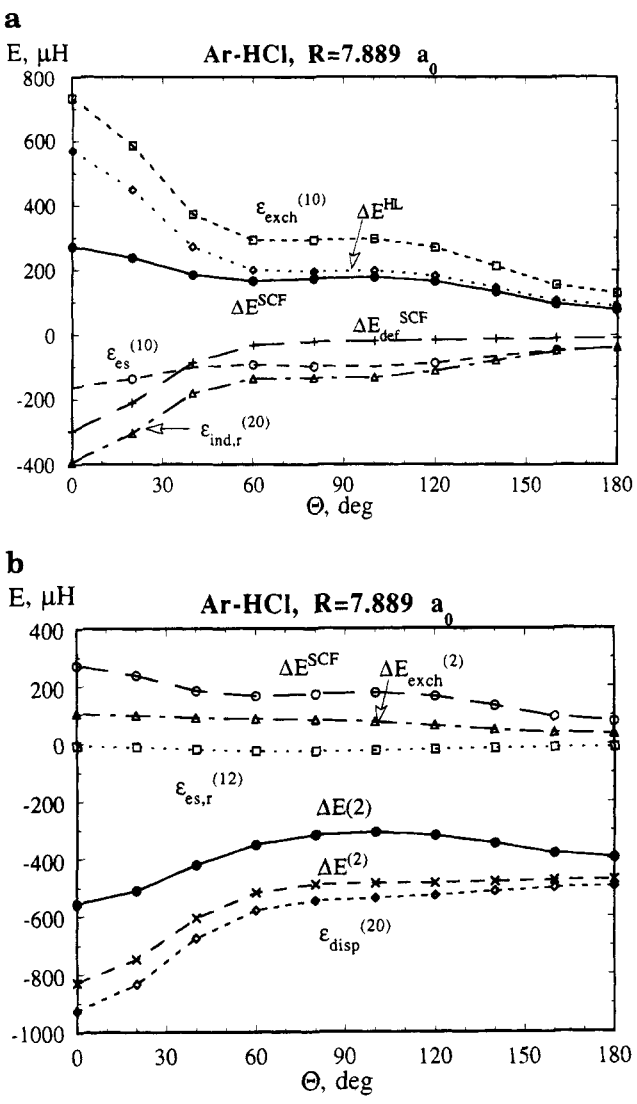

Figure 7. Θ-Dependence of the interaction energy of Ar–HCl; the intersystem distance $R = 7.889\ a_0$ corresponds to the equilibrium separation of the global minimum: (a) the SCF interaction energy and its components; (b) the correlated components of the interaction energy. $\Delta E(2)$ denotes the total interaction energy through the second order of S-MP.

$\epsilon_{es}^{(10)}$, deformation ΔE_{def}^{SCF}, and induction $\epsilon_{ind,r}^{(20)}$ terms reveal approximately reciprocal anisotropy of the exchange term. This has a smoothing effect on the total SCF anisotropy. Overall, the ΔE^{SCF} curve has a maximum at the linear Ar—H—Cl orientation, a minimum at the linear Ar—Cl—H orientation, and is fairly flat for the bent geometries, in the region 40–120°.

The behaviors of various correlation terms are illustrated in Figure 7b. The correlation terms, $\Delta E^{(2)}$ and $\epsilon_{disp}^{(20)}$, behave in a reciprocal manner to ΔE^{SCF}. Both $\Delta E^{(2)}$ and $\epsilon_{disp}^{(20)}$ have a minimum for the linear Ar—H—Cl, a maximum for the linear Ar—Cl—H form, and a flat region 40–120°. Electrostatic correlation and exchange correlation terms are less significant.

The anisotropy of total interaction energy is represented by $\Delta E(2)$. It is different from its components since it results from a delicate balance between SCF and correlation contributions. It has an absolute minimum at the linear Ar—H—Cl configuration, a barrier at about 100°, and a secondary minimum at the linear Ar—Cl—H configuration.

Decomposition of the total interaction energy enables us to analyze which fundamental components determine the anisotropy in a particular region. Whereas the dominant attractive component is always dispersion, and the dominant repulsive term is always exchange, these two terms alone are not sufficient to interpret the anisotropy of the PES. In fact, the induction energy, albeit much smaller than dispersion, is substantially more anisotropic than the latter and plays a crucial role in the determination of the global minimum Ar—H—Cl. Indeed, if we neglect the induction term, a bent structure ($\Theta = 50°$) rather than the linear one becomes the most stable. This is because ΔE_{def}^{SCF} and $\epsilon_{ind,r}^{(20)}$ peak sharply for the collinear H-bonded arrangement. This has been attributed to the fact that the electric fields, due the HCl dipole and quadrupole moments, reinforce one another in this direction, whereas they interfere destructively at the Cl end.[12] This interpretation is qualitatively correct, but the magnitude of both ΔE_{def}^{SCF} and its exchangeless approximation, $\epsilon_{ind,r}^{(20)}$, is much larger than the interaction between the induced-dipole and the lowest permanent moments, the dipole and quadrupole (see ref 183).

The origin of the local minimum for the linear Ar—Cl—H form is also quite interesting. It is due to the minimum of the exchange repulsion at $\Theta = 180°$. This minimum indicates an important feature of the HCl molecule which is a relative depletion of the electron density at the Cl end along the molecular axis.[12,194] It causes the repulsive exchange effect to be weaker for the linear Ar—Cl—H form than for the T-shaped form ($\Theta = 90°$). The electron density which protrudes at $\Theta = 100–120°$ corresponds to π-lone pairs of Cl of the cylindrical symmetry.

It is important to compare our potential and its contributions with the family of accurate empirical potentials of Hutson.[184,195] These potentials are of the general form:

$$V(R,\Theta) = A(\Theta)\exp(-bR) + V_{ind}(R,\Theta) - \sum_{n=6,7,8} C_n(\Theta)D_n(R)R^{-n} \quad (12)$$

The first term is the Born–Mayer repulsion. The second term simulates the induction effects. The last term has the form of the dispersion contribution, but since it is adjusted to make the total potential reproduce the experimental data, it additionally accommodates the deficiencies of the first two terms. Because of this adjustment it is not possible to make a precise comparison with the terms from ref 183 which are "pure" exchange, induction, and dispersion contributions. Nevertheless, qualitative agreement of the exchange and dispersion terms predicted ab initio and in the H6(3) potential[190] of eq 11 proved to be good. The induction term V_{ind} of the H6(3) potential differed from the ab initio induction term since V_{ind} was designed to represent only the dominant asymptotic contribution, while the rest of induction interaction was accommodated into the C_8 term. In the latest improved potential,[179] named H6(4,3,0), the induction term V_{ind} was represented instead by

a "point charge plus quadrupole" model which is expected to be more realistic for the induction energies.

For a prototype system, a determination of the accuracy of the well depths and barrier parameters is of great significance. The best empirical potential of Hutson H6(4,3,0) yields for the primary minimum D_e = 802.0 μH and for the secondary minimum D_e = 675.8 μH.[184] Precise assessment of the accuracy is difficult to obtain (it may vary in different regions), but the absolute well depth is probably accurate to ±14 μH (3 cm^{-1}),[179] which constitutes an error of ±2%. The error for the Ar—Cl—H configuration is expected to be larger, as pointed out in ref 196. Our best ab initio result is 795.4 μH [see Table 6, MP4/WTdf(b-ext)], and is expected to be in error by less than ±5%. This result is indeed very close to the empirical value. The best ab initio result for the secondary minimum well depth amounts to 634.8 μH (obtained at the same MP4/WTdf(b-ext) level). This result is about 6% below the empirical value.

B. H_2O Interaction with Ar and Other Closed-Shell Atoms

Complexes involving water are of particular interest because they are relevant to such important concepts as hydrophilic and hydrophobic interactions and to the solvation effect. In addition, complexes of water with atoms are prototypes of the atom—triatom interactions. While the atom—diatom interactions have been extensively studied and are now fairly well understood, a prototype atom—triatom complex of Ar and H_2O has been the subject of several ab initio[107,197] and spectroscopic studies[198-202] only recently. Other complexes of water and closed-shell atoms have also been investigated, e.g. He—H_2O,[172,203] Kr—H_2O,[204] and Be—H_2O.[205-207] Below we will describe the results for the Ar—H_2O interaction obtained in ref 197 in more detail and then compare it to interactions involving other closed-shell atoms.

The anisotropies of the fundamental components of the Ar—H_2O interaction at the SCF and correlated levels of theory are shown in Figure 8a,b, respectively. The SCF component at R = 7.09 a_0 (cf. Figure 8a) is principally determined by the exchange term which is the largest in magnitude and most strongly anisotropic. It has a saddle point between the hydrogens, maxima at the hydrogens, and a minimum for the T-shaped configuration (Θ = 60°, χ = 0°). These points correspond to the relative concentrations (maxima) and depletions (minima) of the electron density of H_2O in Bader's approach.[208] Interestingly, the lone electron pairs charge concentrations are not detected in a sharp and distinct way. There are only slight irregularities in a slow buildup of repulsion around the right angle in the perpendicular plane (see below).

The SCF deformation is much smaller than the exchange term, but it is strongly anisotropic and noticeably affects the total SCF anisotropy. Indeed, if we neglected this term the minimum of the SCF curve, at Θ = 0°, would be shifted to 60° (this is the minimum of the HL energy). As will be shown below, the induction effect has a great impact on the position of the global minimum on the PES.

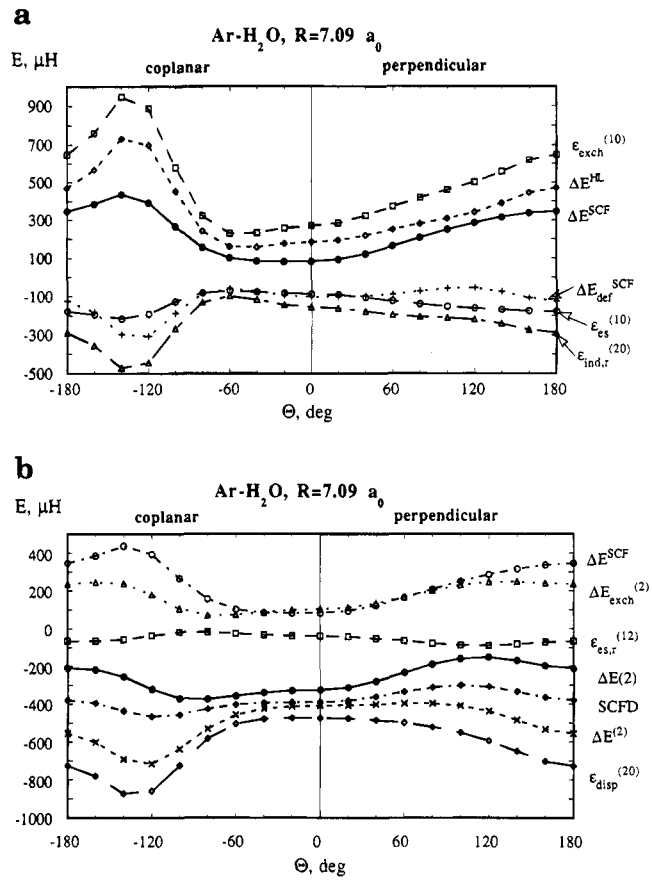

Figure 8. Θ-Dependence of the interaction energy of Ar—H_2O at the intersystem distance R = 7.09 a_0 corresponding to the equilibrium separation of the T minimum: (a) the SCF interaction energy and its components; (b) the correlated components of the interaction energy. $\Delta E(2)$ denotes the total interaction energy through the second order of S-MP.

The behaviors of various correlation terms are illustrated in Figure 8b. The anisotropy of the dispersion energy is roughly reciprocal to that of the exchange energy. Indeed, the minima in one nearly coincide with maxima in the other. However, this pattern is not fully reflected in $\Delta E^{(2)}$, because the $\Delta E^{(2)}_{exch}$ term has the same general shape as ϵ^{HL}_{exch}. Thus it has a smoothing effect on the anisotropy of $\epsilon^{(20)}_{disp}$.

The total PES for Ar—H_2O adopts a very interesting shape. At large R, where the interaction energy energy is dominated by the dispersion term, if R *decreases*, the deepest descending valley corresponds to the H-bond structure. In the short-range region, if R *increases*, the deepest descending valley is related to the T structure (where Ar is located at the face of a triangle formed by two lone pairs and one H atom). In the van der Waals minimum a very flat region is observed which joins these two valleys and makes the T-shaped and hydrogen-bond structures very close in energy without a barrier between them. This picture is in good qualitative agreement with the experimental findings. The calculated well depth of 470 μH from ref 197 provided only a lower bound to the true value and was estimated to be too low by ca. 25%. Although some earlier estimates of D_e were substantially larger (the empirical AW1 potential of Cohen and Saykally predicted D_e of 796.1 μH[199] and

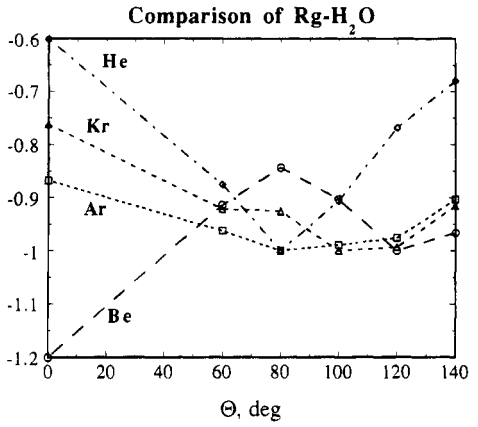

Figure 9. Comparison of qualitative features of potential energy surfaces of He–H_2O, Ar–H_2O, Kr–H_2O, and Be–H_2O (see the text).

the ab initio potential of Bulski et al. a value of 715.9 μH[107]), the recent AW2 potential of Cohen and Saykally[198] has a well depth of 652 μH and thus lies within the error bars predicted in ref 197. On the other hand, our very recent calculations predict D_e around 622 μH with ±5% error.[185] It is more difficult to corroborate the shape of the minimum region. All the above studies differ somewhat on this issue. The potentials AW1 and that of Bulski et al. predict the T-shaped structures with $\Theta = 90°$ and $\Theta = 50°$, respectively. The newer AW2 potential, on the other hand, predicts the hydrogen-bonded structure. While the AW2 potential is in qualitative agreement with ref 197 it does not predict a similarly wide minimum area which is almost isoenergetical between the T-shaped and hydrogen-bonded structures. No doubt, the Ar–H_2O complex warrants further studies.

It is interesting to compare the total PES for different atom–H_2O complexes. The anisotropies of the basic SCF and correlation components are qualitatively *similar* for different atoms and are, to a large extent, *independent* of the intersystem separation. In fact, this is a general feature of the fundamental components if the partner is spherically symmetric. What distinguishes these atom–H_2O complexes from one another is a *different balance* of the fundamental terms. Therefore, the shapes of PESs are different for these complexes and are also strongly dependent on the intersystem separation. To appreciate the qualitative differences in the van der Waals minimum region, in Figure 9 we have schematically drawn the minimal energy paths around water for He, Ar, Kr, and Be. To expose various shapes of the PESs, the plots illustrate angular dependence of the following ratio of the interaction energies: the lowest energy at a particular angle and the global minimum energy. It is seen that for a compact and hard to polarize helium atom there is a distinct minimum at $\Theta = 80°$ (the coplanar T-shaped structure). This structure is stable because of the relatively important role of the exchange component which is minimized in this configuration. For the more polarizable rare gas atoms, Ar and Kr, there is a very flat and wide minimum, ranging from 80° to 120°. Moreover, for Ar this minimum is wider and flatter, while for Kr it is somewhat shifted toward the H-bond structure. This shift is related to the growing role of the induction effect from He to Kr because of the increasing polarizability. To better understand the role of induction effect, the complex with Be atom has also been studied. The Be atom is even more polarizable than Kr and has a very diffuse electron charge cloud. Indeed, this complex reveals distinct minima for two structures that maximize induction attraction: the H-bonded structure, and a C_{2v} structure with Be attached to the O atom. The T-shaped orientation represents a barrier.[205]

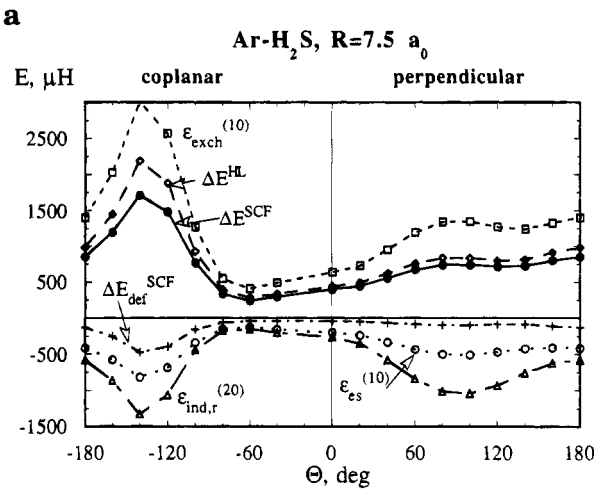

Figure 10. Θ-Dependence of the interaction energy of Ar–H_2S at the intersystem distance $R = 7.5$ a_0 corresponding to the equilibrium separation of the global minimum: (a) the SCF interaction energy and its components; (b) the correlated components of the interaction energy. $\Delta E(2)$ denotes the total interaction energy through the second order of S-MP.

C. H_2S–Ar Interaction

It is interesting to compare Ar–H_2O with its second-row analog Ar–H_2S.[185] One can see in Figure 10a,b that fundamental components are similar. The difference is in the relative magnitude of the induction effect which is weaker for H_2S than for H_2O. Consequently, the H-bonded geometry is no longer attractive enough and the global minimum occurs for the T-shaped geometry (as for He–H_2O) in agreement with experimental data.[209] Interestingly, in contrast to He–H_2O there is also another local minimum, at the H–H edge, separated from the T-shaped one by a barrier. With increasing R, the

valleys ascending from these minima join at the top of this barrier. With further increasing R, the barrier transforms into the dominant long-range valley on the PES. In the long range the H-bonded arrangement has the lowest energy.

Another distinct feature of the H_2S–Ar interaction is a clear indication of the lone pairs by the exchange energy component which shows a maximum at Θ = 80–90°, χ = 90° (see below).

D. NH_3 Interaction with Ar and Other Closed-Shell Atoms

Weak van der Waals complexes of ammonia are as interesting as those of water. Similar to water, ammonia, and amino groups play an important role in various areas of chemistry and biology. The lone pair of NH_3 is a well-known proton acceptor. In contrast to water, experimental studies indicate that ammonia is an extremely reluctant proton donor.[210,211] Perhaps the only case where NH_3 is capable of creating a hydrogen bond is the ammonia dimer.[212,213] For these reasons the Ar–NH_3 complex has become a subject of several ab initio[106,204] and spectroscopic studies.[211,215] Below we describe the Ar–NH_3 interaction in more detail and then compare it to interactions with other closed shell atoms: Kr and Be.

The anisotropies of the fundamental components at the SCF and correlated levels of theory are shown in Figure 11, parts a and b, respectively. Although obtained for Ar–NH_3, these anisotropies are representative of other atom–ammonia complexes. The difference appears only in their magnitude and mutual balance, and consequently in the final shape of total PES.

The Θ dependence of the SCF components of Ar–NH_3 at R = 7.09 a_0 is shown in Figure 11a. The total SCF anisotropy is principally determined by the exchange component (similar to the Rg–H_2O case) which is quite typical for most dispersion bound complexes. The maxima of the exchange and SCF energies are related to the concentrations of electron density around the nitrogen (the lone pair) and at the hydrogens.

The behaviors of the correlation terms are illustrated at Figure 11b. The anisotropy of the $\epsilon_{disp}^{(20)}$ term, which dominates the $\Delta E^{(2)}$ energy, is reciprocal to that of the exchange term. However, $\epsilon_{disp}^{(20)}$ is more isotropic than the exchange term. Consequently, the global minimum of $\Delta E(2)$ occurs for the T-shaped geometry (Θ = 80°, χ = 60°), where the exchange repulsion is minimal. In contrast to water, the induction effect is not strong enough to make the N and H atoms prone to Ar attachment.

The Kr–NH_3[204] is similar to Ar–NH_3. Fundamental contributions have a qualitatively similar character; the induction effect is not substantially enhanced despite the fact that Kr is more polarizable than Ar. Thus the Kr–NH_3 structure is also T-shaped. Only if a rare gas atom is replaced by Be (Figure 12a,b) would a dramatic increase in induction effect shift the position of the minimum to the C_{3v} configuration with Be attached to the nitrogen lone pair.[205] Although the electron concentrations at H

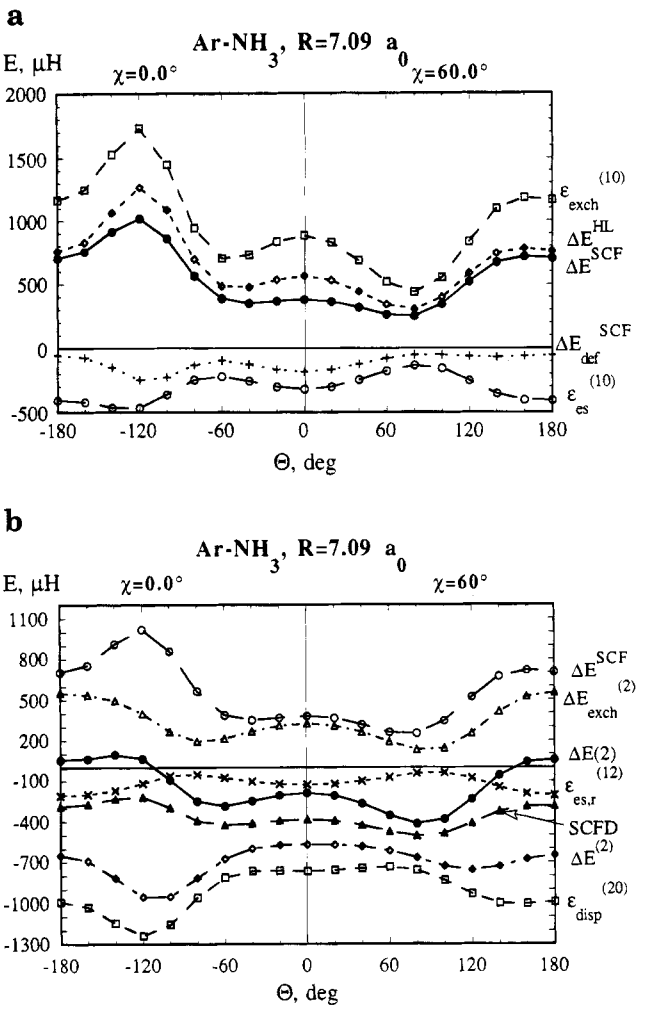

Figure 11. Θ-Dependence of the interaction energy of Ar–NH_3 at the intersystem distance R = 7.09 a_0 corresponding to the equilibrium separation of the global minimum: (a) the SCF interaction energy and its components; (b) the correlated components of the interaction energy. $\Delta E(2)$ denotes the total interaction energy through the second order of S-MP.

atoms also enhance induction, it is not enough to yield a stable H-bonded form.

Interestingly, at large distances the PESs of all three complexes are determined by the deepest valley leading to hydrogens. On closer approach an atom eventually turns either to the middle of a triangle formed by two H atoms and the lone pair (for Ar and Kr) or to the lone pair (Be).

The PES of Ar–NH_3 is in qualitative agreement with another ab initio PES obtained by Bulski et al.,[106] as well as with the PES from inversion of VRT spectra.[211,215] A good comparison of all three potentials is provided in ref 211.

E. Lone Pairs in H_2O, H_2S, and NH_3

The concept of lone electron pairs is deeply rooted in chemistry, and there is no question about its usefulness in the interpretation and prediction of chemical structure and reactivity. In the context of intermolecular interactions, lone pairs have been customarily used to rationalize the configurations of H-bonded dimers in terms of the alignment of a lone pair of a proton acceptor and the H–X bond of a

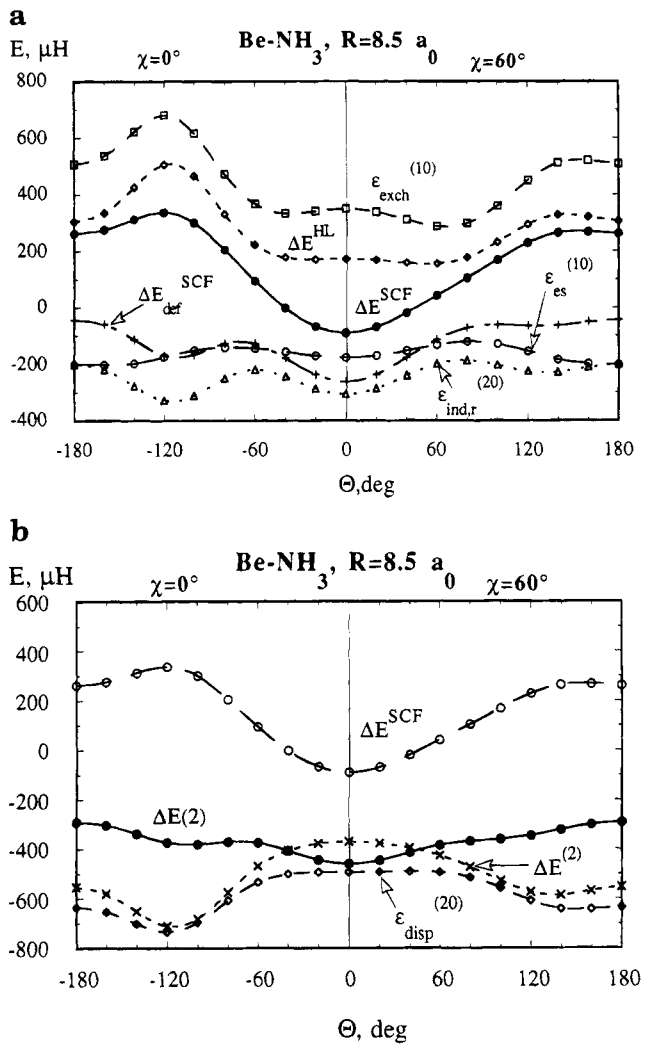

Figure 12. Θ-Dependence of the interaction energy of Be–NH_3 at the intersystem distance R = 8.5 a_0: (a) the SCF interaction energy and its components; (b) the correlated components of the interaction energy. $\Delta E(2)$ denotes the total interaction energy through the second order of S-MP.

proton donor. The long-range theory of intermolecular forces, on the other hand, bypasses the concept of lone pairs completely, as the equilibrium structures are described in terms of interactions between multipole moments. Therefore, an ab initio characterization of lone pairs and their relation to the structural properties of molecular complexes is of great interest.

As noted in the preceding section, the charge concentrations corresponding to lone pairs in the water molecule are not detected in a clear way, except for some irregular slope in the increase of the exchange term for Θ from 0° to 90° at χ = 90°. The presence of charge concentrations is difficult to notice if one examines solely the exchange curve. However, following the gradient of the exchange term, a local maximum appears around 60–80°. Similar maxima are also detected for the gradients of ΔE^{SCF} and $\Delta E(2)$. They indicate that there must be a relative concentration of the electron density in this region. This is in agreement with Bader's analysis of the Laplacian of electron density which revealed a maximum at 68°, which he interpreted as a lone pair.[208]

The existence of lone electron pairs in water has also been discussed by Cohen and Saykally.[198] They noticed that the repulsive wall of their potential extends further from the center of mass at the lone pair angle than it does in between the two lone pairs. Analysis of the gradient of PES (or the repulsive component of PES) may be more conclusive in this regard.

As it turns out, this weak manifestation of electron pairs is typical of water rather than of electron pairs in general. A comparison of water with H_2S and ammonia is interesting in this context. In Ar–H_2S the plot of the exchange term has a very distinct maximum at about 80–90°, and so do the SCF and $\Delta E(2)$ curves, cf. Figure 10. Similar maxima occur in the exchange, SCF and $\Delta E(2)$ curves in NH_3 at Θ = 0°, thus indicating a presence of a lone pair at N (cf. Figure 11a). To conclude, probing with Ar allows us to observe the presence of lone pairs in molecules. In NH_3 and H_2S the lone electron pairs appear very clearly. They constitute one of the structure-determining factors in complexes of NH_3 and H_2S with Ar. However, in H_2O only hints of the lone pairs are seen, and no direct relationship between their directionality and structure can be found. As will be discussed below, in weak molecular complexes involving water, an alignment along the lone pairs of H_2O does not occur (see below).

In this and in the forthcoming sections we often compare the picture of electron density distribution inferred from examining the HL exchange energy with the Bader's plots of the Laplacian of electron density. Some comment on this comparison is in order at this point. A careful examination of Bader's plots leads us to believe that the quantity probed by the HL exchange energy is not the overall density, but the density in the *diffuse region*. The diffuse region is relevant to the overlap of the monomer charge clouds. This explains why the water lone pairs are not clearly visible in our analysis. The lone pairs in water do exist, but they have a short-range character. In the outer region they disappear fairly quickly. The lone pairs of NH_3 and H_2S, on the other hand, disappear more slowly, thereby reaching the outer region.

F. Principles Governing Equilibrium Structures in Rare Gas–Molecule Complexes

van der Waals complexes involving molecules bound to rare gases display a wide diversity of equilibrium structures which elude conventional chemical explanations. Several attempts have been made in the past to reconcile these structural properties with common intuitions. These include the hard sphere–distributed multipole model of Buckingham and Fowler[216] (based on distributed multipole analysis of Stone[217]), the directionality of lone pairs approach by Legon,[218] the so-called molecular mechanics for clusters (MMC) by Dykstra,[219] the HOMO–LUMO approach of Klemperer,[220] the energy partitioning by Hurst et al.[221] (based on the perturbation approach proposed by Hayes and Stone[222]), and many others (e.g. ref 223).

In the preceding sections (A-E) a number of complexes involving Ar bound to a hydride molecule have

been discussed which displayed a variety of equilibrium structures. We are now in a position to rationalize these geometries by examination of the fundamental components of interaction energy. It is clear that two competing factors are involved in the determination of equilibrium structures. In the short range of PES the anisotropy is determined by the HL exchange energy which probes the outer region of the electron density around a molecule. As discussed above, this effect determines the repulsive part of PES. The directionality of PES at the long intersystem separations is determined by the anisotropy of long-range forces, such as dispersion and induction. The equilibrium structures thus result from a delicate balance between the short-range and long-range factors. Depending upon the intrinsic properties of monomers, this balance can be shifted either toward the short-range or toward the long-range effects.

Let us begin with the Ar−CH_4 complex.[224] Each of the C−H bonds represents an area of concentration of electron density which results in strong exchange repulsion. The areas of the molecule which are favorable in terms of the exchange repulsion are, thus, the four faces of the CH_4 tetrahedron. The repulsion due to the HL exchange effect is minimized in the center of each of the faces. The long-range effects in this case constitute the dispersion energy alone, since, due to the absence of low multipoles on methane, the induction effect is negligible. The dispersion energy represents the dominant attractive component. However, its anisotropy cannot overcome the strong directionality of repulsive forces. Ultimately, the equilibrium position of Ar is on one of the faces of CH_4, the positions which are determined by the minimum in the repulsive force.

The complexes of pyramidal molecules with Rg atoms can be viewed as a special case of the Rg−tetrahedral molecule, in which one vertex is replaced by a lone pair. Such is the case of Ar−NH_3 complex. The position of Ar favored by the minimal exchange repulsion is on any face formed by the lone pair and two H atoms and strongly disfavors the areas around the H atoms. The dispersion and induction effects, on the other hand, favor positions facing the H atoms. The dispersion energy is strongly attractive, but the induction effect is relatively weak. Their combined anisotropies are not strong enough to overcome the directionality of the exchange effect, so the equilibrium geometry involves the T structure with Ar located on any of the lone-pair H−H faces of the hypothetical tetrahedron formed by the N−H bonds and the N lone pair. In the Ar−PH_3[225] complex involving the second-row analog of ammonia, the situation is very similar. Despite a strong dispersion attraction, the complex assumes a T configuration, analogous to that in Ar−NH_3, due to the lack of substantial induction contribution.

A tetrahedral model can also be applied to an H_2O molecule by considering a tetrahedron spanned on the two O−H bonds and the two oxygen lone pairs. In Ar−H_2O the exchange effect is minimized on either face which is formed by two lone pairs and one O−H bond. The induction effect has sharp minima next to the H atoms and so does the dispersion energy. However, the anisotropy of the former is much stronger. As a result of this interplay, two configurations of this complex, T-shaped (favored by the exchange effect) and H-bonded (favored by the induction and dispersion effects), are very close in energy. In fact, the calculations involving a less sophisticated basis set indicate that the balance is shifted toward the T structure. However, in the calculations involving a more elaborate basis set which leads to a better saturation of dispersion energy, a slight preference for the H-bonded configuration is observed.[226] The importance of the induction effect in stabilizing the H-bond structure is further underscored when we consider He−H_2O complex.[173] This complex is also stabilized by the dispersion energy; however, due to the small polarizability of the He atom, the induction effect in this complex is much smaller than in Ar−H_2O. As a result, the complex He−H_2O assumes a T configuration which is favored by the exchange effect. Ar−H_2S displays a T-shaped configuration as well.[185] The preference for this configuration can be easily rationalized in terms of a weaker induction effect, roughly attributable to a smaller dipole moment from that of H_2O.

Of the two stable configurations of Ar−HCl, the H-bonded one, Ar—HCl, is far more stable than the non-H-bonded Ar—ClH. Despite the strong preference of the exchange effect for the Ar—ClH structure the induction anisotropy leads to the stronger stabilization of the H-bonded structure. Indeed, as discussed above, the elimination of the induction effect from the total interaction would lead to a bent configuration of the Ar−HCl complex. Interestingly, by choosing a less polarizable Rg atom and a hydrogen halide with smaller dipole moment, the effects of induction can be greatly diminished to the point that the non-H-bonded structure becomes more stable. Such are the cases of He−HCl[227,228] and He−HBr[228] where the He—XH configuration represents a global minimum (cf. Table A1).

A summary of energetics for a number of complexes formed by Ar with molecules of varying properties is shown in Table 10. The complexes of CH_4, NH_3, and H_2S form T-shaped structures, while the complexes of H_2O and HCl form H-bonded configurations. Meanwhile, the proton-donor abilities of molecules gradually increase in the same order. It is clear from the energy partitioning of Table 10 that the property which can be related to the proton-donor abilities is the induction effect. Since the induction effect results from the electrostatic polarization of Ar in the field of molecule, the molecules which we intuitively label as good proton donors are capable of creating a highly directional fields which are maximized along X−H axes.

In a search for more precise measures of molecular ability to form the H-bonded structures, we have introduced the ratio of the induction effect to the dispersion effect.[204] The rationale for using such a ratio is the following: As noted above, both dispersion and induction effects usually peak around the H-bonded geometries; however, this preference for H-bond geometries in both cases has a different origin. The dispersion energy, as a purely correlational term (which does not involve charges and

Table 10. Comparison of Rare Gas–Molecule Complexes[a] (All Values in μH)

				ArH_2O		ArHCl	
	$ArCH_4$ (ref 224)	$ArNH_3$ (ref 214)	ArH_2S (ref 185)	T (ref 197)	HB (ref 197)	non-HB (ref 183)	HB (ref 183)
$\epsilon_{es}^{(10)}$	−86.0	−132.9	−151.8	−80.6	−72.8	−139.5	−163.2
ϵ_{exch}^{HL}	298.9	437.8	547.1	323.1	341.1	472.7	733.5
ΔE_{def}^{SCF}	−13.9	−52.4	−58.9	−85.7	−156.5	−41.0	−298.1
$\epsilon_{ind}^{(20)}$	−64.1	−126.4	−176.5[b]	−114.8	−176.3	−146.3	−343.1
ΔE^{SCF}	199.0	252.5	336.3	156.8	111.7	292.3	272.2
$\epsilon_{es,r}^{(12)}$	−26.2	−42.8	−28.0	−17.8	−11.1	−31.3	−7.4
$\epsilon_{disp}^{(20)}$	−663.9	−757.0	−954.7	−582.6	−542.5	−847.4	−926.6
$\Delta E_{exch}^{(2)}$	62.0	123.0	123.3	71.6	76.9	111.5	105.1

[a] Values originate from S basis set calculations. [b] The value corresponds to $\epsilon_{ind,r}^{(20)}$.

positions of nuclei), prefers the areas of strong overlap of the monomer electron clouds and is largely oblivious to how the electrons are shifted within monomers. The induction energy, although dependent on the overlap too, strongly favors the situations where the electrons are shifted within monomers, i.e. it is sensitive to bond polarization. The ind/disp ratio, best described in the form of $\Delta E_{def}^{SCF}/\epsilon_{disp}^{(20)}$, has proven very useful in our rationalization of why NH_3 does not form H-bond configurations even with very polarizable atoms, such as Kr.[204] It can also be of value in similar analyses of other donor–acceptor complexes such as these discussed in the next section.

The complexes formed by the Be atom have structurally different properties.[205] For example, the Be–NH_3 complex has the C_{3v} structure with Be attached to the lone pair of NH_3. As discussed in section IV.B the position of Be on the C_3 axis is strongly favored by the induction effect which has a deep minimum for this orientation. Conventional wisdom has it that Be–NH_3 is a charge-transfer complex whose directional properties are determined by the HOMO–LUMO interaction. The effects due to delocalization of electrons from the lone pair to the vacant Be orbitals are implicitly included in our ΔE_{def}^{SCF} and $\epsilon_{ind,r}^{(20)}$ (provided the latter is derived in DCBS). The incipient charge transfer manifests itself in these energies by the unusually large $\Delta E_{def}^{SCF}/\epsilon_{disp}^{(20)}$ ratios. One might add at this point that this HOMO–LUMO interaction is not necessarily maximized along lone pairs of electron-donor molecules. Our calculations show that the Be–H_2O complex[205] has the C_{2v} structure, and not a configuration with Be attached to a lone pair of water.

G. Rare Gas–Halogen Molecule Complexes

Since it was experimentally established that two different forms of Rg–halogen molecule complexes exist, a linear form and a T-shaped form, a great deal of attention has been paid to these systems. The Ar–ClF[229] and Kr–ClF[230] complexes adopt linear equilibrium structures, whereas the Rg–Cl_2 systems were found to be T shaped.[231–234] An understanding of the origin of these structures, as well as reliable characterization and modeling of their PESs, proved to be a challenge for experimentalists and theoreticians alike.

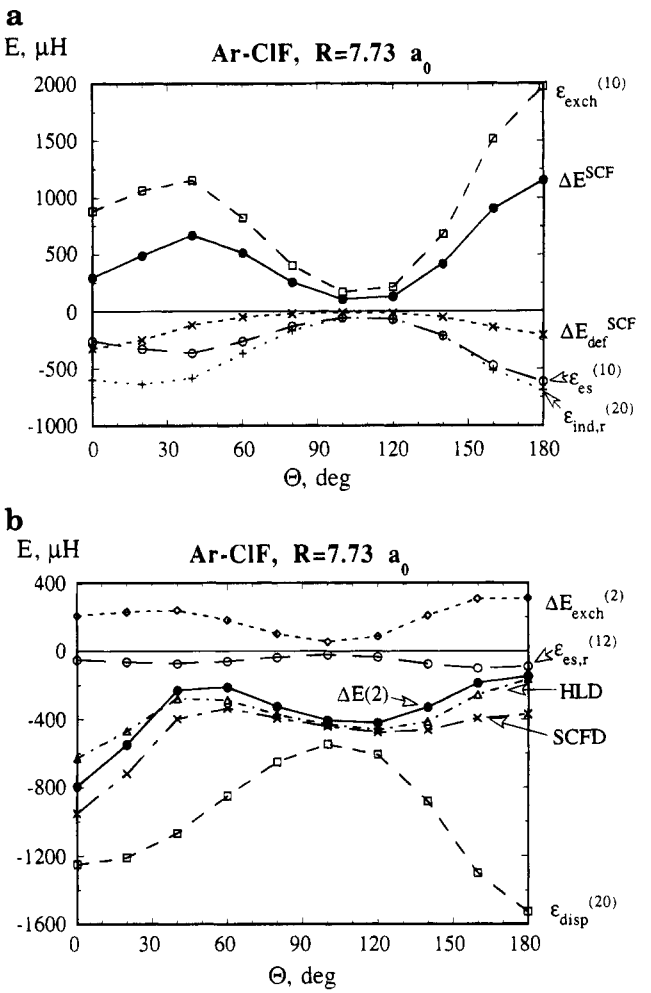

Figure 13. Θ-Dependence of the interaction energy of Ar–ClF at the intersystem distance $R = 7.73$ a_0 corresponding to the equilibrium separation of the global minimum: (a) the SCF interaction energy and its components; (b) the correlated components of the interaction energy. $\Delta E(2)$ denotes the total interaction energy through the second order of S-MP; HLD denotes the $\Delta E^{HL} + \epsilon_{disp}^{(20)}$ approximation; SCFD denotes the $\Delta E^{SCF} + \epsilon_{disp}^{(20)}$ approximation.

1. Ar–ClF

There are two recent ab initio studies of the PES of this complex.[235,236] The anisotropies of fundamental components of Ar–ClF at the SCF and correlated levels, at the distance of the global minimum (R = 7.73 a_0), are shown in Figure 13, parts a and b, respectively, following ref 235. The HL exchange

term (Figure 13a) displays a strong angular dependence with minima at $\Theta = 0°$ and 100°, and maxima at $\Theta = 180°$ and 40°. The SCF interaction energy closely follows the behavior of the HL exchange interaction with minima and maxima at the same Θ values. The less anisotropic SCF deformation component is smaller in magnitude than its nonexchange approximation, $\epsilon_{ind,r}^{(20)}$.

The correlated components are shown in Figure 13b, along with the total interaction energy. The dispersion energy, which provides the most important stabilizing contribution, displays a high degree of anisotropy. It has two minima for $\Theta = 0°$ and 180°, and a maximum for 100°. (The minimum for $\Theta = 180°$ appears deeper than the one for 0° because the Ar—F distance is shorter than Ar—Cl with the present choice of the origin of the coordinate system, see Figure 6d.) Nevertheless, the anisotropy of the total interaction energy (see $\Delta E(2)$ in Figure 13b) more closely resembles that of the SCF energy.

One of the most striking features of the anisotropy of the interaction energy components is the observed minimum in the exchange repulsion for $\Theta = 0°$ which sets a similar trend for the SCF curve (see Figure 13a). The minimum in the exchange repulsion indicates an indentation in the charge distribution around Cl along the molecular axis.

One may conclude that the linear Ar—Cl—F and the T-shaped forms correspond to minima because the exchange repulsion is minimized for those forms. Indeed, the former corresponds to the electron density depletion at the Cl end, and the latter to the electron density depletion in the middle of the bond. The question is, however, why is the linear minimum so much deeper than the T minimum? The second significant factor proves to be the induction effect. There is a relative enhancement of the induction effect for the linear configuration, as the ΔE_{def}^{SCF} term constitutes 22% of the dispersion effect for the linear minimum, but only 2% for the T minimum.

The best estimate of D_e for the global minimum at the MP4/spdf(b-ext) level amounts to 1148 μH (252 cm^{-1}) at $R_e = 7.73$ a_0[237] to be compared with the experimental value of 1061 μH at $R_e = 7.37$ a_0.[229] The accuracy of ab initio D_e is about ±5% and thus the empirical result is expected to be underestimated. The depth of the secondary T minimum estimated at the same level of theory is 710 μH (156 cm^{-1}) at $R_e = 7.23$ a_0, again with ±5% error bars for D_e.[237] There are no experimental data for this structure and previous ab initio estimates were less accurate.[235,236]

The shape of the PES for large R is easy to predict as it is determined by the dispersion and induction components. Therefore, the long-range part of PES exhibits two valleys descending toward smaller R which correspond to two collinear geometries, Ar—Cl—F and Ar—F—Cl, and a barrier in between for bent geometries. For smaller R around the van der Waals minimum the barrier crest splits to form a third, perpendicular valley.

Experimental studies determined that Ar—ClF has a much higher bond energy than the other complexes involving Ar. Also, its bending force constant (k_b) was found to be very high (over 20 times higher than in Ar—HCl). The unusual strength and angular rigidity

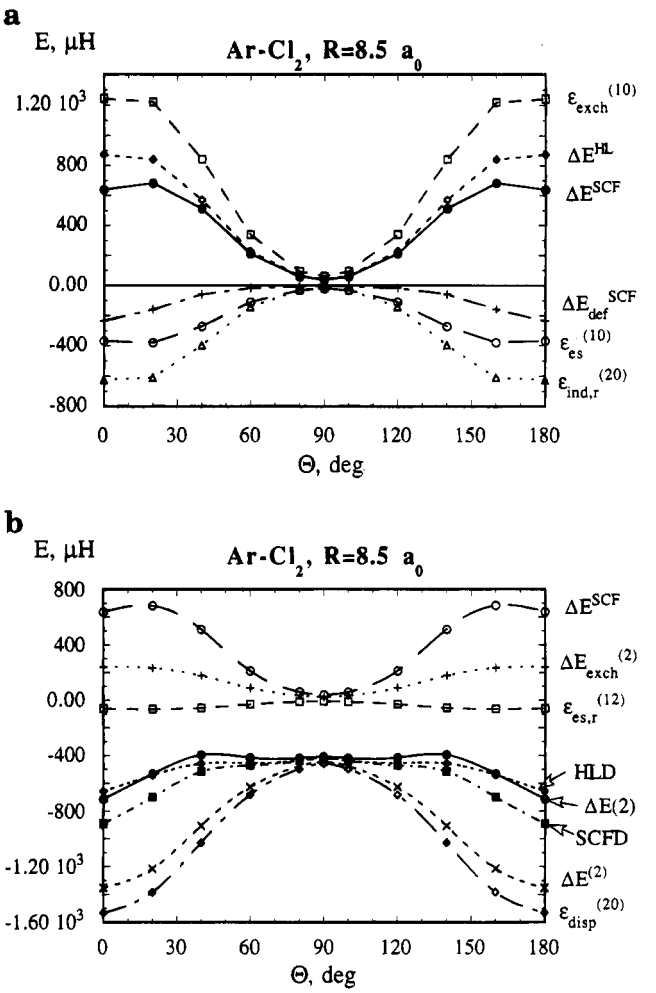

Figure 14. Θ-Dependence of the interaction energy of Ar—Cl_2 at the intersystem distance $R = 8.5$ a_0 corresponding to the equilibrium separation of the global minimum: (a) the SCF interaction energy and its components; (b) the correlated components of the interaction energy. $\Delta E(2)$ denotes the total interaction energy through the second order of S-MP; HLD denotes the $\Delta E^{HL} + \epsilon_{disp}^{(20)}$ approximation; SCFD denotes the $\Delta E^{SCF} + \epsilon_{disp}^{(20)}$ approximation.

of Ar—ClF prompted Harris et al.[229] to explain its properties in terms of an incipient charge transfer from HOMO of Ar to LUMO of ClF. Our calculations indicate that the chief factor in the stabilization of this complex is the depletion in charge distribution at the Cl end of ClF. However, the induction effect, as reflected in the highly attractive ΔE_{def}^{SCF} term, is of some importance too. The charge-transfer hypothesis of ref 229 requires that the SCF-deformation energy should have a significant delocalization component. Indeed, the large def/disp ratio in the linear structure of Ar—ClF suggests this may be the case. Our calculations also examined the sources of the high bending force constant.[235] We found that the induction energy has no effect on k_b, and the rigidity of the van der Waals bond is almost entirely due to the charge depletion on Cl.

2. Ar–Cl_2

The anisotropies of fundamental components of the Ar—Cl_2 interaction at the SCF level and correlated levels of theory at the distance $R = 8.5$ a_0 are shown in Figure 14, parts a and b, respectively, following

ref 237.

The HL exchange term (Figure 14a) displays a strong angular dependence with a minimum at $\Theta = 90°$ and maxima at 0° and 180°. Close to the Cl ends the ϵ_{exch}^{HL} curve flattens, which indicates some depletion of the electron density in this region, similar to the HCl and ClF cases, but to a far lesser degree. Another difference between Cl_2 and ClF is that the maxima and minima of the exchange component are shifted toward F in the ClF case. This is attributed to a shift of the σ-electron density from Cl toward F.[235] The electron density distribution in Cl_2 resembles a dumbbell with slight indentations at its ends. By comparison, the ClF distribution may be viewed as an asymmetric dumbbell with a large dent at the Cl end.

The correlation components are shown in Figure 14b along with the total interaction energy. It is seen that $\Delta E^{(2)}$ is actually determined by the dispersion term. The anisotropies of $\Delta E^{(2)}$ and $\epsilon_{disp}^{(20)}$ favor the Cl ends and strongly disfavor the midpoint of the Cl—Cl bond. Ultimately, the linear minimum is stabilized by the dispersion effect, whereas the T minimum is determined by the least repulsive value of ϵ_{exch}^{HL}.

Our best estimate of D_e for the linear minimum amounts to 1013 μH at $R_e = 8.54$ a_0 and that for the T minimum equals 943 μH at $R_e = 7.16$ a_0. Both values were obtained at the MP4/spdf(b-ext) level and are thus expected to be accurate within ca. ±5%. The energy difference between both minima of ca. 70 μH (15 cm^{-1}), in favor of the linear one, slightly exceeds the error bars.

The shape of the PES at large R may be predicted by examining the anisotropy of the dispersion and induction components. Thus, the long-range part of the PES is characterized by two valleys descending toward smaller R which correspond to two collinear geometries of Ar—Cl_2 (identical because of symmetry), and a barrier for bent geometries. Around the van der Waals minimum the barrier crest splits to form a third, perpendicular valley.

There is a great deal of controversy concerning the geometry of the absolute minimum of Ar—Cl_2. The experimental measurements detect unequivocally the T-shaped form,[233,234] whereas the ab initio calculations consistently predict the linear form as a deeper minimum.[236,237] One plausible argument was advanced by Tao and Klemperer.[236] Namely, the energetical difference favors the linear structure by 70 μH (according to our best estimates[237]). The zero-point energy, on the other hand, favors the T configuration by 82 μH, according to estimates from ref 236. It is doubtful, however, that the harmonic approximation would be valid on such a flat surface. Thus, high-quality dynamics studies are necessary to resolve the problem as to which minimum is preferred.

We should add at this point that in the lowest triplet state of a similar complex, He—Cl_2, the global minimum corresponds to the T configuration[174,238] in agreement with the experimental data.[239] This state is obtained by promoting one electron from π^* orbital to σ^* and results in a change of the shape of the repulsive wall. Due to the fact that the π-symmetry density is diminished and the σ-symmetry density is enhanced, the dumbbell becomes elongated and its ends become convex (as opposed to concave, in the ground state, see above).

Generally, the shape of repulsive wall may have consequences that reach beyond the equilibrium structures of binary complexes. Cl_2 serves as good case in point. The crystal of Cl_2 has been found impossible to describe by using a pair potential involving isotropic atomic interaction sites.[240] To remedy this problem Rodger et al. proposed the use of anisotropic interaction sites which resulted in very good description of properties in all three phases (including lattice dynamics in the solid state!).[241] Our results fully support their idea of representing exchange repulsion around chlorine atom in the anisotropic fashion. The electron density which protrudes in this atom at 20—60° away from the bond axis (in Cl_2, ClF, and HCl) may be interpreted as π-lone pair density which precludes spherically symmetric van der Waals radii.

H. Interaction of CO-Containing Molecules with Ar

The C—O bond in its various valence states is ubiquitous in chemistry and biology. In order to determine how the intrinsic properties of C—O vary depending upon the electronic structure of this bond we have studied the Ar complexes with CO and CO_2 molecules,[242,243] as well as with the simplest molecule containing the carbonyl group, H_2CO.[244] While the chemical properties of these molecules are different, the CO part reveals very similar behavior in the van der Waals complexes with Ar. Below, we describe the Ar—CO complex in more detail and compare it with the other two species.

1. Ar—CO

The PES of the Ar—CO complex has only one minimum related to the T-shaped geometry.[242] The ab initio estimate of bond energy amounts to 496 μH at $R_e = 7.0$ a_0 and $\Theta = 80°$. These values agree very well with the experimental findings of $D_e = 501$ μH at $R_e = 6.86$ a_0 and Θ within the range of 60—80°.[245,246] The approximate MMC model provides similar geometrical parameters (7.20 a_0 and 69°), but considerably overestimates D_e (720 μH).[247]

The anisotropies of fundamental components of Ar—CO interaction at the SCF and correlated levels of theory near the distance of the global minimum ($R = 7.09$ a_0) are shown in Figure 15, parts a and b, respectively. The HL exchange term (Figure 15a) displays a strong angular dependence with a minimum at $\Theta = 80°$, and maxima at $\Theta = 0°$ and $\Theta = 180°$. A much higher maximum around the C atom indicates a more diffuse charge cloud of C than that of O. This feature is also seen in the Bader's plot of the Laplacian of electron density[208] and reflects a larger atomic radius of the C atom. The SCF interaction energy follows the behavior of exchange interaction with minima and maxima at the same Θ values.

The correlated components are shown in Figure 15b, along with the total interaction energy. The dispersion attraction, $\epsilon_{disp}^{(20)}$, which provides the most

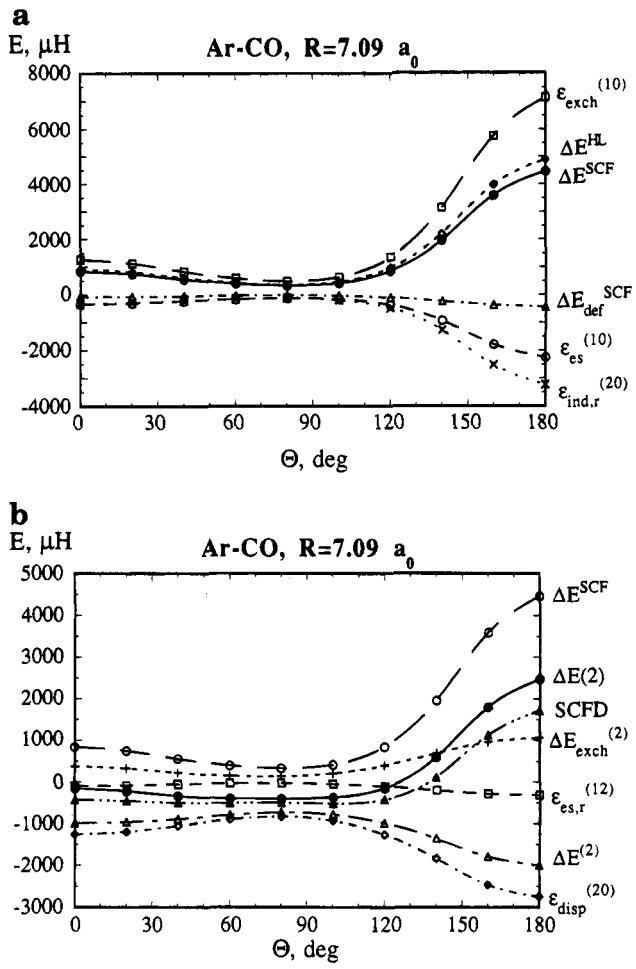

Figure 15. Θ-Dependence of the interaction energy of Ar–CO at the intersystem distance $R = 7.09$ a_0 corresponding to the equilibrium separation of the global minimum: (a) the SCF interaction energy and its components; (b) the correlated components of the interaction energy. $\Delta E(2)$ denotes the total interaction energy through the second order of S-MP; SCFD denotes the $\Delta E^{SCF} + \epsilon_{disp}^{(20)}$ approximation.

important stabilizing contribution, displays a high degree of anisotropy, reciprocal to that of the HL exchange energy. It is maximized at $\Theta = 0°$ and $\Theta = 180°$, and minimized at $\Theta = 80°$. Nevertheless, the anisotropy of the total interaction energy (see $\Delta E(2)$ in Figure 15b) resembles that of the SCF energy. Consequently, the complex adopts the T-shaped form with the Ar atom almost perpendicular to the C–O axis. Two approximate models, HL+disp (HLD) and SCF+disp (SCFD) (see Figure 15b) correctly predict the global minimum structure.

The origin of the anisotropy and the global minimum structure may be interpreted as follows. The CO molecule reveals almost no charge separation, as evidenced by its very small dipole moment. The induction effect is, consequently, small and fairly isotropic. The shape of electron charge cloud resembles that of a dumbbell which agrees with the findings of Bader and Essen.[248] Consequently, the global minimum occurs in the position of the least repulsion, i.e. in the T configuration.

2. Ar–CO_2

The Ar–CO_2 complex PES has a primary minimum related to the T-shaped geometry, and two equivalent secondary minima for the collinear geometries. Ab initio calculations yield the bond energy of 957 μH for the global minimum at $R_e = 6.5$ a_0 and $\Theta = 90°$ [243] in good agreement with the experimental estimate of $D_e = 894$ μH at (6.4 a_0, 90°).[249] The secondary minimum 533 μH at $R_e = 9$ a_0[243] and $\Theta = 0°$ is much deeper than the empirical estimate of 260 μH at $R = 9.4$ a_0.[249] The ab initio well depths are expected to be ±5% accurate.

In the region of C–O bonds the fundamental components reveal similar anisotropy at the terminal oxygens to that in the Ar–CO complex. At the C atom, however, the charge density is depleted, which agrees with the plot of Laplacian of electron density obtained by Bader and Kaith.[250] This depletion is at the roots of the large width and flatness of the primary minimum which coincides with the lowest values of the exchange repulsion term. The induction effect is of secondary importance at both minima, as evidenced by the small ratios def/disp of 7% and 3% at the primary and secondary minima, respectively.

3. Ar–H_2CO

The equilibrium structure of this complex is T-shaped with the Ar atom nearly perpendicular ($\Theta = 100°$) to the CO bond and in the molecular plane of the H_2CO. The ab initio values of R_e and D_e amount to 7.09 a_0 and 780 μH, respectively.[244] The latter value may be underestimated by about 25%. The shape of the total potential surface is complex. Its anisotropy for the in-plane motion of Ar ($\chi = 0°$) resembles that of the Ar–H_2O complex. The anisotropy for the motion of Ar in the perpendicular plane of H_2CO ($\chi = 90°$) is very similar to that of the Ar–CO complex. The induction effect is not significant, as the ratio def/disp amounts to only 11%. The position of the global minimum is determined by the minimal exchange repulsion. As in the case of H_2O, only slight hints of the oxygen lone pairs can be seen in H_2CO. It is conceivable that H_2CO undergoes hindered internal rotation in this complex, as suggested in the experimental microwave study.[251]

I. Concluding Remarks on Anisotropy of Potential Energy Surfaces

The shape of PESs of van der Waals complexes depends on the intrinsic properties of the monomers involved, such as charge distribution, anisotropy of polarizability, and on the ability to generate directional fields. It also varies with the intersystem distance. At short intersystem separations the shape of the electron charge cloud, as reflected by the HL interaction energy, represents the determining factor. At the long separations, where the overlap effects vanish, the properties which are related to the long-range energy components play a significant role in determining the shape of PES. For example, at short distances, and around the equilibrium, the He atom occupies the repulsion-favored T position. At long distances, however, the optimal orientation of He is along the O–H bond of water. By increasing the polarizability of the Rg partner, the balance of the opposing forces can be tilted toward the long-range components. For example, in Kr–H_2O the preferable position of Kr is along the O–H bond already near

the equilibrium distance. In yet another case of the Be−H_2O complex, the optimal attachment of Be is either to the O or to the H end of H_2O. Clearly, the PESs of these three complexes are qualitatively different. However, if we compare all the components of interaction energy in these systems, except for electrostatic, their anisotropies are nearly identical. The diverse PESs in the three cases result from a different balance of exchange, dispersion, and induction components, and in certain instances from a different role of the electrostatic contribution. The similarities are not limited to the H_2O atom case. As will be shown in the forthcoming section, if H_2O interacts with another molecule, we can by freezing the partner in space and rotating H_2O around its center of mass, easily recognize that the exchange, dispersion, and induction anisotropies are strikingly similar to those in H_2O−Rg. Furthermore, the three components have similar shapes even in the H_2O− ion interactions. The electrostatic components show no similarity among the different types of interaction because they are most sensitive to the plus−minus charge separation in the molecule.

These considerations clearly justify the transferability of exchange, dispersion, and induction parameters from molecule−Rg interactions to molecule−molecule interactions. The remaining part of the interaction energy in the latter case corresponds to the multipole electrostatics, which can be easily described in the form of multipole expansion. In view of the fact that it is the *anisotropy* of components which is characteristic of a given molecule, the transferable parameters must be *anisotropic*. In particular, our data clearly support the notion of anisotropic exchange parameters, the idea that has been suggested in the past by Stone and Price.[240] Some attempts to characterize the anisotropy of the exchange repulsion have already been undertaken.[252]

In the next section we will extend the above findings concerning the interactions between a molecule and a spherically symmetric species by substituting the latter for an anisotropic molecule.

J. H_2O−Nonpolar Molecules Interactions

The lack of distinct directionality is often regarded as one of the features that distinguishes the van der Waals interactions from hydrogen bonding. In order to understand the differences between these two types of interaction we can first examine whether there are any intrinsic similarities between them. The study of the Rg−H_2O interactions has revealed the essential elements of the interaction energy in a typical van der Waals complex. When the Rg atom in this complex is substituted by another molecule, the potential energy surface becomes more complex, primarily due to the appearance of new intermolecular degrees of freedom. Furthermore, the interactions of two nonspherical charge distributions lead to the appearance of multipole electrostatic terms which are by nature very anisotropic. The evaluation of the resulting PES is, no doubt, more difficult, and the question arises as to what extent this task could be simplified by applying the insights gained in studying molecule−Rg system to the molecule−molecule system. Let us consider a substitution of Ar in H_2O−Ar by molecules of gradually changing properties, such as octopolar CH_4,[168] quadrupolar H_2,[253] and N_2,[254,255] and weakly polar CO.[256,257]

1. H_2O−CH_4

Probing the H_2O molecule with Rg and Be revealed that water displays a particular ability to form van der Waals bonds if the other species approaches from two distinct directions, either along the O−H bond or from the oxygen side along its C_2 axis. Due to its tetrahedral symmetry, CH_4 can be approached from three distinct directions: the face (F), edge (E), and vertex (V). In the H_2O case, the exchange repulsion is large at the H end and much smaller at the O end. In the CH_4 case, the exchange repulsion favors the F orientation and strongly precludes the V orientation. This eliminates a large number of possibilities, and we are left with three plausible candidates for the equilibrium orientation: F-H, V-O, and E-H, all three involving the H-bonded configurations. As discussed above, a good measure of the H-bond abilities is provided via the induction effect, and this effect, as shown in Table 10, is much stronger when the O−H bond acts as a proton donor than when the C−H bond does. Thus the structure F-H, which involves the C···H−O hydrogen bond, should be more stable than the V-O, which involves the C−H···O bond. The E-H structure also involves the C···H−O bond; however, the exchange repulsion on the edge of CH_4 is expected to be higher than on the face, thus the E-H structure should slide down to the F-H minimum. So far these intuitions have been based solely on the properties of H_2O and CH_4 uncovered through the interactions with Ar. The ab initio calculations fully confirm these predictions.[168] Indeed, the F-H structure represents the global minimum some 99 cm^{-1} more stable than the V-O. The estimated bond energy, D_e, for this configuration amounts to 1320 μH at the C−O separation of 6.8 a_0.[168] This value is underestimated by ca. 10% due to the unsaturation of dispersion energy. The examination of the energy components indicates that the stability of F-H structure results from the weakest exchange repulsion in this orientation, despite the fact that all the other attractive components favor either V-O ($\epsilon_{es}^{(10)}$) or E-H ($\epsilon_{disp}^{(20)}$, ΔE_{def}^{SCF}). The actual ratio def/disp is nearly equal in F-H and V-O configurations.

2. H_2O−H_2

Analogous reasoning suggests that the H_2 molecule can be attached to H_2O either from the O side or along the O−H bond axis. The orientation of H_2 with respect to H_2O is expected to be determined by the electrostatics. The latter could be rationalized by considering that the negatively charged O atom should attract the positive end of the H_2 quadrupole (H atoms), and the H atoms of H_2O should attract the negatively charged midpoint of the H_2 molecule. This leads to two possible structures of the H_2O−H_2 complex. One in which the H_2 approaches the O atom collinearly with the C_2 axis (H−H−OH_2) and the second, in which H_2 is perpendicular to the O−H bond (HO−H−H_2). Both structures are nearly equal in energy, 898 vs 838 μH.[253] These estimates are

most likely underestimated by some 25%. The O approach is favored by the smaller exchange repulsion and by the electrostatic contribution, while the approach along the O−H axis is favored by the other components. As one might have expected, the def/disp ratio strongly favors the O−H approach of H_2.

It should be mentioned at this point that neither CH_4 (in V-O configuration of CH_4−H_2O)[168] nor H_2 (in H−H−OH_2)[253] prefer the orientation along the lone pairs of H_2O. If the potential energy surfaces are properly calculated (i.e. using the counterpoise procedure), the preferred orientations are along the C_2 axis, although the uncorrected surfaces show in both cases minima corresponding to the approach along the lone pairs. This underscores the importance of BSSE removal in gradient optimizations.

3. H_2O–N_2

This interaction is analogous to H_2O−H_2, except for the fact that the quadrupole moment of N_2 is negative instead of positive. As a result, the N_2 molecule approaches the O end in such a way that its bond axis is perpendicular to the C_2 axis of water. In the approach along the O−H bond, the two bond axes, N_2 and O−H, are (nearly) collinear. The latter H-bonded configuration is now the most stable with $D_e = 1943\ \mu$H at R(H−N) = 2.45 Å (accuracy of ±5%). This configuration is also strongly favored by the def/disp ratio in addition to the electrostatic term.[254]

4. H_2O–CO

In this complex the H-bonded configuration is also the most stable, with CO attached along the O−H bond. As above, the orientation of CO is determined by electrostatics. At the HF level, which wrongly predicts the direction of the dipole moment of CO, the orientation H−O−H−CO is predicted as more stable. However, the second-order MP level of correlation already corrects this deficiency, and the second-order electrostatic correlation $\epsilon_{es,r}^{(12)}$ effectively inverses the complex to the correct H−O−H−OC configuration. Actually, both minima are expected to coexist. However, at the correlated level, the latter becomes more stable. The estimate of D_e for this minimum is 2970 μH.[257] The dispersion energy in this calculation is most likely underestimated by some 25%. Due to a peculiar role of electrostatic component in this interaction, though, the overall error bounds are difficult to establish. A more reliable value of well depth in this complex might be obtained from the CCSD(T) calculations.

In summary, a great deal of information is transferable from the Rg−molecule to the molecule−molecule interactions. The optimal orientations of monomers in the latter can be predicted by examination of the favorable exchange and induction sites in the Rg−molecule interactions followed by superimposing the molecule−molecule electrostatic effects. In fact, the similarities go much deeper. We noticed that in the molecule−molecule interactions A−B, if molecule A is kept fixed in space and B rotates around its center of mass, the interaction energy components, except for electrostatics, show very similar anisotropy as in the Ar−B complex. Analogously, if molecule B is fixed and A rotated, the components, except for electrostatics, resemble these of the Ar−A interaction. One example is shown below for the H_2O−CO complex in Figure 16.[257] The figure describes the situation of H_2O fixed and CO rotated (by Θ) around its center of mass. The interaction energy components (indicated as solid lines), exclusive of electrostatics, show clear resemblance to those of Ar−CO interaction (cf. Figure 15a,b). The electrostatic terms, $\epsilon_{es}^{(10)}$ and $\epsilon_{es,r}^{(12)}$, have a crucial effect on the optimal CO orientation in this complex. Although, the former is larger in magnitude, the latter is capable of inverting CO to attain the energetically lower H−O−H−OC orientation.

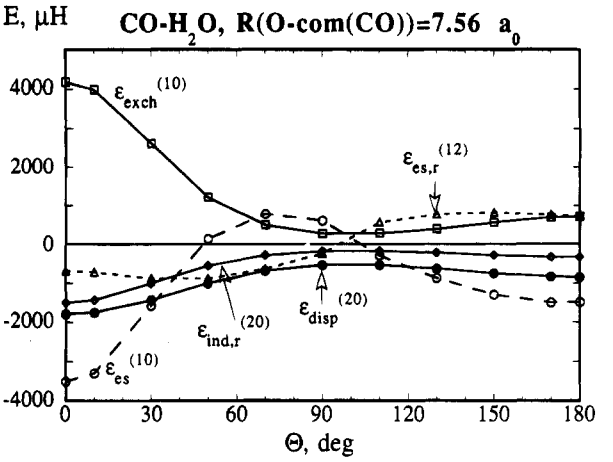

Figure 16. Θ-Dependence of the fundamental components in H_2O−CO at the distance between the O atom of H_2O and the CO center of mass equal to 7.56 a_0. The H_2O molecule is fixed in space and CO rotates by Θ around its center of mass.

K. Interactions between Polar Molecules

van der Waals complexes of polar molecules are primarily bound by the electrostatic interaction. The electrostatic interaction is believed to be responsible for the equilibrium monomer orientations.[216,221] The induction and dispersion components provide additional attraction and they are usually of similar magnitude. We will illustrate these interactions by using three important and representative examples: the HF dimer, the water dimer, and the ammonia dimer.

1. HF Dimer

A fairly complete summary of ab initio calculations has been published recently by Racine and Davidson (ref 258 and references therein). Here, only the most extensive and reliable calculations will be mentioned. First, it is important to comment upon the experimental results. The dissociation energy, D_0, measured by Miller's group,[259] amounts to 4838 μH with an error of less than 5 μH. In order to obtain the binding energy, D_e, which may be directly compared with the ab initio data, the zero-point energy must be included. The problem with the reliable calculation of the latter is that the harmonic approximation proved to be very inaccurate. Quack and Suhm[187] succeeded in calculating the anharmonic zero-point energy for the dimer of 2093 μH to the accuracy of ±10 μH. The anharmonic contribution is significant,

about 289 μH. By using the above zero-point energy, the best empirical estimate of D_e may be obtained as 7116 μH, which is probably no more in error than by $\pm$10 μH. Only this value may be legitimately compared with an ab initio calculated well depth.

The most exhaustive calculations of the PES (in terms of the number of points) has been performed by Kofranek et al.[186,260] who used the coupled electron pair approximation (CEPA). These calculations were used to construct the best semiempirical PES of Quack and Suhm.[187] Since CEPA neglects triples, and the basis set was relatively small (of the "spd" quality), D_e was not very accurate.

Some of the reliable values of D_e include those of Rybak et al.[36] obtained at the MP4 level of theory (6400 μH), and results of Racine and Davidson[258] at the CCSD(T) level of theory (6500 μH). The I-MP result of 7000 μH is worth mentioning. However, it neglected the repulsive exchange correlation contribution. The discrepancy with the empirical value is, thus significant, ca. 10%. The basis sets used in both cases were roughly of the "spdf" standard (no higher than f symmetry polarization functions nor bond functions were used) and, indeed, our "spdf"-quality basis set in Table 6 (Sdf) yields a similar D_e of ca. 6600 μH. However, as shown in Table 6, these results may be improved considerably by adding bond functions. The most elaborate WTdf(b-ext) basis set yields D_e = 6942 μH[185] within 3% of the experimental value. The major contributors to this increment are the dispersion and induction energies. An even better agreement is obtained at the CCSD(T)/Sdf(b-ext) level with D_e equal to 7085 μH.[185] We should be aware, though, that justification of such a close agreement (i.e. below 3%) demands a careful reevaluation of even minor assumptions, such as what equilibrium geometries of monomers and of the dimer should be used, and how they are related to the experimental geometries which are vibrationally averaged. In our calculation[185] the effects of geometry relaxation were estimated at ca. 5 μH.

It is interesting to analyze the source of binding in the HF dimer. One can see in Table 6 that the proportion of attractive components, electrostatic–induction–dispersion, is 9.9:3.0:2.5. The electrostatic energy is an unquestionable leader.

2. H_2O Dimer

Of all van der Waals dimers, the water dimer, and in particular the determination of its binding energy, has been the subject of the largest number of ab initio studies. For a comprehensive bibliography the reader is referred to a recent paper by van Duijneveldt-van de Rijdt and van Duijneveldt[102] and to the recent review by Scheiner[261] (cf. also ref 262). In contrast to $(HF)_2$, D_o has not been determined with spectroscopic accuracy and the commonly accepted experimental range for D_e is frustratingly wide, 8600 $\pm$ 1100 μH (5.4 $\pm$ 0.7 kcal/mol).[263] In fact, the ab initio estimates of van Duijneveldt-van de Rijdt and van Duijneveldt should be considered as more reliable. Their R(O–O) of 5.573 a_0 is very close to experimental, and the authors offer many indirect arguments that their result of D_e = 7540 $\pm$ 160 μH (4.73 $\pm$ 0.1 kcal/mol) is reliable.[102] One might add here that the basis set and methodological standards of this work are expected to produce an error no larger than 5% (0.2 kcal/mol). These results also closely agree with the extended calculations of Rybak et al.[36] which resulted in D_e = 7490 $\pm$ 320 μH (4.7 $\pm$ 0.2 kcal/mol) by means of I-MP and "spdf" quality basis set, and those by Feller[166] with D_e = 7100 $\pm$ 560 μH (4.46 $\pm$ 0.35 kcal/mol) by means of MP4 with the aug-cc-pVTZ basis which is an "spdf" quality basis set.

In summary, the growing evidence from high-quality ab initio calculations suggests that the well depth of the water dimer potential is far less than the commonly accepted value of 5.4 kcal/mol. The value D_e = 7540 $\pm$ 160 μH (4.73 $\pm$ 0.1 kcal/mol) obtained by van Duijneveldt-van de Rijdt and van Duijneveldt is the most reliable. In fact, the same strategy applied to the HF dimer yields D_e within 3% of the empirical value. The existing analytical potentials for water which were designed to match D_e of ca. 5.4 kcal/mol are bound to fail. Hopefully, the far-IR spectroscopy measurements will help resolve the present discrepancy between ab initio data and experiment.[264]

It is interesting to analyze the source of binding in the H_2O dimer. Close to the minimum, the proportion of attractive components, electrostatic–induction–dispersion, is 11.2:2.7:2.9, which is remarkably similar to the HF dimer case in that the electrostatic energy is the major factor.

3. NH_3 Dimer

Among the three dimers considered in this section, the NH_3 dimer is the most difficult and controversial. Even the equilibrium structure is a matter of hot debate, not to mention quantitative results for D_e.[212,213,265–266] (See also ref 267 for popularized account of this debate.)

The microwave studies seemed to support a cyclic asymmetric dimer (χ = 60°, in Figure 6h) with a rigid structure and a small dipole moment.[265,266] The ab initio calculations,[268–273] by and large, predicted a nonrigid dimer with very flat minimum region encompassing the cyclic symmetric (C_{2h}) and H-bonded (C_s) structure as shown in Figure 17. A small dipole moment was postulated to result from vibrational averaging.[269,271] A similar picture has emerged from the VRT study by Loeser et al.[212] and its analysis by van Bladel et al.[213] which found the dimer nonrigid in a number of degrees of freedom. Although it is now widely accepted that the dimer can move almost freely between a cyclic symmetric and an H-bonded structure, the qualitative details vary from one ab initio study to another. The first study employing moderate basis sets found that the cyclic centrosymmetric dimer (χ = 0° in Figure 6h) is more stable than the H-bonded C_s structure.[269] The more extensive studies, which applied the larger basis sets and gradient optimization,[271,272] indicated that a nearly linear hydrogen-bonded geometry was the equilibrium configuration, and the barrier to proton donor–acceptor interchange was small (e.g. 160 μH in the study by Hasset et al.[271]). The debate concerning the equilibrium structure appeared to have been resolved in favor of the linear H-bonded structure. However, in their recent study employing the extended basis

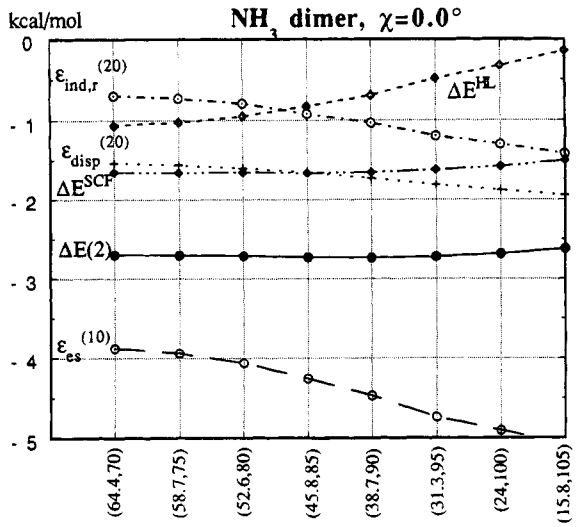

Figure 17. Lowest energy path between the cyclic (see Figure 6j) and the hydrogen-bonded structure of $(NH_3)_2$ calculated with S basis set. The values on the horizontal axis correspond to (Θ,Θ') angles; for a given value of Θ' the angle Θ was optimized.

sets and bond functions, Tao and Klemperer[273] suggested the centrosymmetric cyclic structure as the absolute minimum. The energy difference between this minimum and the hydrogen-bond geometry was found to be extremely small (54 μH), of the order of 1% of the total interaction energy. The cyclic minimum appeared as a result of the use of bond functions, which according to the authors' assertion, alleviated the geometrical bias inherent to the atom-centered basis sets. Shortly thereafter the calculations by Cybulski,[274] which employed energy partitioning and the most elaborate basis set so far, called the results of Tao and Klemperer[273] into question. He demonstrated that some slight improvements in the basis set of ref 273 led to the minimum of the C_s symmetry. One important finding of this work is that the inclusion of bond functions may cause large distortions (percentage-wise) in the electrostatic correlation, $\epsilon_{es,r}^{(12)}$, term. The magnitude of these distortions was found to strongly depend on the quality of the basis set on the H atoms, and on the position of bond functions (as discussed earlier, section III.A.2, the position of bond functions does not affect the dispersion energy). Cybulski's results showed that these distortions, which were of the order of the $C_{2h}-C_s$ energy difference, led to the higher stabilization of the C_{2h} minimum in the work of Tao and Klemperer.[273] When the basis set effects on $\epsilon_{es,r}^{(12)}$ were minimized, the C_s minimum was found to be more stable than C_{2h} by some 45 μH. When the $\epsilon_{es,r}^{(12)}$ term was totally eliminated (by using the SCF+disp model), the C_s structure appeared more stable by 150 μH. It seems that the interpretation given by Tao and Klemperer[273] that using bond functions reduces the geometrical bias of atom-centered basis sets might have been too optimistic. It is clear that the inclusion of bond functions causes distortions in the electrostatic correlation effect due to the appearance of an auxiliary center in the electrostatic term. Thus, contrary to Tao and Klemperer's suggestions, the bond functions may *cause a geometrical bias*. To minimize this bias it is necessary to saturate the electrostatic correlation effect (which may be difficult in view of the fact that it is an intrasystem correlation effect), or at least minimize the basis set effects on this term. Notwithstanding the uncertainties in the nature of the minimum region, the value of $D_e = 4753$ μH (MP2) provided by Tao and Klemperer should be, according to our experience, reliable within ±5%. (Cybulski's result at the same level amounts to 4712 μH.[274]) Clearly, further studies of the interconversion path of the NH_3 dimer are necessary. Elucidation of the shape of this region is absolutely necessary to obtain a better agreement between the experimentally observed properties of this dimer and those calculated via the vibrational averaging using the existing PES.[213] A review of the latest results on the subject of vibrational averaging in this system by van der Avoird et al. can be found in this volume.[275]

It is interesting to analyze the source of binding in the NH_3 dimer. Close to the minimum, the ratio of attractive components, electrostatic–induction–dispersion, is 9.2:3.6:6.2, which differs markedly from the HF dimer, and the H_2O dimer in that the role of dispersion energy is dramatically enhanced. This also means that the NH_3 dimer should be more basis set demanding than $(HF)_2$ and $(H_2O)_2$.

Among the three dimers the HF dimer appears to be the most thoroughly studied, both ab initio and experimentally. The water dimer seems to be well characterized by ab initio calculations, but more accurate experimental measurements are necessary. Finally, for the ammonia dimer a great deal of fine experimental data exists at present, but their analysis requires a highly reliable ab initio PES which has not been generated so far. This system reveals the most interesting dynamics involving wide amplitude motions of monomers and possibly the interchange tunneling.[213]

V. Ab Initio Studies of Nonadditive Effects

In section II.F the theoretical aspects of many-body interactions have been described. Because the electrostatic component of interaction energy is additive, there are only three fundamental components of any nonadditive interaction: exchange, induction, and dispersion. The perturbational contents of the S-MP perturbation theory nonadditivies in any given order are listed in Table 3. In the study of nonadditive energies the following strategy proves useful: The S-MP calculations are carried out to evaluate the three-body components of ΔE^{SCF}, $\Delta E^{(2)}$, and $\Delta E^{(3)}$, and next, these components are analyzed in terms of I-MP-derived ϵ_{exch}^{HL}, $\epsilon_{ind,r}^{(20)}$ (or $\epsilon_{ind}^{(20)}$), $\epsilon_{ind,r}^{(30)}$, and $\epsilon_{disp}^{(30)}$ nonadditivities.[122,123,190,191,276–279] In the case of purely dispersion-bound clusters this strategy may be insufficient, as the accurate treatment of the dispersion nonadditivity requires advanced correlational approaches which allow for the inter–intra correlation coupling[125] (see below). In forthcoming sections the studies of nonadditive effects in a number of clusters ranging from nonpolar to polar will be discussed. The coordinate systems used in these studies are displayed in Figure 18.

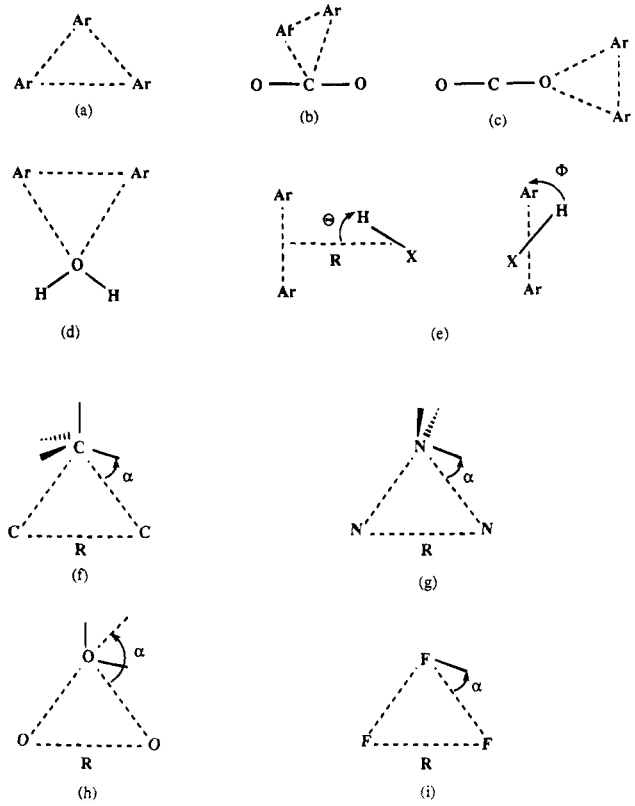

Figure 18. Definition of geometrical parameters of trimers discussed in section V. For clarity in f, g, h, and i only one monomer is explicitly shown.

A. Comparison of Nonadditive Interactions in Trimers Involving Ar_2

In trimers containing a pair of rare gas atoms the total nonadditivity is repulsive for geometries which are close to trimer minima. Table 11 shows a comparison of a few trimers which contain an atom, quadrupolar molecule, and polar molecule in addition to Ar_2 (the geometries of these trimers are shown in Figure 18). In triangular Ar_3 the nonadditivity is dominated by two opposing effects: the HL exchange nonadditivity which is attractive, and the dispersion nonadditivity which is repulsive. The three-body $\Delta E^{(2)}$, which in this case is governed by second-order exchange effects, is also sizable. A similar pattern is retained in trimers containing a quadrupolar molecule. In trimers containing a polar molecule the polarization nonadditivity becomes equally important to the other components.

To illustrate the dependence of nonadditive terms upon the orientation of a molecule in a trimer we display (Table 11) two configurations for Ar_2CO_2[243] and Ar_2HCl[122,279] trimers corresponding in each case to the global and secondary minima. The dispersion and second-order exchange nonadditivities vary weakly with orientation. The HL exchange nonadditivity, on the other hand, is very strongly orientation dependent and so is the induction nonadditivity. While the latter can be easily explained by considering the direction of the polarizing field, the former seems to elude simple rationalization. For example, in the equilibrium Ar_2HCl triangular complex where the H−Cl, pointing with its H end, is perpendicular to the Ar—Ar axis (Figure 18e, $\Theta = 0°$), the exchange nonadditivity is repulsive, while in the secondary minimum Ar_2ClH, where the HCl molecule is rotated 180°, this effect is negative. As discussed in section II.F, the concept of electrostatic interactions involving the "exchange quadrupole" on Ar_2 can help rationalize at least the sign of this effect. The interaction of exchange quadrupole with the positive end of HCl should be repulsive, as is the case of the Ar_2HCl configuration, and the interaction of the exchange quadrupole with the negative end of HCl should be attractive, as is the case of Ar_2ClH. In the second system, Ar_2CO_2, the sign of the exchange nonadditivity in the two configurations of the Ar_2CO_2 cluster (see Figure 18b,c) can also be explained in terms of this model if we keep in mind that the quadrupole moment of CO_2 is negative. The same explanation can be used to justify the large negative value of the HL exchange nonadditivity in Ar_2H_2O. This complex has a configuration in which the C_2 axis of water is perpendicular to the Ar—Ar axis and H_2O points to Ar_2 with its O end (see Figure 18d). Below we will justify such semiqualitative predictions on the rigorous basis.

B. Comparison of Nonadditive Effects in Trimers of Hydrides

A summary of the calculated values of nonadditive interaction in five such trimers is shown in Table 12. One of the trimers is composed of nonpolar monomers; the remaining ones are polar. All the clusters are considered in the geometry of the equilateral triangle with C_3 (or C_{3h}) point group symmetry. The orientational angles of the monomers with respect to the triangle skeleton are optimal (or nearly so).

Of the five trimers, the $(CH_4)_3$ trimer behaves more like Ar_3 than the other polar clusters. This is, of course, due to the fact that the first nonvanishing multipole moment of CH_4 is the octopole moment and its van der Waals radius is close to that of Ar. Obviously, the anisotropy of the three-body interaction in $(CH_4)_3$ is more complex than that of Ar_3.

The nonadditivity in polar clusters is entirely dominated by the polarization effect. The HL exchange nonadditivity is 1 to 2 orders of magnitude smaller than the polarization, and so is the three-body dispersion. The overall three-body interaction is thus well approximated at the SCF level. As stated before, the best representation of the polarization nonadditivity is via the three-body SCF-deformation term. Its nonexchange approximation, $\epsilon_{ind}^{(20)}$, may underestimate it by nearly half (as in the case of $(HF)_3$), which is largely due to the neglect of the exchange effects, as well as the absence of orbital relaxation.

The values in Table 12 may create the impression that the exchange nonadditivity is unimportant in polar clusters considered here. However, the values presented describe the situation in the equilibrium trimers. As the monomer orientations are allowed to vary, this impression is only partially valid (see Figures 19−22). The dependence of the SCF components, HL exchange and SCF deformation, is shown as a function of the angle α which describes the orientation of monomers with respect to the triangle skeleton (orientation angles are varied in the

Table 11. Nonadditive Terms in Ar_2-Containing Trimers (All Values in μH)

nonadditivity	Ar_3[a]	Ar_2CO_2[b]	Ar_2CO_2[c]	Ar_2H_2O[d]	Ar_2HCl[e]	Ar_2ClH[f]	Ar_2HF[g]
ϵ_{exch}^{HL}	−14.6	0.8	−10.7	−14.7	4.8	−0.9	24.9
ΔE_{def}^{SCF}	−1.4	1.4	1.1	5.9	11.5	0.8	30.8
$\epsilon_{ind-r,mult}^{(30)}$	0				10.7	−0.2	27.6
ΔE^{SCF}	−16.0	2.2	−9.6	−8.8	16.3	−0.1	55.7
$\Delta E^{(2)}$	9.2	3.1	5.7	6.2	8.3	4.6	−10.0
$\epsilon_{disp}^{(30)}$	19.6	23.3	16.4	9.5	30.6	19.0	21.5
$\Delta E^{(3)}$	17.7	22.7	15.3	9.4	26.3	17.7	20.2
$\Delta E(3)$	10.9	27.9	11.5		50.9	22.2	65.9

[a] From ref 276, equilateral triangle geometry, R(Ar—Ar) = 7 a_0. [b] From ref 243, geometry in Figure 18b, r(Ar—Ar) = 7.1 a_0, r(C—Ar) = 7 a_0. [c] From ref 243, geometry in Figure 18c, r(Ar—Ar) = 7.1 a_0, r(C—Ar) = 9 a_0. [d] From ref 197, geometry in Figure 18d, r(Ar—Ar) = 7.5 a_0, r(O—Ar) = 7.09 a_0. [e] From refs 122 and 183, geometry in Figure 18e, $\Theta = 0°$, R = 6.564 a_0. [f] From refs 122 and 279, geometry in Figure 18e, $\Theta = 180°$, R = 6.409 a_0. [g] From ref 122, geometry in Figure 18e, $\Theta = 0°$, R = 5.631 a_0.

Table 12. Nonadditive Terms in Trimers of Hydrides (Geometries Shown in Figure 18f–i) (All Values in μH)

nonadditivity	$(CH_4)_3$[a]	$(NH_3)_3$[b]	$(H_2O)_3$[c]	$(HCl)_3$[d]	$(HF)_3$[e]
ϵ_{exch}^{HL}	−5.2	−68.7	−89.8	−3.7	−175
ΔE_{def}^{SCF}	−0.3	−1233.2	−1558.1	−389	−2364
$\epsilon_{ind}^{(20)}$	−0.2	−835.3	−942.3	−265	−1297
ΔE^{SCF}	−5.6	−1301.9	−1648.0	−393	−2539
$\Delta E^{(2)}$	3.7	4.6	23.5	5.9	−112
$\epsilon_{disp}^{(30)}$	15.5	65.0	36.0	19	15
$\Delta E^{(3)}$	15.4	65.0	46.5	25	75
$\Delta E(3)$	13.5	−1232.3	−1578.0	−362	−2576

[a] From ref 191, R = 7.899 a_0, $\alpha = 70°$. [b] From ref 190, R = 6.236 a_0, $\alpha = 15°$. [c] From ref 277, R = 5.67 a_0, $\alpha = 75°$. [d] From ref 278, R = 7.814 a_0, $\alpha = 24.3°$. [e] From ref 278, R = 5.16 a_0, $\alpha = 26.9°$.

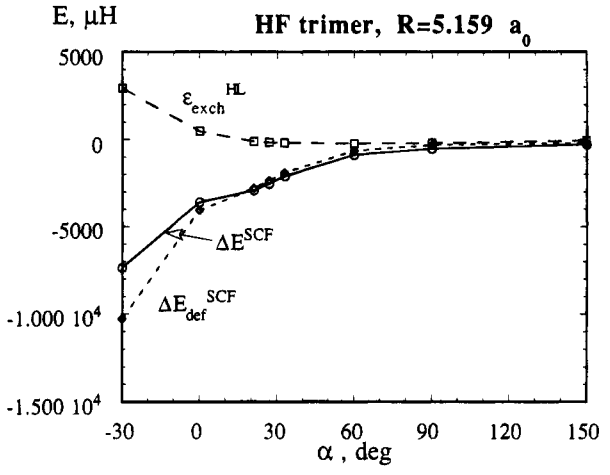

Figure 19. α-Dependence of the three-body components of the SCF nonadditive interaction of $(HF)_3$ in a C_{3h} geometry, R = 5.159 a_0.

concerted fashion). In $(HF)_3$ the SCF nonadditivity is indeed nearly fully determined by the SCF-deformation term. Some role of exchange is present when the H atoms point to the center of the triangle ($\alpha = 30°$) which causes strong steric repulsion. The H_2O trimer is similar in this regard; the SCF-deformation nonadditivity is clearly dominant. In the trimer of ammonia, though, the anisotropy of the SCF nonadditivity closely resembles that of the HL exchange, albeit the curves are far apart on the energy scale. Finally, in the CH_4 trimer the SCF deformation is not important at all, and the entire nonadditivity is a combination of the exchange effects

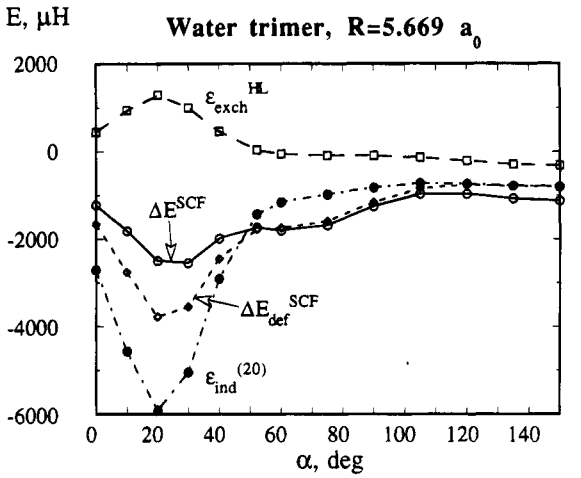

Figure 20. α-Dependence of the three-body components of the SCF nonadditive interaction of $(H_2O)_3$ in a C_{3h} geometry, R = 5.669 a_0.

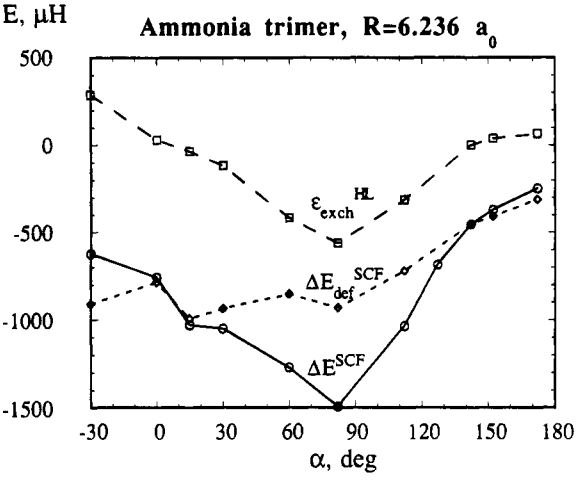

Figure 21. α-Dependence of the three-body components of the SCF nonadditive interaction of $(NH_3)_3$ in a C_{3h} geometry, R = 6.236 a_0.

(HL and second order) and of dispersion. We may thus conclude that in the trimers of polar systems the polarization effect dominates the overall nonadditivity if strong proton donors (HF, H_2O) are involved. The exchange nonadditivity, on the other hand, plays a significant role in trimers involving weak proton donors.

A comment regarding the basis set dependence of nonadditive energies in polar clusters is in order at this point. As discussed previously (see section

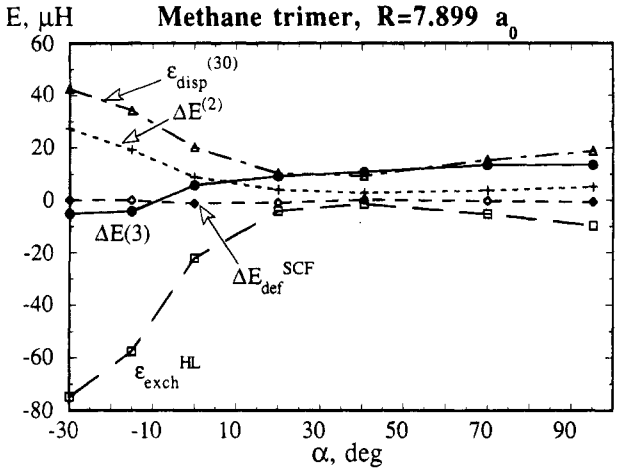

Figure 22. α-Dependence of the three-body components of the SCF nonadditive interaction of $(CH_4)_3$ in a C_{3h} geometry, R = 7.899 a_0.

III.A.2), the two most basis set dependent components of the interaction energy are the electrostatic and dispersion energies (at any level). The former is additive, so this factor is entirely eliminated from the nonadditive interactions. The latter plays only a minor role in polar clusters, as shown above. Thus the basis set dependence of many-body energies in these clusters is limited to the effects pertaining to the exchange and induction energies. These components, as demonstrated in section III.A.2, are fairly basis set independent and can be easily saturated in basis sets of moderate size. The fact that these terms are derived within the TCBS regimen only improves their description. Therefore, in the polar cluster calculations we may expect that the three-body effects will be better saturated than their two-body counterparts.[278] It is recommended that more computational effort in terms of basis set size be devoted to the two-body interactions.

C. Water Trimer

Among the hydrogen-bonded trimers $(H_2O)_3$ has been the most thoroughly studied. The early MBERS experiments indicated that the trimer has no dipole moment, i.e. it is probably cyclic.[280] Ab initio studies at a moderate level of sophistication confirmed that the structure is indeed cyclic and found a nonsymmetric (i.e. chiral) trimer with two free O—H bonds above the plane of the three O atoms, and the third O—H bond below.[281] In 1992 Pugliano and Saykally[282] directly observed one intermolecular IR transition which they assigned to an inversion motion between the two enantiomers of $(D_2O)_3$ with a tunneling splitting superimposed (see also ref 283). They postulated that the interconversion between the enantiomers involves the flipping of one of the free O—H bonds to the other side of the O_3 plane. This work precipitated a number of theoretical studies of the structure, energetics, and dynamics of the trimer.[284-287] Calculations at higher levels confirmed the earlier predictions that the trimer is the cyclic C_1 species. A fairly reliable trimer stabilization energy of Xantheas[285b] obtained at MP2/aug-cc-pVTZ level amounts to −22100 μH (−13.87 kcal/mol) out of which ca. 16% corresponds to the three-body interaction. This result is probably accurate to within 5−10%. Unfortunately, no MP3 values were reported in this work[285b] to better judge the quality of the three-body contribution. Our own earlier calculations with the idealized C_{3h} geometry of $(H_2O)_3$ (R = 5.669 a_0, and no monomer relaxation) yield a smaller percentage contribution of the nonadditive effects (less than 10%).[277] Another reliable study by van Duijneveldt-van de Rijdt and van Duijneveldt[286] yields the trimer D_e = 23400 μH (14.7 kcal/mol) and D_0 = 16200 μH (10.2 kcal/mol) at MP2. A detailed ab initio study of pathways to rearrangement, which included three flipping coordinates, established that the barrier to interconversion of the two enantiomers is very low of ca. 160 ± 160 μH (or 0.1 ± 0.1 kcal/mol)[287] and involves a transition state with the flipping O−H lying in the O_3 plane. Studies of the PES and nuclear dynamics of this trimer will no doubt continue. It is clear, that any PES of this trimer which would be suitable for dynamics studies must include the three-body interaction.

D. Prototypical Anisotropic Trimers: Ar_2HCl and Ar_2HF

One of the main problems which arises in studies of nonadditivity is the fact that the pair potentials are usually unknown experimentally. This is particularly true of the interactions involving molecular species. This fact generally precludes the verification of the calculated three-body potentials using experimental information, as it is often done in the case of rare gases where such pair potentials are known with very high precision. There exists a handful of Rg−molecule systems where the accurate semiempirical two-body potentials have recently been derived by the inversion of the microwave and IR data. For example, the potentials for Ar−HF[288] and Ar−HCl[195] interactions have been advanced by Hutson with spectroscopic accuracy. Given the fact that the Ar−Ar potential is accurately known, the Ar_2HCl and Ar_2HF clusters have become extremely attractive targets for the study of nonadditive forces.

The most interesting region of PES for these clusters involves variations of angles Θ and Φ as defined in Figure 18e. These angles are related to the three bending vibrational frequencies which correlate with the j = 1 rotational states of free HX (X = F, Cl). These frequencies have recently been observed spectroscopically by Saykally and co-workers for Ar_2HCl.[289]

The three-body effects provide a sizable contribution to the interaction energy of both clusters.[122] In the equilibrium Ar_2HF trimer (Θ = 0°) the total nonadditivity evaluated through the MP3 amounts to 66 μH. In the equilibrium Ar_2HCl trimer (Θ = 0°) the analogous value amounts to 51 μH. Due to the basis set unsaturation of the dispersion component, both values are likely to be underestimated. The three-body effects modify the shapes of the total potentials in both clusters.[279] For the in-plane variations of Θ, the nonadditivity in Ar_2HCl makes the potential well shallower in the equilibrium region and around the secondary minimum (Figure 23). In Ar_2HF it leads to the appearance of a double minimum near the equilibrium with the barrier of ca. 12

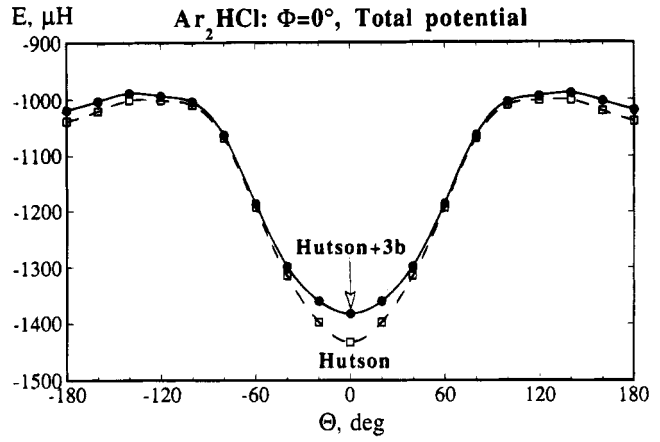

Figure 23. Total interaction of Ar_2HCl as a function of the Θ angle at $\Phi = 0°$ and $R = 6.564$ a_0 (see Figure 18e). The dashed line describes the two-body potential; the solid line corresponds to the sum of the two-body potential and the ab initio three-body potential. The two-body potential is the semiempirical Ar−HCl potential of Hutson (ref 195); the Ar—Ar interaction which is constant during this motion is omitted.

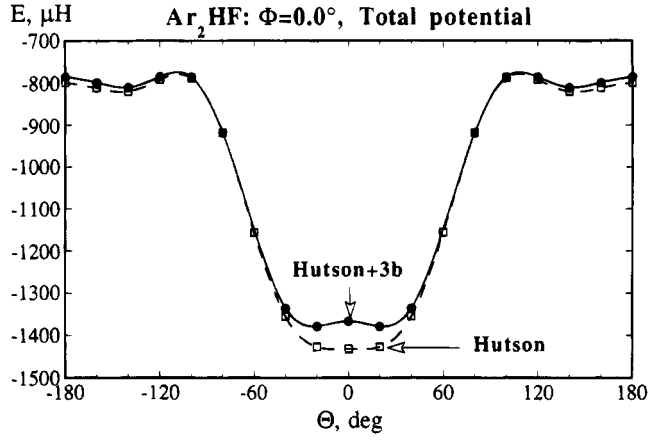

Figure 24. Total interaction of Ar_2HF as a function of the Θ angle at $\Phi = 0°$ and $R = 5.631$ a_0 (see Figure 18e). The dashed line describes the two-body potential; the solid line corresponds to the sum of the two-body potential and the ab initio three-body potential. The two-body potential is the semiempirical Ar−HF potential of Hutson (ref 288); the Ar—Ar interaction which is constant during this motion was omitted.

μH (Figure 24). These conclusions follow from the comparison of our ab initio three-body terms with the accurate two-body potentials of Hutson.[195,288] For the out-of-plane Θ variations, the three-body terms have smoothing effects on the potentials for Ar_2HCl and Ar_2HF.

The behavior of fundamental nonadditive components for Ar_2HCl is shown in Figure 25a (SCF components) and in Figure 25b (correlated components). It should be stressed that in both trimers the overall nonadditive component follows rather well the behavior of the SCF nonadditivity. The total nonadditivity displays a sharp maximum at $\Theta = 0°$, a minimum near $\Theta = 90°$, and another flat maximum around $\Theta = 180°$. This shape results from an interplay of the three fundamental nonadditivities (see Figure 25a). The broad minima are chiefly determined by the exchange effect. In the equilibrium region, the induction effect displays a strong anisotropy. The dispersion effect, which is quite

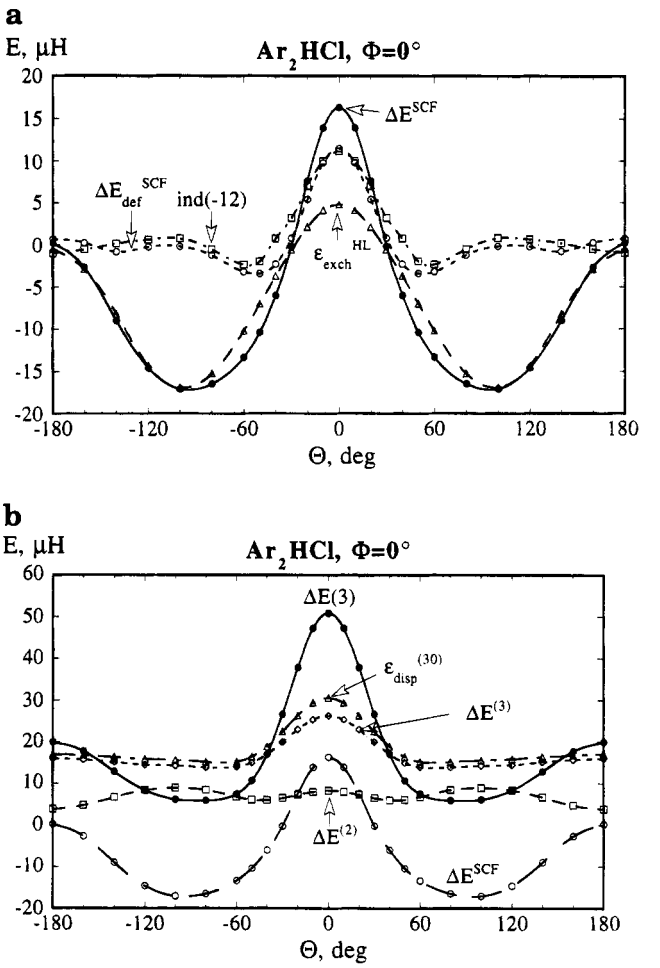

Figure 25. Θ-Dependence (at $\Phi = 0°$, $R = 6.564$ a_0) of the nonadditive components in Ar_2HCl: (a) the SCF nonadditivity and its three-body components (exchange ($\epsilon_{exch}^{(HL)}$), SCF-deformation (ΔE_{def}^{SCF})); "ind(−12)" denotes the multipole approximated $\epsilon_{ind,r}^{(30)}$ term evaluated through R^{-12}; (b) the correlated three-body components; "$\Delta E(3)$" denotes the total three-body contribution evaluated through the third order of S-MP.

sizable in Ar_2HCl (and less so in Ar_2HF), is much less anisotropic than the other two. Both dispersion and induction effects can be modeled using the multipole expansion. The analytical formula for the exchange term can be based on the "exchange quadrupole" model proposed by Cooper and Hutson.[117] As discussed previously in section II.F, these authors proposed to interpret the anisotropic part of the three-body exchange effect in terms of the electrostatic interaction between the overlap-induced quadrupole moment of Ar_2 (the so-called exchange quadrupole) and permanent moments of HX. Such an approach can be easily verified by the ab initio calculation of the electrostatic effect in the system in which we replace the trimer Ar_2HX by a dimer composed of the Ar_2 and HX monomers. The three-body HL exchange term can then be defined as the following sum:

$$\epsilon_{exch,ABC}^{HL} = ES3 + X3 \qquad (14)$$

where ES3 is expressed as:

$$\mathrm{ES3} = \epsilon_{es}^{(10)}(\mathrm{Ar_2{-}HX}) - \epsilon_{es}^{(10)}(\mathrm{Ar'{-}HX}) - \epsilon_{es}^{(10)}(\mathrm{Ar''{-}HX})$$

where Ar′ and Ar″ are the two participating Ar atoms. ES3 is thus a nonexpended electrostatic energy change arising due to the exchange-induced rearrangement in the electron density of Ar_2, and X3 its exchange counterpart. More insights into the properties of these terms are gained via the examination of their radial (R coordinate in Figure 18e) dependence.[279] As it turns out, ES3 varies as R^{-n} while X3 decays exponentially. It is known that the HL-exchange nonadditivity can be expanded in powers of the intermolecular overlap integral S. ES3 was shown to gather terms proportional to S^2. The S^2 terms contain among other things Coulomb integrals which decay as R^{-n}.[116] X3, on the other hand, includes terms which are proportional to S^3 (and higher powers) which decay exponentially. We can thus conclude that ES3 represents the effect of exchange within pairs of monomers and is of the long-range character. X3 involves effects of exchange among all three monomers and has a short-range character. The former should be strongly anisotropic and dominate asymptotically, while the latter should be important only at short distances. As was mentioned earlier, ES3 can be easily described using the multipole expansion. It is yet unclear how to model the X3 term.

It should be mentioned that two semiempirical attempts have already been undertaken by Hutson and co-workers to reconstruct the three-body potential of Ar_2HCl on the basis of spectroscopic data.[117,290] Such an effort requires an assumption of some model of the three-body potential. Upon its addition to the two-body potentials, the Schroedinger equation for nuclear motions is solved for spectroscopic observables. The adjustable parameters in the potential can then be set to accurately reproduce the vibrational frequencies and rotational constants. This is not a trivial undertaking, since, as we tried to demonstrate above, the understanding of various nonadditive components, and the means of their representation, is a task which has only just begun. Certainly, the ab initio approach represents an invaluable tool toward such an understanding. The availability of the semiempirical three-body potentials, on the other hand, is essential to assessing the accuracy and the basis set dependence of ab initio terms. Both semiempirical attempts[117-290] were quite successful in that they provided significant new insights into the dynamics of Ar_2HCl. They also stimulated a great deal of experimental work on this cluster.[289]

E. Dispersion Nonadditivity in Rare Gas Trimers

Nonadditivity of interaction energy in clusters of rare gases is dominated by two effects of different origins. One is the exchange nonadditivity, and the other is the dispersion effect. The former can be routinely calculated with very good accuracy. Already, the Hartree−Fock level calculations provide quite a satisfactory description of the exchange nonadditivity. The latter, however, requires advanced correlated treatments. These unequal requirements have in the past led to some problems with the modeling of bulk properties (see ref 114 and references therein). The problem is well summarized in the quote from this review:[114] "A central question is concerned with why the model of reliable two-body potential plus triple-dipole dispersion (DDD) often works so effectively when it is known that other nonadditive interactions of the same magnitude as DDD are not included in the model". Clearly, our present methods of calculation of dispersion nonadditivity are inadequate, and a proper framework for the accurate treatment of this term should be established.

The two-body dispersion energy has been the subject of exhaustive studies, and the methods of its evaluation are pretty well established due to the efforts of Jeziorski, Szalewicz, and co-workers (see section II.A). By using the I-MP formalism,[35,37] supported by the diagrammatic many-body perturbation theory,[32,33] the following hierarchy of dispersion-type corrections is obtained which can be easily classified according to the degree of the intrasystem correlation effects on dispersion:

two-body:

$$\epsilon_{disp}^{(20)},\ \epsilon_{disp}^{(21)},\ \epsilon_{DQ,disp}^{(22)},\ \epsilon_{SDQ,disp}^{(22)},\ \epsilon_{SDQT,disp}^{(22)} \quad (15)$$

where the second index in the $\epsilon_{disp}^{(ij)}$ corrections refers to the intrasystem correlation operator. Using similar arguments, we proposed an analogous series for the three-body dispersion effects:[125]

three-body:

$$\epsilon_{disp}^{(30)},\ \epsilon_{disp}^{(31)},\ \epsilon_{DQ,disp}^{(32)},\ \epsilon_{SDQ,disp}^{(32)},\ \epsilon_{SDQT,disp}^{(32)} \quad (16)$$

In this series the first term, $\epsilon_{disp}^{(30)}$, describes the three-body dispersion nonadditivity arising among the monomers represented at the Hartree−Fock (i.e. uncorrelated) level. The subsequent terms denote the corrections to dispersion resulting from varying levels of correlation of the monomer wave functions. For example, $\epsilon_{SDQT,disp}^{(32)}$ denotes the component of the dispersion effect if monomers are correlated with single-, double-, triple-, and quadruple-excitations. It is apparent that the three-body effects require a one order higher treatment than their two-body analogs. Thus, if the two-body dispersion effects are reproduced up through the full (22) order, the similar balance of intra−inter effects in the three-body case would require the full (32) order calculations. This would be rather cumbersome and impractical. However, a conclusion of great practical importance can be drawn from the similarity of the series of eqs 15 and 16; namely, the convergence properties of both series should be analogous. Thus, if the sum of the first series, eq 15, is known (e.g. from ab initio calculations or semiempirical data) a fairly good estimate of the sum of eq 16 can be obtained, thus providing bounds to the three-body dispersion effect.[125]

The relationship between S-MP and I-MP perturbation theories provides an additional computational advantage in that it allows for the following mapping of the many-body dispersion terms:

The map describes the dispersion components (right)

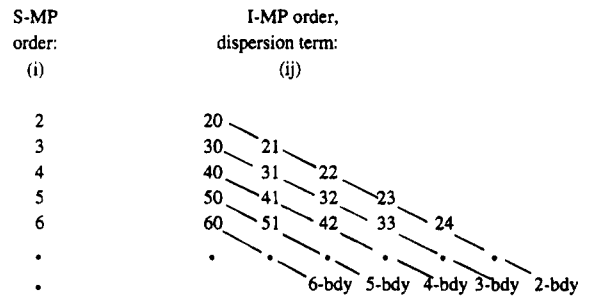

which are implicitly present in the supermolecular $\Delta E^{(i)}$ terms of the corresponding order (left). For example, the calculation of the combined dispersion effect which encompasses all the terms of the series of eq 15 requires the supermolecular MP4 treatment including S, D, T, and Q excitations. By the same token, to account for all the three-body terms which appear in eq 16, it is necessary to carry out the fifth-order MP perturbation theory calculations (with inclusion of S, D, T, and Q excitations, as well).

Alternatively, we can turn to the coupled cluster theory with single-, double-, and noniterative triple excitations (CCSD(T)), since CCSD(T) may be viewed as the infinite-order limit of MP perturbation theory with the S, D, Q, and T excitations

$$\Delta E_{ABC}^{CCSD(T)} \approx \sum_{i=0}^{\infty} \Delta E_{SDQT,ABC}^{(i)} \qquad (17)$$

where "≈" sign reminds us that the T excitations in CCSD(T) theory are not exact. The supermolecular CCSD(T) calculations of the three-body effect should implicitly include all the three-body dispersion terms present in the series eq 16.

In summary, the accurate treatment of the dispersion nonadditivity requires ab initio treatments which are highly correlated. The supermolecular CCSD(T) approach, although lacking in insights into the internal structure of dispersion effect, is, so far, the most efficient means of calculating the three-body dispersion term. One should also keep in mind that calculations of this sort are very time-consuming. Severe basis set dependency of many-body dispersion effects represents another, equally cumbersome, aspect of these calculations. Basis set saturation of the dispersion effect requires polarization functions of very high angular symmetries. It is possible to circumvent the use of such immense basis sets by using sets of bond functions of a lower symmetry centered in the middle of van der Waals bonds, in addition to atom-centered basis sets. Such a procedure yields the two-body dispersion energies with an accuracy of ca. 5%. Some benchmark results obtained with CCSD(T) method and bond functions for three rare gas trimers are shown in Table 13.

F. Concluding Remarks on Nonadditivity Calculations

Ab initio calculations of the three-body component of interaction potential are more complex than those for pair interactions and involve more computational effort. Some experience in this field which follows from the relationship between S-MP and I-MP perturbation theories should be briefly summarized.

Table 13. S-MP and CCSD(T) Nonadditive Interactions (in μH) for He_3, Ne_3, and Ar_3 in Configurations of Equilateral Triangle[a]

nonadditive term	He_3 (R = 5.6 a_0)	Ne_3 (R = 6.0 a_0)	Ar_3 (R = 7.0 a_0)
ΔE^{SCF}	−0.870	−0.567	−15.78
$\Delta E^{(2)}$	0.155	0.204	11.39
$\Delta E^{(3)}$	0.275	1.440	21.94
$\Delta E(3)$	−0.440	1.077	17.55
$\Delta E^{CCSD(T)}$	−0.334	1.66	14.46
accurate[b]	−0.34	1.81	16.6

[a] From ref 125. [b] Estimated on the basis of convergence properties of eqs 15 and 16.

I-MP offers many clues concerning the origins of three-body interactions. It describes a three-body interaction as a superposition of three fundamental nonadditivities: exchange, induction, and dispersion. These fundamental components can be described at various levels of inclusion of the intramonomer correlation. From a practical standpoint, the ability to predict which effect dominates in a given cluster is of primary importance in choosing a strategy of calculations and in a selection of basis set. In the clusters of polar molecules the three-body interaction is dominated by the induction nonadditivity. However, in the trimers formed by weak proton donors the exchange nonadditivity may be of some importance.[276] The dispersion effect is usually negligibly small. In the trimers formed by a molecule and two Rg atoms all the three fundamental nonadditivities are important. When the molecule is polar, the exchange term may be the most anisotropic of the three.[122,279] In the trimers involving negative ions it is expected that all the three terms should play an equal role.[291] In complexes involving positive ions only the induction nonadditivity needs to be included.[292] Finally, in the trimers of rare gases the dispersion and exchange nonadditivities are present.[42,114,125]

The bulk of exchange and induction nonadditivities is reproduced already at the HF level. The three-body dispersion energy of monomers described at the HF level, which is a pure correlation effect, appears at the third-order UCHF level of theory. The four-body UCHF dispersion energy appears in the fourth order, and so on.

For these reasons one can recommend the following strategy of S-MP calculations of nonadditive effects. In our experience, the clusters of polar molecules can be treated with sufficient accuracy at the MP3 level. This is because in these clusters the dispersion nonadditivity is of a secondary importance, and its UCHF treatment should be satisfactory. The remaining fundamental nonadditivities (exchange, induction) are very well reproduced through this level. In fact, the supermolecular HF calculations already provide reasonable estimates of nonadditive energies in these trimers. The calculations for dispersion-bound clusters should follow a different route. In this case, a reliable description of the three-body dispersion energy requires a correlated description of the monomer wave functions, mandating at least the MP5 treatment that includes S, D, T, and Q excitations, or CCSD(T) calculations. If the same level of accuracy is desired for the four-body dispersion

energy, a treatment which is one order higher must be used, i.e. MP6, for example. Of course such calculations would be prohibitively expensive. A more realistic approach in this case is to treat all many-body dispersion terms at the UCHF level. This means the pair energies are treated at MP2, the three-body energies at MP3, and the four-body energies at the MP4DQ level.[42]

As in any supermolecular calculations the energies of monomers, dimers, and all the appropriate n-mers should be derived in the basis set of the entire cluster. If the monomers become relaxed within the cluster, an additional account should be made of the one-body terms.

The construction of analytical formulae for the many-body potentials is in general nontrivial. Both dispersion and induction nonadditivities can be represented using the multipole expansion. As for the exchange effect, in certain types of clusters it can be modeled by the electrostatic interactions involving the exchange-induced distortions of electron density.[117,279]

VI. Summary and Outlook

We have demonstrated in this review that the state-of-the-art molecular electronic structure theory, implemented in the form of S-MP perturbation theory in conjunction with I-MP perturbation theory, offers useful and intellectually rewarding insights into the nature of intermolecular interactions. A study of simple models involving a molecule bound to a spherically symmetric species can reveal the properties of a molecule which determine its anisotropic behavior in a more complex molecular setting. The energy partitioning technique was shown to be of great value in the analysis of the shapes of PESs in the entire range of intersystem distances. By examining a variety of dimers bound by forces ranging from typical van der Waals to hydrogen bonding and donor−acceptor interactions, we found that the anisotropies of fundamental components, exchange, induction, and dispersion, are strikingly similar. The different anisotropies of total PESs in these systems result from a different relative balance of these components and from electrostatics. The role of other structure-determining factors, such as the presence of lone pairs (or charge-density indentations) and abilities of molecules to generate directional fields, has also been discussed. Studies of this type are crucial to a better understanding of the hydrogen bonding, hydrophobic interactions, and other interaction-related problems in chemistry and biology.

Three-body interactions were also discussed in this review on the basis of a number of simple model trimers. These interactions represent additional anisotropic factors which must be included when the structural and dynamic properties of clusters are to be described accurately. There is no single physical source of nonadditive behavior. The nonadditive interaction, for the most part, is a superposition of three fundamental components each with different physical origin. Through the individual analysis of these components we can develop notions helpful in determining in which instances these effects are important and how they can be adequately modeled. This review intended to document the first step in this direction.

One lesson learned from previous ab initio calculations of potentials energy surfaces is that they are of value only if determined with high precision. From our present standpoint, the sources of error in these surfaces have been well understood and in many instances circumvented. The S-MP and I-MP techniques supplemented by CCSD(T) allow calculations of highly accurate correlated PESs. However, basis set saturation remains a very demanding task. It requires both the theoretical insight into the nature of the interaction and the technology to handle a large number of basis set functions. Although the basis set problem has not been satisfactorily solved, significant progress has been achieved. At present, calculations of PESs of the most difficult dispersion-bound complexes with an error of 25% have become fairly routine. At this level of accuracy a variety of structural and energetical aspects of van der Waals interactions may be reliably addressed. We demonstrated such calculations for a number of complexes. Modest improvements of basis sets in the form of bond functions were shown to provide the accuracy of ±5% due to the efficient saturation of the dispersion term. This technique should be applied with some caution since it may adversely affect some of the interaction energy components. Yet these problems can be easily avoided, and in the coming years this technique will be perfected. It is also hoped that the basis set saturated values of the energy components will soon be obtained by using systematic sequences of basis sets, composed of independent sets designed to saturate intra- and intersystem correlation effects. Such results derived for some model systems will serve as invaluable benchmark data.

So far the accuracy of PESs has been assessed on the basis of semiempirical data in those rare instances where such data are available. It is anticipated that additional, independent information on accurate surfaces will come from nonempirical sources, such as, e.g., numerical treatments which sidestep the use of basis set entirely. One such approach, quantum Monte Carlo, has recently proved successful in the He dimer calculations.[293] Another treatment, diffusion Monte Carlo, was recently shown to permit the adjustment of potential energy surfaces to match the experimentally observed properties of molecular complexes.[254,294] One should expect other calculations of this sort in the near future.

So far the quantitative accuracy of PESs has been achieved for dimers involving up to ca. 50 electrons. The question arises now as to whether the interactions involving much larger systems, say, protein fragments, DNA bases, zeolites, etc., can be described with similar accuracy. As the systems approached by ab initio methods become more complex, this problem, no doubt, will be addressed. The insights gained at the present stage, such as the role of individual energy components, transferability of interaction parameters, etc., will guide future development in this area.

The main thrust of future ab initio studies of intermolecular interaction will be directed toward a better understanding of condensed phases. A study

Appendix Table A1. Structural and Energetical Characteristics (R_e and D_e) for the Rare Gas–Molecule Complexes Discussed in This Review from ab Initio Calculations[a]

complex	geometry	ab initio R_e, D_e	comment	experiment
		Rare Gas Atom–HX Complexes		
ArHCl	primary minimum Ar···H–Cl	R_e = 7.89 a_0 D_e = 795.4 (±5%)	MP4/WTdf(b-ext) (ref 185)	R_e = 7.57 a_0 D_e = 801.9 ± 14 (ref 184)
	secondary minimum Ar···Cl–H	R_e = 6.82 a_0 D_e = 634.8 (±5%)	MP4/WTdf(b-ext) (ref 185)	R_e = 6.82 a_0 D_e = 675.7 ± 14 (ref 184)
HeHCl	primary minimum He···Cl–H	R_e = 6.4 a_0 D_e = 146.1 (±5%)	MP4/spdf(b-ext) (ref 228)	R_e = 6.54 a_0 D_e = 149.0 (ref 227)
	secondary minimum He···H–Cl	R_e = 7.3 a_0 D_e = 140.2 (±5%)	MP4/spdf(b-ext) (ref 228)	R_e = 7.28 a_0 D_e = 128.9 (ref 227)
HeHBr	primary minimum He···Br–H	R_e = 7 a_0 D_e = 99 (30–40%)	MP2/spd (ref 228)	
	secondary minimum He···H–Br	R_e = 8 a_0 D_e = 92 (30–40%)	MP2/spd (ref 228)	
		Closed-Shell Atom–H_2X Complexes		
HeH_2O	T-shaped, coplanar	R_e = 6.6 a_0, Θ = 80°, χ = 0° D_e = 110 (25%)	MP4/spdf (ref 172)	
ArH_2O	coplanar, from T-shaped to H-bonded	R_e = 7.09–7.56 a_0, Θ = 80°–120°, χ = 0° D_e = 490 (25%)	MP4/spdf (ref 197)	R_e = 6.871 a_0, Θ = 125°, χ = 0° D_e = 651.57 (ref 198)
KrH_2O	coplanar, from T-shaped to H-bonded	R_e = 7.5 a_0, Θ = 100°, χ = 0° D_e = 472 (30–40%)		
BeH_2O	primary minimum C_{2v}	R_e = 6.5 a_0, Θ = 0° D_e = 802	MP4/spdf (ref 204)	
	secondary minimum coplanar, H-bonded	R_e = 7.5 a_0, Θ = 120°, χ = 0° D_e = 734	MP4/spdf (ref 205)	
ArH_2S	primary minimum coplanar, T-shaped	R_e = 7.5 a_0, Θ = 80°, χ = 0° D_e = 523 (30–40%)	MP2/spd (ref 185)	Θ = 90° (ref 209)
	secondary minimum C_{2v}	R_e = 8.0 a_0, Θ = 180° D_e = 460 (30–40%)	MP2/spd (ref 185)	
		Closed-Shell Atom–H_3X Complexes		
$ArNH_3$	T-shaped	R_e = 7.09 a_0, Θ = 80°, χ = 60° D_e = 414 (30–40%)	MP2/spd (ref 214)	R_e = 7.24 a_0 D_e = 466 (ref 215)
$KrNH_3$	T-shaped	R_e = 7.5 a_0, Θ = 80°, χ = 60° D_e = 492 (30–40%)	MP2/spd (ref 204)	
$BeNH_3$	C_{3v}	R_e = 6.5 a_0, Θ = 0° D_e = 1185	MP4/spdf (ref 205)	
$ArPH_3$	T-shaped	R_e = 7.09 a_0, Θ = 75°, χ = 60° D_e = 333 (30–40%)	MP2/spd (ref 225)	
		Rare Gas Atom–XY Halogens Complexes		
ArClF	primary minimum Ar···Cl–F	R_e = 7.73 a_0 D_e = 1148.0 (±5%)	MP4/spdf(b-ext) (refs 235 and 237)	R_e = 7.37 a_0 D_e = 1061 (ref 229)
	secondary minimum T-shaped	R_e = 7.23 a_0, Θ = 107° D_e = 710.1 (±5%)	MP4/spdf(b-ext) (refs 235 and 237)	
$ArCl_2$	primary minimum Ar···Cl–Cl	R_e = 8.54 a_0, Θ = 0° D_e = 1013.5 (±5%)	MP4/spdf(b-ext) (ref 237)	
	secondary minimum T-shaped	R_e = 7.16 a_0, Θ = 90° D_e = 943.9 (±5%)	MP4/spdf(b-ext) (ref 237)	R_e = 7.03 a_0 D_e = 966 (ref 233b)
$HeCl_2$ (^{1}X)	primary minimum He···Cl–Cl	R_e = 8.03 a_0, Θ = 0° D_e = 205.5 (±5%)	MP4/spdf(b-ext) (ref 174)	
	secondary minimum T-shaped	R_e = 6.6 a_0, Θ = 90° D_e = 185.7 (±5%)	MP4/spdf(b-ext) (ref 174)	R_e = 6.71 a_0 D_e = 174.1 (ref 239)
$HeCl_2$(^{3}A″)	primary minimum T-shaped	R_e = 6.6 a_0, Θ = 90° D_e = 138	UMP2/spdf (refs 174 and 238)	R_e = 6.73 a_0 D_e = 146.8 (ref 239)
	secondary minimum He···Cl–Cl	R_e = 9.4 a_0, Θ = 0° D_e = 90	UMP2/spdf (refs 174 and 238)	
H_2Cl_2	primary minimum T-shaped (Θ = 0°, Θ′ = 90°)	R_e = 7.75 a_0 D_e = 894 (±5%)	MP4/spdf(b-ext) (ref 270)	
	secondary minimum T-shaped (Θ = 90°, Θ′ = 0°)	R_e = 6.6 a_0 D_e = 587 (±5%)	MP4/spdf(b-ext) (ref 270)	
		Rare Gas Atom–CO-Containing Molecule Complexes		
ArCO	T-shaped, bent	R_e = 7.0 a_0, Θ = 80° D_e = 496 (±5%)	MP4/spdf(b-ext) (ref 242)	R_e = 6.86 a_0 D_e = 501 (ref 245) R_e = 7.20 a_0, Θ = 60–80° (ref 246)
HeCO	T-shaped, bent	R_e = 6.4 a_0, Θ = 70° D_e = 100 (±5%)	MP4/spdf(b-ext) (ref 242)	
$ArCO_2$	primary minimum T-shaped	R_e = 6.5 a_0, Θ = 90° D_e = 957 (±5%)	MP4/expdf(b-ext) (ref 243)	R_e = 6.4 a_0 D_e = 894 (ref 249)
	secondary minimum collinear	R_e = 9 a_0, Θ = 0° D_e = 533 (±5%)	MP4/spdf(b-ext) (ref 243)	R_e = 9.4 a_0 D_e = 260 (ref 249)
ArH_2CO	T-shaped, coplanar	R_e = 7.09 a_0, Θ = 100° D_e = 779 (20–30%)	MP4/spdf (ref 244)	coplanar, T-shaped (ref 251)

[a] The percent error estimates of D_e are given in parentheses. (For example, ±5% means plus/minus 5% of the reported value; 30–40% means plus 30–40% of the reported value.) In general, a precision of the ab initio determination of the angle and R were 10° and 0.25 a_0. The level of theory and the type of basis set are indicated in the "comment" column.

of larger clusters, which permits the observation of the properties of matter in transition between molecular and condensed bulk behavior, will be undertaken. Future applications will involve problems of interest to surface chemistry, enzymatic catalysis, supramolecular chemistry, structure–function–dynamics relations in biomolecules, and a number of other areas of science which require knowledge of intermolecular potential energy surfaces. These applications mandate further investigations of pair interactions and many-body forces at the fundamental level.

In contrast to van der Waals interactions of closed-shell species, the studies of complexes involving open-shell moieties are in their infancy.[295,296] From the experimental point of view this is a result of difficulties in generating these short-lived species. Ab initio studies are hampered by the fact that the electronic theory of open-shell systems is much more involved, and to a large extent still presents a theoretical challenge. The unrestricted MP (UMP) approach is expected to be useful in many cases,[297,298] and the intermolecular UMP (I-UMP) should be developed. However, applications of S-UMP and I-UMP are essentially limited to the cases where the spin contamination is not severe, and where such problems as bond breaking and curve crossing do not occur. There is, thus, a great need for treatments which involve multiconfigurational reference states. In fact, such approaches have already been successfully attempted by a number of researchers.[105,299–303] Studies of this type type are likely to intensify in the near future.

VII. Abbreviations

BSE	basis set extension
BSSE	basis set superposition error
CC	coupled cluster
CCSD	coupled cluster singles and doubles
CCSD(T)	coupled cluster singles, doubles, and noniterated triples
CEPA	coupled electron pair approximation
CHF	coupled Hartree–Fock
CI	configuration interaction
CP	counterpoise
DCBS	dimer-centered basis set
HF	Hartree–Fock
HL	Heitler–London
HOMO	highest occupied molecular orbital
ICF	interacting correlated fragments
I-MP	intermolecular Møller–Plesset perturbation theory
LUMO	lowest unoccupied molecular orbital
MBPT	many-body perturbation theory
MCBS	monomer centered basis set
MC	Monte Carlo
MMC	molecular mechanics for clusters
MP	Møller–Plesset perturbation theory
MP2	Møller–Plesset perturbation theory through the second order
MP3	Møller–Plesset perturbation theory through the third order
MP4	Møller–Plesset perturbation theory through the fourth order
MR-SDCI	multireference singles and doubles configuration interaction
PES	potential energy surface
Rg	rare gas
RS	Rayleigh–Schroedinger
SCF	self-consistent field
S-MP	supermolecular Møller–Plesset perturbation theory
TCBS	trimer-centered basis set
TDHF	time-dependent Hartree–Fock
UCHF	uncoupled Hartree–Fock
UMP	unrestricted Møller–Plesset perturbation theory
VRT	vibration–rotation–tunneling
WT	well-tempered

VIII. Acknowledgments

Many results described in this review represent a group effort of many collaborators. We wish to thank S. M. Cybulski, S. Scheiner, R. Moszyński, B. Kukawska-Tarnawska, J. Sadlej, P. Cieplak, M. Gutowski, R. A. Kendall, and P. Piecuch. We would also like to thank R. Burcl who performed some calculations solely for the purpose of this review. Special thanks go to M. Gutowski, B. Jeziorski and R. J. Saykally for offering us their comments on the manuscript. This work was supported by the National Institutes of Health (GM36912), the National Science Foundation (CHE-9215082), and by the Polish Committe for Scientific Research KBN (2 0556 91 01).

IX. References

(1) Maitland, G. C.; Rigby, M.; Smith, E. B.; Wakeham, W. A. *Intermolecular Forces*; Clarendon Press: Oxford, 1981.
(2) *Structure and Dynamics of Weakly Bound Molecular Complexes*; Weber, A., Ed.; NATO ASI Series C; Reidel: Dordrecht, 1987; Vol. 212.
(3) *Dynamics of Polyatomic van der Waals Complexes*; Halberstadt, N., Janda, K. C., Eds.; NATO ASI Series B; Plenum: New York, 1990; Vol. 227.
(4) Legon, A. C.; Millen, D. J. *Chem. Rev.* **1986**, *88*, 635.
(5) Miller, R. E. *J. Phys. Chem.* **1986**, *90*, 3301.
(6) Miller, R. E. *Adv. Mol. Vib. Collision Dyn.* **1991**, *1*, 83.
(7) Nesbitt, D. J. *Chem. Rev.* **1988**, *88*, 843.
(8) Cohen, R. C.; Saykally, R. J. *J. Phys. Chem.* **1992**, *96*, 1024; *Annu. Rev. Phys. Chem.* **1991**, *42*, 369.
(9) Saykally, R. J.; Blake, G. A. *Science* **1993**, *259*, 1570.
(10) McIlroy, A.; Nesbitt, D. J. *Adv. Mol. Vib. Collision Dyn.* **1991**, *1*, 109.
(11) Novick, S.; Leopold, K.; Klemperer, W. In *Atomic and Molecular Clusters*; Bernstein, E., Ed.; Elsevier: Amsterdam, 1990.
(12) Hutson, J. M. *Annu. Rev. Phys. Chem.* **1990**, *41*, 123.
(13) Hutson, J. M. *Adv. Mol. Vib. Collision Dyn.* **1991**, *1*, 1.
(14) *Intermolecular Interactions: From Diatomics to Biopolymers*; Pullman, B., Ed.; Wiley: New York, 1978.
(15) *Intermolecular Forces*; Pullman, B., Ed.; Reidel: Dordrecht, Holland, 1981.
(16) *The Hydrogen Bond-Recent Development in Theory and Experiment*; Schuster, P., Zundel, G., Sandorfy, C., Eds.; North-Holland: Amsterdam, 1976.
(17) *Molecular Interactions*; Ratajczak, H., Orville-Thomas, W. J., Eds.; Wiley: Chichester, UK, 1980; Vol. 1.
(18) Intermolecular Complexes. *The Role of van der Waals Systems in Physical Chemistry and in the Biodysciplines*; Hobza, P., Zahradník, R., Eds.; Academic: Prague, 1988.
(19) *Hydrogen Bonds*; Schuster, P., Ed.; *Top. Curr. Chem.* **1984**, No. 120.
(20) Scheiner, S. In *Aggregation Processes in Solution*; Wyn-Jones, Gormally, E., Eds.; Elsevier: Amsterdam, 1983; pp 462–508.
(21) *Theoretical Models of Chemical Bond*; Maksic, Z. B., Ed.; Springer-Verlag: Berlin, 1991.

(22) Schuster, P.; Karpfen, A.; Beyer, A. In *Molecular Interactions*; Ratajczak, H., Orville-Thomas, W. J., Eds.; Wiley: Chichester, UK, 1980; Vol. 1.
(23) Kołos, W. In *New Horizons of Quantum Chemistry*; Lowdin, P.-O., Pullman, B., Eds.; Reidel: Dordrecht, 1983.
(24) Hobza, P.; Zahradník, R. *Chem. Rev.* **1988**, *88*, 871.
(25) Chałasiński, G.; Gutowski, M. *Chem. Rev.* **1988**, *88*, 943.
(26) Buckingham, A. D.; Fowler, P. W.; Hutson, J. M. *Chem. Rev.* **1988**, *88*, 963.
(27) Møller, C.; Plesset, M. S. *Phys. Rev.* **1934**, *46*, 618.
(28) Pople, J. A.; Seeger, R.; Krishnam, R. *Int. J. Quantum Chem. Symp.* **1977**, *11*, 149.
(29) Krishnam, R.; Pople, J. A. *Int. J. Quantum Chem.* **1978**, *14*, 91.
(30) Bartlett, R. J. *Ann. Rev. Phys. Chem.* **1981**, *32*, 359.
(31) Bartlett, R. J. *J. Phys. Chem.* **1989**, *93*, 1697.
(32) Jørgensen, P.; Simons, J. *Second-Quantized-Based Methods in Quantum Chemistry*; Academic Press: New York, 1981.
(33) Wilson, S. *Electron Correlation in Molecules*; Clarendon Press: Oxford, 1984.
(34) Jeziorski, B.; Kołos, W. In *Molecular Interactions*; Ratajczak, H., Orville-Thomas, W. J., Eds.; Wiley: New York, 1982; Vol. 3, p 1.
(35) Szalewicz, K.; Jeziorski, B. *Mol. Phys.* **1979**, *38*, 191.
(36) Rybak, S.; Jeziorski, B.; Szalewicz, K. *J. Chem. Phys.* **1991**, *95*, 6576.
(37) Williams, H. L.; Szalewicz, K.; Jeziorski, B.; Moszyński, R.; Rybak, S. *J. Chem. Phys.* **1993**, *98*, 1279.
(38) Jeziorski, B.; Moszyński, R.; Ratkiewicz, A.; Rybak, S.; Szalewicz, K.; Williams, H. L. SAPT: A Program for Many-Body Symmetry-Adapted Perturbation Theory Calculations of Intermolecular Interaction Energies. In *Methods and Techniques in Computational Chemistry: METECC-94*; Clementi, E., Ed.; STEF: Gagliari, 1993; Vol. B.
(39) Chałasiński, G.; Szczęśniak, M. M. *Mol. Phys.* **1988**, *63*, 205.
(40) Moszyński, R.; Rybak, S.; Cybulski, S. M.; Chałasiński, G. *Chem. Phys. Lett.* **1990**, *166*, 609.
(41) Cybulski, S. M.; Chałasiński, G.; Moszyński, R. *J. Chem. Phys.* **1990**, *92*, 4357.
(42) Chałasiński, G.; Szczęśniak, M. M.; Cybulski, S. M. *J. Chem. Phys.* **1990**, *92*, 2481.
(43) Cybulski, S. M.; Chałasiński, G. *Chem. Phys. Lett.* **1992**, *197*, 591.
(44) Moszyński, R.; Cybulski, S. M.; Chałasiński, G. *J. Chem. Phys.* **1994**, *100*, 4998.
(45) Frisch, M. J.; Trucks, G. W.; Head-Gordon, M.; Gill, P. M. W.; Wong, M. W.; Foresman, J. B.; Johnson, B. G.; Schlegel, H. B.; Robb, M. A.; Replogle, E. S.; Gomperts, R.; Andres, J. L.; Raghavachari, K.; Binkley, J. S.; Gonzalez, C.; Martin, R. L.; Fox, D. J.; Defrees, D. J.; Baker, J.; Stewart, J. J. P.; Pople, J. A. *Gaussian 92*; Gaussian, Inc.: Pittsburgh, PA, 1992.
(46) Hehre, W. J.; Radom, L.; Schleyer, P. v. R.; Pople, J. A. *Ab Initio Molecular Orbital Theory*; Wiley: New York, 1986.
(47) London, F. *Z. Phys. Chem. (B)* **1930**, *11*, 222.
(48) Eisenschitz, R.; London, F. *Z. Phys.* **1930**, *60*, 491.
(49) London, F. *Trans. Faraday Soc.* **1937**, *33*, 8.
(50) Margenau, H.; Kestener, N. R. *Theory of Intermolecular Forces*; Pergamon: Oxford, 1971.
(51) Hirschfelder, J. O.; Curtiss, C. F.; Bird, R. B. *Molecular Theory of Gases and Liquids*; Wiley: New York, 1954.
(52) Hirschfelder, J. O.; Meath, W. J. *Adv. Chem. Phys.* **1976**, *12*, 3.
(53) Piecuch, P. In *Molecules in Physics, Chemistry and Biology*; Kluwer Academic Publishers: Dordrecht, 1988; Vol. 2, p 417.
(54) Magnasco, V.; McWeeny, R. In *Theoretical Models of Chemical Bonding*; (Theoretical Treatment of Large Molecules and Their Interactions; Maksic, Z. B., Ed.; Springer: New York, 1991; Part 4, p 133.
(55) Morokuma, K.; Kitaura, K. In *Molecular Interactions*; Ratajczak, H., Orville-Thomas, W. J., Eds.; Wiley: New York, 1982; Vol. 1, p 21.
(56) Curtiss, L. A.; Pochatko, A. J.; Reed, A. E.; Weinhold, F. *J. Chem. Phys.* **1985**, *82*, 6833. Gladening, E. D.; Streitwieser, A. *J. Chem. Phys.* **1994**, *100*, 2900.
(57) Gutowski, M.; Piela, L. *Mol. Phys.* **1988**, *64*, 337.
(58) Frey, R. F.; Davidson, E. R. *J. Chem. Phys.* **1989**, *90*, 5555.
(59) Clementi, E.; Corongui, G.; Chakravorty, S. In *Modern Techniques in Computational Chemistry: MOTECC-90*; Clementi, E., Ed.; ESCOM Sci. Publ.: Leiden, 1990; p 343.
(60) Hirschfelder, J. O. *Chem. Phys. Lett.* **1967**, *1*, 325.
(61) Jeziorski, B.; Kołos, W. *Int. J. Quantum Chem.* **1977**, *12*, Suppl. 1, 91.
(62) Chipman, D. M.; Hirschfelder, J. O. *J. Chem. Phys.* **1973**, *59*, 2838.
(63) Klein, D. J. *Int. J. Quantum Chem.* **1987**, *32*, 377.
(64) Adams, W. H. *Int. J. Quantum Chem.* **1990**, *S24*, 531; **1991**, *S25*, 165.
(65) Tang, K. T.; Toennies, J. P. *J. Chem. Phys.* **1991**, *95*, 5918.
(66) Jeziorski, B.; Szalewicz, K.; Chałasiński, G. *Int. J. Quantum Chem.* **1978**, *14*, 271.
(67) Jeziorski, B.; Schwalm, W. A.; Szalewicz, K. *J. Chem. Phys.* **1980**, *73*, 6215.
(68) Ćwiok, T.; Jeziorski, B.; Kołos, W.; Moszyński, R.; Szalewicz, K. *J. Chem. Phys.* **1992**, *97*, 7555.
(69) Jeziorski, B.; Bulski, M.; Piela, L. *Int. J. Quantum Chem.* **1976**, *10*, 281.
(70) Claverie, P. In *Intermolecular Interactions: From Diatomics to Biopolymers*; Pullman, B., Ed.; Wiley: New York, 1978; p 69.
(71) Jeziorski, B.; van Hemert, M. C. *Mol. Phys.* **1976**, *31*, 713.
(72) Kochanski, E. *J. Chem. Phys.* **1973**, *58*, 5823.
(73) Moszyński, R.; Jeziorski, B.; Ratkiewicz, A.; Rybak, S. *J. Chem. Phys.* **1993**, *99*, 8856.
(74) Salter, E. A.; Trucks, G. W.; Bartlett, R. J. *J. Chem. Phys.* **1989**, *90*, 1752.
(75) Cybulski, S. M. *J. Chem. Phys.* **1992**, *97*, 7545.
(76) Amos, R. D. *Adv. Chem. Phys.* **1987**, *67*, 99.
(77) Cybulski, S. M. *J. Chem. Phys.* **1992**, *96*, 8225.
(78) Moszyński, R.; Jeziorski, B.; Szalewicz, K. *Int. J. Quantum Chem.* **1993**, *45*, 409.
(79) McWeeny, R. *Croat. Chem. Acta* **1984**, *57*, 865.
(80) Knowles, P. J.; Meath, W. J. *Mol. Phys.* **1987**, *60*, 1143.
(81) Jaszuński, M.; McWeeny, R. *Mol. Phys.* **1985**, *55*, 1275.
(82) Visser, F.; Wormer, P. E. S.; Stam, P. *J. Chem. Phys.* **1983**, *76*, 4973.
(83) Rijks, V.; Wormer, P. E. S. *J. Chem. Phys.* **1988**, *88*, 5704.
(84) Thakkar, A. J.; Hettema, H.; Wormer, P. E. S. *J. Chem. Phys.* **1992**, *97*, 3252.
(85) Wormer, P. E. S.; Hettema, H. *J. Chem. Phys.* **1992**, *97*, 5592.
(86) Sadlej, A. J. *J. Chem. Phys.* **1981**, *75*, 320.
(87) Casimir, H. B. G.; Polder, D. *Phys. Rev.* **1948**, *73*, 360.
(88) Ćwiok, T.; Jeziorski, B.; Kołos, W.; Moszyński, R.; Rychlewski, J.; Szalewicz, K. *Chem. Phys. Lett.* **1992**, *195*, 67.
(89) Gutowski, M.; Chałasiński, G.; van Duijneveldt-van de Rijdt, J. G. C. M. *Int. J. Quantum Chem.* **1984**, *26*, 971.
(90) Jankowski, P.; Jeziorski, B.; Rybak, S.; Szalewicz, K. *J. Chem. Phys.* **1991**, *95*, 6576.
(91) Moszyński, R.; Jeziorski, B.; Szalewicz *J. Chem. Phys.* **1994**, *100*, 1312. Moszyński, R.; Jeziorski, B.; Rybak, S.; Szalewicz; Williams, H. L. *J. Chem. Phys.* **1994**, *100*, 5080.
(92) Moszyński, R.; Jeziorski, B.; Szalewicz, K. *Chem. Phys.* **1992**, *166*, 329.
(93) Cybulski, S. M.; Scheiner, S. *Chem. Phys. Lett.* **1990**, *166*, 57.
(94) Gutowski, M.; Olszewski, K.; Piela, L. *J. Phys. Chem.* **1990**, *94*, 5710.
(95) Jeziorska, M.; Jeziorski, B.; Čižek. *Int. J. Quantum Chem.* **1987**, *32*, 149.
(96) Moszyński, R.; Jeziorski, B. To be published.
(97) Liu, B.; McLean, A. D. *J. Chem. Phys.* **1980**, *72*, 3418.
(98) Liu, B.; McLean, A. D. *J. Chem. Phys.* **1989**, *91*, 2348.
(99) Vos, R. J.; van Lenthe, J. H.; van Duijneveldt, F. B. *Mol. Phys.* **1989**, *67*, 1011.
(100) Vos, R. J.; van Lenthe, J. H.; van Duijneveldt, F. B. *J. Chem. Phys.* **1990**, *93*, 643.
(101) Vos, R. J.; Hendriks, R.; van Duijneveldt, F. B. *J. Comput. Chem.* **1990**, *11*, 1.
(102) van Duijneveldt-van de Rijdt, J. G. C. M.; van Duijneveldt, F. B. *J. Chem. Phys.* **1992**, *97*, 6649.
(103) Saebo, S.; Tong, W.; Pulay, P. *J. Chem. Phys.* **1993**, *98*, 2170.
(104) Kapuy, E.; Kozmutza, C. *J. Chem. Phys.* **1991**, *94*, 5565.
(105) Roeggen, I.; Ahmadi, G. R.; Wind, P. A. *J. Chem. Phys.* **1993**, *99*, 277.
(106) Bulski, M.; Wormer, P. E. S.; van der Avoird, A. *J. Chem. Phys.* **1991**, *94*, 491.
(107) Bulski, M.; Wormer, P. E. S.; van der Avoird, A. *J. Chem. Phys.* **1991**, *94*, 8097.
(108) van der Pol, A.; van der Avoird, A.; Wormer, P. E. S. *J. Chem. Phys.* **1990**, *92*, 7498.
(109) Wormer, P. E. S. Ph.D. Dissertation, Nijmegen, 1975.
(110) Wormer, P. E. S.; Mulder, F.; van der Avoird, A. *Int. J. Quantum Chem.* **1977**, *11*, 959.
(111) (a) Lengsfield, B., III; McLean, A. D.; Yoshimine, Liu, B. *J. Chem. Phys.* **1983**, *79*, 1891. (b) Dyall, K. G.; McLean, A. D. *J. Chem. Phys.* **1992**, *97*, 8424.
(112) McLean, A. D.; Liu, B.; Barker, J. A. *J. Chem. Phys.* **1988**, *89*, 6339.
(113) Meath, W. J.; Aziz, R. A. *Mol. Phys.* **1984**, *52*, 225.
(114) Meath, W. J.; Koulis, M. *Theochem* **1991**, *226*, 1.
(115) Kołos, W.; Leś, A. *Chem. Phys. Lett.* **1972**, *14*, 167.
(116) Bulski, M.; Chałasiński, G. *Theor. Chim. Acta* **1980**, *56*, 199.
(117) Cooper, A. R.; Hutson, J. M. *J. Chem. Phys.* **1993**, *98*, 5337.
(118) Cooper, A. R.; Jain, S.; Hutson, J. M. *J. Chem. Phys.* **1993**, *98*, 2160.
(119) Jansen, L. *Phys. Rev.* **1962**, *125*, 1798.
(120) Jansen, L. *Adv. Quantum Chem.* **1965**, *125*, 119.
(121) Piecuch, P. *Int. J. Quantum Chem.* **1993**, *47*, 263.
(122) Szczęśniak, M. M.; Chałasiński, G.; Piecuch, P. *J. Chem. Phys.* **1993**, *99*, 6732.
(123) Cybulski, S. M. *Chem. Phys. Lett.*, in press.
(124) Axilrod, B. M.; Teller, E. *J. Chem. Phys.* **1943**, *11*, 299.
(125) Chałasiński, G.; Szczęśniak, M. M.; Kendall, R. A. *J. Chem. Phys.* **1994**, in press.
(126) Liu, B.; McLean, A. D. *J. Chem. Phys.* **1973**, *59*, 4557.

(127) Gutowski, M.; Chałasiński, G. *J. Chem. Phys.* **1993**, *98*, 5540.
(128) van Lenthe, J. H.; van Duijneveldt-van de Rijdt, J. G. C. M.; van Duijneveldt, F. B. *Adv. Chem. Phys.* **1987**, *69*, 521.
(129) Gutowski, M.; van Duijneveldt-van de Rijdt, J. G. C. M.; van Lenthe, J. H.; van Duijneveldt, F. B. *J. Chem. Phys.* **1993**, *98*, 4728.
(130) Szczęśniak, M. M.; Scheiner, S. *J. Chem. Phys.* **1986**, *84*, 6328.
(131) Boys, S. F.; Bernardi, F. *Mol. Phys.* **1970**, *19*, 553.
(132) Yang, J.; Kestner, N. R. *J. Phys. Chem.* **1991**, *95*, 9214. Yang, J.; Kestner, N. R. *J. Phys. Chem.* **1991**, *95*, 9221.
(133) Tao, F.-M.; Pan, Y.-K. *J. Phys. Chem.* **1991**, *95*, 3582.
(134) Tao, F.-M.; Pan, Y.-K. *J. Phys. Chem.* **1991**, *95*, 9811.
(135) Tao, F.-M.; Pan, Y.-K. *J. Phys. Chem.* **1992**, *96*, 7145.
(136) Eggenberger, R.; Gerber, S.; Huber, S.; Searls, D. *Chem. Phys. Lett.* **1991**, *183*, 223.
(137) van Duijneveldt, F.; van Duijneveldt-van de Rijdt, G. C. J. M.; van Lenthe, J. H. *Chem. Rev.* **1994**, *94*, this issue.
(138) Mayer, I.; Vibok, A. *Int. J. Quantum Chem.* **1991**, *40*, 139.
(139) Mayer, I.; Vibok, A. *Int. J. Quantum Chem.* **1992**, *43*, 801.
(140) Sadlej, A. *J. Chem. Phys.* **1991**, *95*, 6705.
(141) Cook, D. B.; Sordo, T. L.; Sordo, J. A. *J. Chem. Soc., Chem. Commun.* **1990**, *2*, 185.
(142) Karlstrøm, G.; Sadlej, A. J. *Theor. Chim. Acta* **1982**, *61*, 1.
(143) Cullen, J. M. *Int. J. Quantum Chem.* **1991**, *S25*, 193.
(144) Davidson, E. R.; Chakravorty, S. J. *Chem. Phys. Lett.* **1994**, *217*, 48.
(145) Scheiner, S. In *Reviews in Computational Chemistry*; Lipkowitz, K. B., Boyd, D. B., Eds.; VCH: Weinheim, 1991; p 165.
(146) Parasuk, V.; Almlöf, J.; DeLeeuw, B. *Chem. Phys. Lett.* **1991**, *176*, 1.
(147) Latajka, Z.; Scheiner, S.; Chałasiński, G. *Chem. Phys. Lett.* **1992**, *196*, 384.
(148) Chałasiński, G.; van Lenthe, J.; Groen, T. *Chem. Phys. Lett.* **1984**, *110*, 369.
(149) Gutowski, M.; Verbeek, J.; van Lenthe, J.; Chałasiński, G. *Chem. Phys.* **1987**, *111*, 271.
(150) Chałasiński, G.; Gutowski, M. *Mol. Phys.* **1985**, *54*, 1173.
(151) Chałasiński, G.; Jeziorski, B.; Andzelm, J.; Szalewicz, K. *Mol. Phys.* **1977**, *33*, 971.
(152) Werner, H. J.; Meyer, W. *Mol. Phys.* **1976**, *31*, 855.
(153) Latajka, Z.; Scheiner, S. *J. Comput. Chem.* **1987**, *8*, 663; **1987**, *8*, 674. Latajka, Z. *Theochem* **1991**, *251*, 245; **1990**, *205*, 13.
(154) Szczęśniak, M. M.; Scheiner, S. *Collect. Czech. Chem. Commun.* **1988**, *53*, 2214.
(155) Sadlej, A. J. *Collect. Czech. Chem. Commun.* **1988**, *53*, 1995; *Theor. Chim. Acta* **1991**, *79*, 123; **1992**, *81*, 339. Kellö, V.; Sadlej, A. J. *Theor. Chim. Acta* **1992**, *83*, 351.
(156) van Duijneveldt-van de Rijdt, J. G. C. M.; van Duijneveldt, F. B. *Theochem* **1982**, *89*, 185.
(157) Huzinaga, S.; Kłobukowski, M.; Tatewaki, H. *Can. J. Chem.* **1985**, *63*, 1812.
(158) Huzinaga, S.; Kłobukowski, M. *Theochem* **1988**, *167*, 1.
(159) Dingle, T.; Huzinaga, S.; Klobukowski, M. *J. Comput. Chem.* **1989**, *10*, 753.
(160) Dunning, T. H., Jr. *J. Chem. Phys.* **1989**, *90*, 1007. Kendall, R. A.; Dunning, T. H., Jr.; Harrison, R. J. *J. Chem. Phys.* **1992**, *96*, 6796. Woon, D. E.; Dunning, T. H., Jr. *J. Chem. Phys.* **1993**, *98*, 1358.
(161) Almlöf, J.; Taylor, P. R. *J. Chem. Phys.* **1987**, *86*, 4070.
(162) Almlöf, J.; Taylor, P. R. *J. Chem. Phys.* **1990**, *92*, 551.
(163) Partridge, H. *J. Chem. Phys.* **1989**, *90*, 1043; **1987**, *87*, 6643.
(164) Woon, D. E. *J. Chem. Phys.* **1994**, *100*, 2838.
(165) Woon, D. E. *Chem. Phys. Lett.* **1993**, *204*, 29.
(166) Feller, D. *J. Chem. Phys.* **1992**, *96*, 6104.
(167) van Duijneveldt-van de Rijdt, J. G. C. M.; van Duijneveldt, F. B. *J. Comput. Chem.* **1992**, *13*, 399.
(168) Szczęśniak, M. M.; Chałasiński, G.; Cybulski, S. M.; Cieplak, P. *J. Chem. Phys.* **1993**, *98*, 3078.
(169) (a) Tao, F.-M.; Pan, Y.-K. *J. Chem. Phys.* **1992**, *97*, 4989. (b) Tao, F.-M.; Pan, Y.-K. *Chem. Phys. Lett.* **1992**, *194*, 162.
(170) Tao, F.-M. *J. Chem. Phys.* **1992**, *98*, 3049.
(171) Chałasiński, G.; Szczęśniak, M. M. *Croat. Chem. Acta* **1992**, *65*, 17.
(172) Kukawska-Tarnawska, B.; Chałasiński, G.; Szczęśniak, M. M. *J. Mol. Struct.* **1993**, *297*, 313.
(173) Hobza, P.; Bludsky, O.; Selzle, H. L.; Schlag, E. W. *J. Chem. Phys.* **1992**, *97*, 335.
(174) Chałasiński, G.; Gutowski, M.; Szczęśniak, M. M.; Sadlej, J.; Scheiner, S. *J. Chem. Phys.*, in press.
(175) Diercksen, G. H. F.; Sadlej, A. *J. Chem. Phys.* **1989**, *156*, 269.
(176) Černušak, I.; Noga, J.; Diercksen, G. H. F.; Sadlej, A. J. *Chem. Phys.* **1988**, *125*, 255.
(177) Saxe, P.; Schaefer, H. F., III; Handy, N. C. *Chem. Phys. Lett.* **1981**, *79*, 202. Harrison, R. J.; Handy, N. C. *Chem. Phys. Lett.* **1983**, *95*, 386.
(178) Diercksen, G. H. F.; Kellö, V.; Sadlej, A. J. *Chem. Phys.* **1985**, *96*, 59.
(179) Kutzelnigg, W. In *Theoretical Models of Chemical Bonding*; Part 2 (The Concept of the Chemical Bond), Maksic, Z. B., Ed.; Springer: New York, 1990; p 1.
(180) Chałasiński, G.; Funk, D. J.; Simons, J.; Breckenridge, W. H. J. *Chem. Phys.* **1987**, *87*, 3569.
(181) Aziz, R. A.; Chen, H. H. *J. Chem. Phys.* **1977**, *67*, 5719.
(182) Tang, K. T.; Toennies, J. P. *J. Chem. Phys.* **1984**, *80*, 3726.
(183) Chałasiński, G.; Szczęśniak, M. M.; Kukawaska-Tarnawska, B. *J. Chem. Phys.* **1991**, *94*, 6677.
(184) Hutson, J. M. *J. Phys. Chem.* **1992**, *96*, 4237.
(185) Burcl, R.; Szczęśniak, M. M.; Chłasiński, G. Unpublished results.
(186) Kofranek, M.; Lischka, H.; Karpfen, A. *Chem. Phys.* **1988**, *121*, 137.
(187) Quack, M.; Suhm, M. A. *J. Chem. Phys.* **1991**, *95*, 28.
(188) Miller, R. E. *Acc. Chem. Res.* **1990**, *23*, 10.
(189) Szczęśniak, M. M.; Brenstein, R. J.; Cybulski, S. M.; Scheiner, S. *J. Phys. Chem.* **1990**, *94*, 1781.
(190) Szczęśniak, M. M.; Kendall, R. A.; Chałasiński, G. *J. Chem. Phys.* **1991**, *95*, 5169.
(191) Szczęśniak, M. M.; Chałasiński, G.; Cybulski, S. M.; Scheiner, S. *J. Chem. Phys.* **1990**, *93*, 4243.
(192) Szczęśniak, M. M.; Chałasiński, G.; Cybulski, S. M. To be published.
(193) Ahlrichs, R.; Bohm, H. J.; Brode, S.; Tang, K. T.; Toennies, P. J. *J. Chem. Phys.* **1988**, *88*, 6290; (Erratum) *J. Chem. Phys.* **1993**, *98*, 3579.
(194) Bader, R. F.; Keaveny, I.; Cade, P. E. *J. Chem. Phys.* **1967**, *47*, 3381.
(195) Hutson, J. M. *J. Chem. Phys.* **1988**, *89*, 4550.
(196) Elrod, M. J.; Host, B. C.; Steyert, D. W.; Saykally, R. J.; Hutson, J. M. *Mol. Phys.* **1993**, *79*, 245.
(197) Chałasiński, G.; Szczęśniak, M. M.; Scheiner, S. *J. Chem. Phys.* **1991**, *94*, 2807.
(198) Cohen, R. C.; Saykally, R. J. *J. Chem. Phys.* **1993**, *98*, 6007.
(199) Cohen, R. C.; Saykally, R. J. *J. Phys. Chem.* **1990**, *94*, 7991.
(200) Hutson, J. M. *J. Chem. Phys.* **1990**, *92*, 157.
(201) Bissonnette, C.; Clary, D. C. *J. Chem. Phys.* **1992**, *97*, 8111.
(202) Nesbitt, D. J.; Lascola, R. *J. Chem. Phys.* **1992**, *97*, 8096.
(203) Maluendes, S.; McLean, A. D.; Green, S. *J. Chem. Phys.* **1992**, *96*, 8150. Green, S.; DeFrees, D. J.; McLean, A. D. *J. Chem. Phys.* **1991**, *94*, 1346.
(204) Chałasiński, G.; Szczęśniak, M. M.; Scheiner, S. *J. Chem. Phys.* **1993**, *97*, 8181.
(205) Chałasiński, G.; Szczęśniak, M. M.; Scheiner, S. *J. Chem. Phys.* **1993**, *98*, 7020.
(206) Hasse, F.; Sauer, J.; Kellö, V. *Chem. Phys. Lett.* **1990**, *174*, 19.
(207) Curtiss, L. A.; Pople, J. A. *Chem. Phys. Lett.* **1991**, *185*, 159.
(208) Bader, R. F. W. *Atoms in Molecules—A Quantum Theory*; Oxford University: Oxford, 1990.
(209) Viswanathan, R.; Dyke, T. R. *J. Chem. Phys.* **1985**, *82*, 1674.
(210) Suni, I. I.; Lee, S.; Klemperer, W. *J. Phys. Chem.* **1991**, *95*, 2859.
(211) Schmuttenmaer, C. A.; Cohen, R. C.; Loeser, J. G.; Saykally, R. J. *J. Chem. Phys.* **1991**, *95*, 9.
(212) Loeser, J. G.; Schmuttenmaer, C. A.; Cohen, R. C.; Elrod, M. J.; Steyert, D. W.; Saykally, R. J.; Bumgarner, R. E.; Blake, G. A. *J. Chem. Phys.* **1992**, *97*, 4727.
(213) van Bladel, J. W. I.; van der Avoird, A.; Wormer, P. E. S.; Saykally, R. J. *J. Chem. Phys.* **1992**, *97*, 4750.
(214) Chałasiński, G.; Cybulski, S. M.; Szczęśniak, M. M.; Scheiner, S. *J. Chem. Phys.* **1989**, *91*, 7809.
(215) Nelson, D. D.; Fraser, G. T.; Peterson, K. I.; Zhao, K.; Klemperer, W.; Lovas, F. J.; Suernam, R. D. *J. Chem. Phys.* **1986**, *85*, 5512. Fraser, G. T.; Nelson, C. D.; Charo, A.; Klemperer, W. *J. Chem. Phys.* **1985**, *82*, 2335.
(216) Buckingham, A. D.; Fowler, P. W. *J. Chem. Phys.* **1983**, *79*, 6426; *Can. J. Chem.* **1985**, *63*, 1985.
(217) Stone, A. J. *Chem. Phys. Lett.* **1981**, *83*, 233. Stone, A. J.; Alderton, M. *Mol. Phys.* **1985**, *56*, 1047.
(218) Legon, A. C. *Chem. Soc. Rev.* **1990**, *19*, 197.
(219) Dykstra, C. E. *J. Am. Chem. Soc.* **1989**, *111*, 6168.
(220) Klemperer, W. *J. Mol. Structure* **1980**, *59*, 161.
(221) Hurst, G. J. B.; Fowler, P. W.; Stone, A. J.; Buckingham, A. D. *Int. J. Quantum Chem.* **1986**, *29*, 1223.
(222) Hayes, I. C.; Stone, A. J. *Mol. Phys.* **1984**, *53*, 83; **1984**, *53*, 69.
(223) Kisiel, Z. *J. Phys. Chem.* **1991**, *95*, 7605.
(224) Szczęśniak, M. M.; Chałasiński, G.; Cybulski, S. M. *J. Chem. Phys.* **1992**, *96*, 463.
(225) Latajka, Z.; Scheiner, S. *J. Mol. Struct.* **1989**, *198*, 205.
(226) Burcl, R.; Chałasiński, G.; Szczęśniak, M. M. To be published.
(227) Willey, D. R.; Choong, V.-E.; De Lucia, F. C. *J. Chem. Phys.* **1992**, *96*, 898.
(228) Chałasiński, G.; Szczęśniak, M. M. Unpublished results.
(229) Harris, S. J.; Novick, S. E.; Klemperer, W.; Falconer, W. E. *J. Chem. Phys.* **1974**, *61*, 193.
(230) Novick, S. E.; Harris, S.; Janda, K. C.; Klemperer, W. *Can. J. Phys.* **1975**, *53*, 2007.
(231) Cline, J. I.; Evard, D. D.; Thommen, F.; Janda, K. C. *J. Chem. Phys.* **1986**, *84*, 1165.
(232) Evard, D. D.; Thommen, F.; Janda, K. C. *J. Chem. Phys.* **1986**, *84*, 3630.

(233) (a) Evard, D. D.; Cline, J. I.; Janda, K. C. *J. Chem. Phys.* **1988**, *88*, 5433. (b) Halberstadt, N.; Sema, S.; Roncero, O.; Janda, K. C. *J. Chem. Phys.* **1992**, *97*, 341.
(234) Xu, Y.; Jager, W.; Ozier, I.; Gerry, M. C. L. *J. Chem. Phys.* **1993**, *98*, 3726.
(235) Sadlej, J.; Chałasiński, G.; Szczęśniak, M. M. *J. Chem. Phys.* **1993**, *99*, 3700.
(236) Tao, F.-M.; Klemperer, W. *J. Chem. Phys.* **1992**, *97*, 440.
(237) Sadlej, J.; Chałasiński, G.; Szczęśniak, M. M. *Theochem* **1994**, *307*, 187.
(238) Cybulski, S. M.; Burcl, R.; Szczęśniak, M. M.; Chałasiński, G.; Gutowski, M. To be published.
(239) Beneventi, L.; Casavecchia, P.; Volpi, G. G.; Bieler, C. R.; Janda, K. C. *J. Chem. Phys.* **1993**, *98*, 178.
(240) Stone, A. J.; Price, S. L. *J. Phys. Chem.* **1988**, *92*, 3325.
(241) Rodger, P. M.; Stone, A. J.; Tildesley, D. J. *Mol. Phys.* **1988**, *63*, 173; *J. Chem. Soc., Faraday Trans. 2* **1987**, *83*, 1689; *Mol. Simul.* **1992**, *8*, 145.
(242) Kukawska-Tarnawska, B.; Chałasiński, G.; Olszewski, K. *J. Chem. Phys.* **1994**, *101*, 4964.
(243) Sadlej, J.; Szczęśniak, M. M.; Chałasiński, G. Manuscript in preparation.
(244) Sadlej, J.; Szczęśniak, M. M.; Chałasiński, G. *J. Chem. Phys.* **1993**, *99*, 5211.
(245) Mirsky, K. *Chem. Phys.* **1980**, *46*, 445.
(246) Ogata, T.; Jager, W.; Ozier, I.; Gerry, M. C. L. *J. Chem. Phys.* **1993**, *98*, 9399.
(247) Parish, C. A.; Augspurger, J. D.; Dykstra, C. E. *J. Phys. Chem.* **1992**, *96*, 2069.
(248) Bader, R. F. W.; Essen, H. *J. Chem. Phys.* **1984**, *80*, 1943.
(249) Bohac, E. J.; Marshal, M. D.; Miller, R. E. *J. Chem. Phys.* **1992**, *97*, 4890.
(250) Bader, R. F.; Kaith, T. A. *J. Chem. Phys.* **1993**, *99*, 3685.
(251) Novick, S. E.; Suernam, R. D.; Lovas, R. F.; Fraser, G. T. 43rd Symp. Molec. Spectroscopy, Ohio State University, 1988. Novick, S. *J. Chem. Phys.* **1993**, *99*, 7506.
(252) Wheatley, R. J.; Price, S. L. *Mol. Phys.* **1990**, *69*, 507.
(253) Zhang, Q.; Chenyang, L.; Ma, Y.; Fish, F.; Szczęśniak, M. M.; Buch, V. *J. Chem. Phys.* **1992**, *96*, 6033.
(254) Sandler, P.; Jung, ah. J.; Szczęśniak, M. M.; Buch, V. *J. Chem. Phys.* **1994**, *101*, 1378.
(255) Andrews, L.; Davies, S. R. *J. Chem. Phys.* **1985**, *83*, 4983.
(256) Yaron, D.; Peterson, K. I.; Zolandz, D.; Klemperer, W.; Lovas, F. J.; Suernam, R. D. *J. Chem. Phys.* **1990**, *92*, 7095.
(257) Sadlej, J.; Buch, V. *J. Chem. Phys.* **1994**, *100*, 4272.
(258) Racine, S. C.; Davidson, E. R. *J. Phys. Chem.* **1993**, *97*, 6367.
(259) Dayton, D. C.; Jucks, K. W.; Miller, R. E. *J. Chem. Phys.* **1989**, *71*, 2703.
(260) Bunker, R. P.; Kofranek, M.; Lischka, H.; Karpfen, A. *J. Chem. Phys.* **1988**, *89*, 3002.
(261) Scheiner, S. *Annu. Rev. Phys. Chem.* **1994**, *45*, in press.
(262) Chakravorty, S. J.; Davidson, E. R. *J. Phys. Chem.* **1993**, *97*, 6373.
(263) Curtiss, L. A.; Frurip, D. J.; Blander, M. *J. Chem. Phys.* **1979**, *71*, 2703.
(264) Pugliano, N.; Cruzan, J. D.; Loeser, J. G.; Saykally, R. J. *J. Chem. Phys.* **1993**, *98*, 6600.
(265) Nelson, D. D.; Fraser, G. T.; Klemperer, W. *J. Chem. Phys.* **1985**, *83*, 6201.
(266) Nelson, D. D.; Klemperer, W.; Fraser, G. T.; Lovas, F. J.; Suernam, R. D. *J. Chem. Phys.* **1987**, *87*, 6364.
(267) Baum, R. R. *Chem. Eng. News* **1992**, Oct. 19.
(268) Sagarik, K. P.; Ahlrichs, R.; Brode, S. *Mol. Phys.* **1986**, *57*, 1247.
(269) Latajka, Z.; Scheiner, S. *J. Chem. Phys.* **1986**, *84*, 341.
(270) Szczęśniak, M. M. Unpublished results.
(271) Hassett, D. M.; Marsden, C. J.; Smith, B. J. *Chem. Phys. Lett.* **1991**, *183*, 449.
(272) Frisch, M. J.; Del Bene, J. E.; Binkley, J. S.; Schaefer, H. F. *J. Chem. Phys.* **1986**, *84*, 2279.
(273) Tao, F. M.; Klemperer, W. *J. Chem. Phys.* **1993**, *99*, 5976.
(274) Cybulski, S. M. *Chem. Phys. Lett.*, in press.
(275) Van der Avoird, A.; Wormer, P. E. S.; Moszyński, R. *Chem. Rev.* **1994**, *94*, this issue.
(276) Szczęśniak, M. M.; Chałasiński, G. *J. Mol. Structure (Theochem)* **1992**, *261*, 37.
(277) Chałasiński, G.; Szczęśniak, M. M.; Cieplak, P.; Scheiner, S. *J. Chem. Phys.* **1991**, *94*, 2873. Unfortunately, the geometrical input for the d−d structure in this work was erroeneous. Consequently, the calculated values for this structure are wrong. The erratum containing the correct values will be published. In the meantime, the correct data can be obtained from the authors upon request (e-mail: maria@proton.chem.oakland.edu).
(278) Chałasiński, G.; Cybulski, S. M.; Szczęśniak, M. M.; Scheiner, S. *J. Chem. Phys.* **1989**, *91*, 7048.
(279) Cybulski, S. M.; Szczęśniak, M. M.; Chałasiński, G. *J. Chem. Phys.*, in press.
(280) Dyke, T. R.; Muenter, S. *J. Chem. Phys.* **1972**, *57*, 5011.
(281) Honegger, E.; Leutwyler, S. *J. Chem. Phys.* **1988**, *88*, 2582.
(282) Pugliano, N.; Saykally, R. J. *Science* **1992**, *257*, 1937.
(283) Liu, K.; Loeser, J. G.; Elrod, M. J.; Host, B. C.; Rzepiela, J. A.; Pugliano, N.; Saykally, R. J. *J. Am. Chem. Soc.* **1994**, *116*, 3507.
(284) Mo, O.; Yanes, M.; Elguero, J. *J. Chem. Phys.* **1992**, *97*, 6628.
(285) (a) Xantheas, S.; Dunning, T. H. *J. Chem. Phys.* **1993**, *98*, 8037. (b) Xantheas, S. *J. Chem. Phys.* **1994**, *100*, 7523.
(286) van Duijneveldt-van de Rijdt, J. G. C. M.; van Duijneveldt, F. B. *Chem. Phys.* **1993**, *175*, 271.
(287) Schutz, M.; Burgi, T.; Leutwyler, S.; Burgi, H. B. *J. Chem. Phys.* **1993**, *99*, 5228.
(288) Hutson, J. M. *J. Chem. Phys.* **1992**, *96*, 6752.
(289) Elrod, M. J.; Steyert, D. W.; Saykally, R. J. *J. Chem. Phys.* **1991**, *95*, 3182; **1991**, *95*, 3182. Elrod, M. J.; Loeser, J. G.; Saykally, R. J. *J. Chem. Phys.* **1993**, *98*, 5352.
(290) Hutson, J. M.; Beswick, J. A.; Halberstadt, N. *J. Chem. Phys.* **1989**, *90*, 1337.
(291) Burcl, R.; Cybulski, S. M.; Szczęśniak, M. M.; Chałasiński, G. To be published.
(292) Kelterbaum, R.; Turki, N.; Rahmouni, A.; Kochanski, E. *J. Chem. Phys.* **1994**, *100*, 1589.
(293) Anderson, J. B.; Traynor, C. A.; Boghosian, B. M. *J. Chem. Phys.* **1993**, *99*, 345.
(294) Franken, K. A.; Dykstra, C. E. *J. Chem. Phys.* **1994**, *100*, 2865.
(295) Heaven, M. C. *J. Phys. Chem.* **1993**, *97*, 8567.
(296) Heaven, M. C. *Annu. Rev. Phys. Chem.* **1992**, *43*, 283.
(297) Chałasiński, G.; Simons, J. *Chem. Phys. Lett.* **1988**, *148*, 289.
(298) Chałasiński, G.; Kukawska-Tarnawska, B. *J. Phys. Chem.* **1990**, *94*, 3450.
(299) Esposti, D. A.; Werner, H.-J. *J. Chem. Phys.* **1990**, *93*, 3351.
(300) Kochanski, E.; Flower, D. R. *Chem. Phys.* **1981**, *57*, 217.
(301) Offer, R. A.; van Hemert, M. C. *J. Chem. Phys.* **1993**, *99*, 3836.
(302) van Lenthe, J. H.; van Duijneveldt, F. B. *J. Chem. Phys.* **1984**, *81*, 3168.
(303) Bililign, S.; Gutowski, M.; Simons, J.; Breckenridge, W. H. *J. Chem. Phys.* **1993**, *99*, 3815; **1994**, *100*, 8212.